BIBLIOGRAPHIC INFORMATION

PB95-192076

Report Nos:

Title: Adaptive Dynamic Analysis Considering Structural Lifespan: An Approach Based on Fuzzy Mathematics.

Date: Aug 94

Authors: S. Wadia-Fascetti and H. A. Smith.

Performing Organization: Stanford Univ., CA. John A. Blume Earthquake Engineering Center.

Sponsoring Organization: *National Science Foundation, Arlington, VA.*Shimizu Corp., Tokyo (Japan). Ohsaki Research Inst.

Contract Nos: NSF-BCS-9058316

Type of Report and Period Covered: Research rept.

Supplemental Notes: Also pub. as Stanford Univ., CA. John A. Blume Earthquake Engineering Center rept. no. REPT-113.

NTIS Field/Group Codes: 89D (Structural Analyses)

Price: PC A08/MF A02

Availability: Available from the National Technical Information Service, Springfield, VA. 22161

Number of Pages: 171p

Keywords: *Fuzzy sets, *Structural response, *Earthquake damage, *Uncertainty, Structural vibration, Dynamic response, Degradation, Stiffness, Structural failure, Earthquake engineering, Structural engineering, Errors, Calibration, Structural analysis, *Adaptive dynamic analysis.

Abstract: In this research a new analysis procedure is proposed which integrates system identification objectives and fuzzy set mathematics to formulate an adaptive analysis model capable of considering the changes a structure experiences during its lifespan. The adaptive model quantify the uncertainties associated with dynamic parameters at three stages during the structure's lifespan: calibration, degradation, and damage. The adaptive model proposed here, unlike conventional system identification techniques, does not require experimental response data from the as-built structure. Instead, fuzzy set mathematics is used to represent the level of confidence of various design assummptions, and the vertex method is used to develop a fuzzy set which bounds the structure's dynamic parameters.

The John A. Blume Earthquake Engineering Center

Department of Civil Engineering
Stanford University

ADAPTIVE DYNAMIC ANALYSIS CONSIDERING STRUCTURAL LIFESPAN: AN APPROACH BASED ON FUZZY MATHEMATICS

by
Sara Wadia-Fascetti
and
H. Allison Smith

A report on research sponsored in part by

the Shimizu Corporation and the
National Science Foundation,
Grant No. BCS-9058316

Report No. 113

August 1994

The John A. Blume Earthquake Engineering Center was established to promote research and education in earthquake engineering. Through its activities our understanding of earthquakes and their effects on mankind's facilities and structures is improving. The Center conducts research, provides instruction, publishes reports and articles, conducts seminars and conferences, and provides financial support for students. The Center is named for Dr. John A. Blume, a well-known consulting engineer and Stanford alumnus.

Address

The John A. Blume Earthquake Engineering Center
Department of Civil Engineering
Stanford University
Stanford, California 94305

ADAPTIVE DYNAMIC ANALYSIS CONSIDERING STRUCTURAL LIFESPAN: AN APPROACH BASED ON FUZZY MATHEMATICS

Sara Wadia-Fascetti
and
H. Allison Smith

The John A. Blume Earthquake Engineering Center
Department of Civil Engineering
Stanford University
Stanford, CA 94305-4020

A report on research sponsored in part by
the Shimizu Corporation and the
National Science Foundation, Grant BCS - 9058316

Report no. 113
August 1994

Abstract

In this research a new analysis procedure is proposed which integrates system identification objectives and fuzzy set mathematics to formulate an adaptive analysis model capable of considering the changes a structure experiences during its lifespan. The adaptive models quantify the uncertainties associated with dynamic parameters at three stages during the structure's lifespan; calibration, degradation, and damage. The adaptive model proposed here, unlike conventional system identification techniques, does not require experimental response data from the as-built structure. Instead, fuzzy set mathematics is used to represent the level of confidence of various design assumptions, and the vertex method is used to develop a fuzzy set which bounds the structure's dynamic parameters.

The calibration model, the first of the three categories considered in the adaptive model, quantifies the error between the dynamic parameters predicted by the analytical structural model and those of the actual structure. The error in the dynamic parameters is based on the modeling uncertainties for the structural masses and the structural stiffness. Quantification of the fundamental uncertainties and the use of the calibration model makes it possible to predict the potential values of the higher-level dynamic parameters. The degradation model uses the results from the calibration model and uncertainty in the rate of degradation of fundamental parameters to predict the uncertainty in the dynamic parameters during the structure's lifespan.

It has been well accepted that the excitation acting on a structure (due to an earthquake) is dependent on the site's proximity to the fault rupture, earthquake magnitude, and local site conditions. In this study the uncertainty in the excitation is modeled through the development of the fuzzy response spectra. The fuzzy spectrum used in the dynamic analysis is selected based on the local soil conditions and the site's proximity to the potential earthquake. Each spectrum provides the analyst with a

range of frequency content and maximum responses for the possible earthquake. The forced vibration analysis is performed by superimposing the fuzzy spectrum with the adaptive models (which quantify the potential sources of error in structure's dynamic properties) to quantify the uncertainty in the response for the structure.

A case study of the Santa Clara County Office Building, located is San Jose, California, is presented. This structure's dynamic behavior has been studied extensively since its instrumentation with the California Strong Motion Instrumentation Program. The dynamic parameters obtained from the calibration model and the ground motion models are compared to the actual parameters of the structure. It is found that the calibration model is capable of bounding the dynamic properties (natural frequencies and maximum building response) of the structure at high levels of confidence.

Acknowledgments

This report was performed in collaboration with the Ohsaki Research Institute of the Shimizu Corporation, Tokyo, Japan in an investigation of design issues for structures with extended lifespans. Our conterpart at the Ohsaki Research Institute is Dr. Yasuhiro Hayashi. The contents of this report is a reproduction of the senior author's Ph.D. dissertation.

The research presented in this report was supported by the Ohsaki Research Institute of the Shimizu Corporation and the National Science Foundation Grant BCS-9058316. Additonally, the San Diego Super Computing Center made available their super computers for use in this project. The support provided by these organizations is gratefully acknowledged.

Professor Anne S. Kiremidjian and Dr. Weimin Dong of Risk Management Systems have provided invaluable advise throughout the duration of this project. Dr. William Joyner, of the United States Geological Survey and Dr. Yasuhiro Hayashi, from the Ohsaki Research Institute of the Shimizu Corporation in Japan, have also provided valuable technical advise to this project. Mr. Jarnail Ghumman, from the County of Santa Clara, was very helpful in providing the structural blueprints of the Santa Clara County Office Building which is presented in this report as a case study. The authors are grateful for the help obtained from these individuals.

Any opinions, findings, conclusions, and recommendations expressed in this dissertation are those of the authors and do not represent those of the aforementioned sponsors and colleagues.

Contents

Tables

Figures

Notation

a, b, c, d	thresholds used to define fuzzy sets;
A	cross-sectional area;
b	slopes describing parametric degradation;
c	viscous damping coefficient;
$\mathbf{C}$	assembled system damping matrix;
D	dynamic amplification factor;
E	material modulus of elasticity;
$\mathcal{E}_{cal}(\alpha)$	calibration error at membership α, denoted as E_{cal} in the figures;
$\mathcal{E}_{deg}(\alpha)$	degradation error at membership α, denoted as E_{deg} in the figures;
$\mathcal{E}_{dam}(\alpha)$	damage error at membership α;
$\mathbf{F}(t)$	time dependent forcing function acting on structure;
$\mathcal{F}$	fuzzy set for structural natural frequency, denoted as F in the figures;
$I_{x,y,z}$	moment of inertia about the x, y, and z axes, respectively;
k	stiffness;
$\mathbf{K}$	assembled system stiffness matrix;
l	length of a finite element;
L_d	dead loads considered in analysis;
L_l	live loads considered in analysis;
m	distributed mass of a structural element, and the number of modes superimposed in dynamic analysis;
$\mathbf{M}$	assembled system mass matrix;
M_b	external bending moment applied to a structural joint;
r	ratio of two natural frequencies (used in CQC);
$S_{d,v,a}$	psuedo displacement, velocity, and acceleration, respectively;
T	structural period;
$U_{1,2}$	standard uniform variates;

$\mathbf{v}$	vector containing time dependent structural response for each dof where the first and second derivatives in time denote velocity and acceleration, respectively;
$V_{\max}$	maximum velocity ;
x	distance from site to the rupture zone and a lognormal variate;
x'	a normal variate;
$\mathbf{X}_A(x)$	characteristic function for crisp set analysis;
$\mathcal{X}(\alpha)$	parameter used to define the mass fuzzy sets, varies with α, denoted as X in figures;
y	modal coordinate (or time dependent response);
α	alpha-cut descriptor;
β_i	ratio of input frequency to the system's ith natural frequency;
γ	dimensionless parameter, used to scale spring stiffness;
ζ	standard deviation of a lognormal distribution;
θ_r	rotational joint deformation;
κ	spring stiffness with units $\frac{\text{lb-ft}}{\text{rad}}$;
λ	mean of a lognormal distribution;
μ	mean of a normal distribution;
$\mu_A(x)$	membership function for parameter, x which defines the fuzzy set A;
ν	Poisson's ratio;
ξ	modal critical damping factor;
ρ_{ij}	term which represents the coupling between modes i and j (used for CQC);
σ	standard deviation for a normal distribution;
υ	rate of corrosion;
ϕ	eigenvector denoting mode shape (orthonormal);
ω	circular natural frequency;

Superscripts:

*	denotes dynamic analysis in the time domain (i.e. modal analysis);
^{c}	denotes calibration error;
^{dg}	denotes degradation error;
^{dm}	denotes damage error;
^{U,L}	upper or lower bound for an α-cut;

Subscripts:

$_{i}$	ith degree-of-freedom;
$_{o}$	initial deterministic estimate;
$_{n}$	mode of vibration;
$_{\alpha}$	descriptor which denotes a level of membership a fuzzy set A (A_{α});

CHAPTER 1

Introduction

Engineers spend considerable amounts of time in the design and analysis of structures to withstand dynamic loads. The structural design process ensures that the structural members will be able to resist the required loads, and that the structure's dynamic behavior will be appropriate. Engineering codes have been developed to help structural engineers and designers make decisions pertaining to the selection of structural members. In addition to being able to withstand their own loads, these structures also must be able to resist loads due to external factors such as winds and earthquakes. Very often, the engineer will calculate deterministic values for design parameters and compare them to what the codes present as acceptable. These codes are developed solely for the maintenance of human life and do not consider additional factors such as nonstructural damage and occupant comfort. Ignoring these additional factors in the dynamic analyses increases the uncertainty inherent in the analytical model.

By studying the dynamic behavior of a structure, the analyst assesses the acceptability of accelerations and drifts at various story heights. Stiffening the structure, which will reduce the story drifts, also will increase the accelerations and attract higher levels of dynamic forces to the structure. Consequently, the selected structural members must be able to resist these new forces. In the case of structural dynamics, very often decisions can be made which can reduce the damage to a structure, although the codes rarely address such issues. In order to improve the decision making capabilities of the structural engineer, a method is needed which quantifies the error associated with the parameters used in design. The designer needs a method which can be applied easily and intuitively to aid in his decision making process.

System identification techniques have been used to determine the dynamic behavior of a constructed facility. These techniques have helped researchers not only

determine the true dynamic characteristics of the building, but to evaluate the potential changes of the structure's dynamic characteristics. There are numerous structures which have been instrumented for use in this type of research. Through the identification of the dynamic characteristics of these structures, it is possible to study the possible degradation and damage characteristics of a particular structure due to dynamic loadings such as earthquakes. Implementation of system identification procedures require an instrumented building and a dynamic excitation, with the "identified" results typically including the natural frequencies, mode shapes, and modal damping characteristics.

Much work in the past has focused on understanding and quantifying the various sources of modeling error using system identification and probabilistic techniques. However, more important than understanding the errors themselves, is an accurate understanding of the implications of the errors and their effects on structural response. Errors in the analytical model can cause the response predicted by the original model to differ significantly from the response of the prototype structure.

In structural engineering and design, there are two major sources of uncertainty in analysis: uncertainties associated with the representation of the structural model and uncertainties associated with the representation of the excitation acting on the structure. Previous research has focused on quantifying uncertainties in excitation models including development of stochastic techniques for estimating dynamic loading time histories. Since most of the uncertainty in the dynamic response of a structure is due to the uncertainty in the dynamic loading (such as earthquakes and extreme winds), relatively little work has been done to quantify the approximations associated with structural models. Since the characterization for the input motion is extremely complex, a significant part of the design codes is devoted to the adequate representation of the earthquake load. Consequently, the designer performs the dynamic analyses (in the case of noncritical structures) assuming that the finite element representation of the structure accurately predicts the structural dynamic properties. However, the assumptions made by the engineer and those inherent in the analysis procedures can cause the predicted response to deviate significantly from the actual structural behavior.

Dynamic analysis of a structural design typically only considers the dynamic properties of the "as-designed" structure while ignoring the dynamic characteristics that may occur during the structure's lifespan. Dynamic structures are typically designed and constructed with a design life of 50 to 60 years. However, many of these structures have already been standing much longer than their design life. Many engineering offices in Japan [Hay95] are designing buildings which will stand for several hundred years. Consequently, an understanding of the degradation and damage potential for the structural members will help the analyst make decisions pertaining to the structural design which consider the structure's lifespan. Additionally, an understanding of the long-term degradation properties for the fundamental parameters will enable the designer to predict the structure's dynamic properties as a function of time. This will enable the structure to be designed with its entire lifespan in consideration, hence an adaptive design of the structure.

This thesis addresses the issues related to the quantification of uncertainty in dynamic parameters through the development of a methodology based on fuzzy logic which is capable of managing uncertainties. Section 1.1 defines the problem to be addressed in this work. The scope for this research is addressed in Section 1.2. Finally, the organization for the remainder of this thesis is presented in Section 1.3.

1.1 Statement of the Problem

The objective of this thesis, is to develop an analysis methodology capable of quantifying dynamic uncertainties throughout the structure's lifespan. This methodology is applied to three stages of the structure's life: calibration, degradation, and damage. These three types of error [SW92] represent the potential sources of discrepancy between the initial (finite element) design model for a structure and its as-built characteristics. Calibration error is the discrepancy between the design model and the as-built system in its pristine condition. Degradation error occurs due to the gradual degradation of structural characteristics as the building ages, and represents the uncertainty between the aged structure and the calibrated as-built structure. Damage error represents the difference between the degraded calibrated structure and the

structure after a damaging event.

By dividing the lifespan of a structure into these three categories, it is then possible to quantify the uncertainty of the dynamic parameters as errors in the analytical model. Calibration error, occurs due to simplifications and assumptions made in formulating the design finite element model. Sources of calibration error are approximations in discretizing the structure in the finite element representation, failure to represent accurately the connections between structural members, and inability to represent effectively various characteristics such as structural damping and foundation conditions. Often, for example, there are inconsistencies on the construction site which affect the stiffness of various structural joints (such as tightening joints to proper specifications) which contribute to the calibration error.

Degradation error occurs due to the gradual degradation of structural characteristics as the building ages. During the lifespan of a structure, fatigue and the aging of the building materials causes a gradual decrease in structural stiffness and an increase in structural damping [Tar88, Cif84]. Thus, in addition to the calibration error between the design model and the as-built structure, there is an increasing discrepancy between the characteristics of an aged structure and the pristine, as-built structure.

The final form of discrepancy between the initial design model and the real-life structure is damage error which occurs when a building undergoes a major excitation such as an earthquake, hurricane, or other design-level event. Though the structure's original design specifications allow certain levels of these events to occur without causing significant structural damage, the accumulation of damage and the occasional event which exceeds design specifications can inflict drastic changes in a structure and alter its serviceability and structural integrity.

Calibration errors are denoted by an initial misrepresentation of the actual dynamic characteristics of the structure by the structural model. The additional errors due to degradation and damage to the structure increase the uncertainty in the analytical model's prediction of the dynamic parameters. These three errors are depicted in Figure 1.1 which denotes the possible change in natural frequency over a structure's lifespan. The calibration error is represented by the initial pre-calibrated frequency, ω_o, and the possible calibration error, $\mathcal{E}_{cal}$. The long-term aging characteristics of the

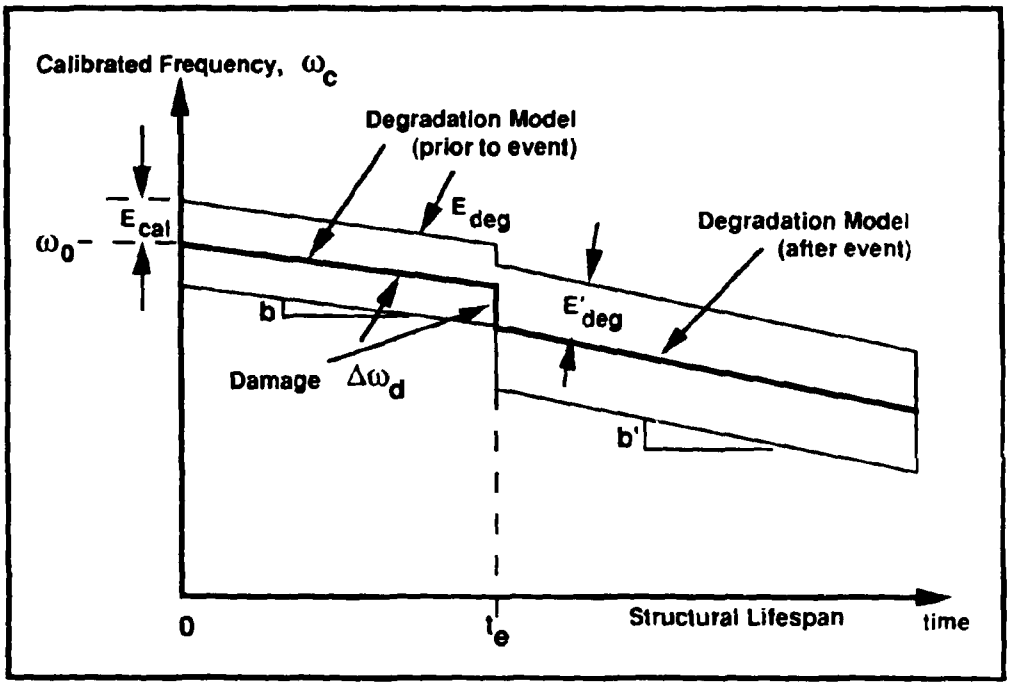

Figure 1.1: Illustration of uncertainty in frequency over structural lifespan.

structure are represented by the gradual decrease in the frequency and is governed by the slope b shown in the figure. Degradation error (which is a function of time) prior to a damaging event is denoted as $\mathcal{E}_{deg}$. The possible damage to the structure is represented by $\Delta\omega_d$ which is the drastic change in frequency and occurs due to a damaging event such as an earthquake at time $t = t_e$. Finally, the degradation process will continue after the structure has been damaged. This degradation is represented in the figure by the error, $\mathcal{E}'_{deg}$, and slope, b'.

By providing the engineer with a mathematical representation of the modeling errors, this procedure helps eliminate the uncertainties that typically are considered using engineering judgement alone. The proposed analysis methodology must have the following characteristics:

1. Have the potential to be standardized for use on many structures.

2. Be intuitive and straight-forward such that the method can be implemented by a practicing engineer.

3. Contain the information and accuracy required for the designer's decision making purposes.

4. Minimize the computations necessary in its implementation.

5. Consider the uncertainty in the input motion to the structure.

6. Facilitate the incorporation of additional uncertainties into the models as the practitioner sees fit.

The iterative design process and the sources of uncertainty to this process must be considered in the development of the adaptive design models. The shaded regions in Fig. 1.2 denote the stages in the iterative design process which are considered in the adaptive analysis models. There are a number of uncertainties contributing to structural analysis which must be considered in the development of the modeling procedures. For the purpose of illustration, these uncertainties have been divided into those contributing to calibration error and degradation/damage error and are shown in Figs. 1.3 and 1.4, respectively. Finally, the uncertainty associated with the input motion to the structure is shown in Fig. 1.5. Due to the large number of contributing uncertainties information (shown in these figures), the following section presents a refined scope for this thesis.

1.2 Scope of the Project

The parameters considered in this project are the modal parameters of a structure characteristic of its dynamic behavior and the response of the structure. The parameters include the natural frequencies of the structure, ω_n, where n denotes the mode of vibration, the frequency ratios (the ratio of the input frequency to ω_n) which are denoted by β_n, and the structural response of the degrees of freedom, x_i, $\dot{x}_i$, and $\ddot{x}_i$ where i denotes the degree-of-freedom.

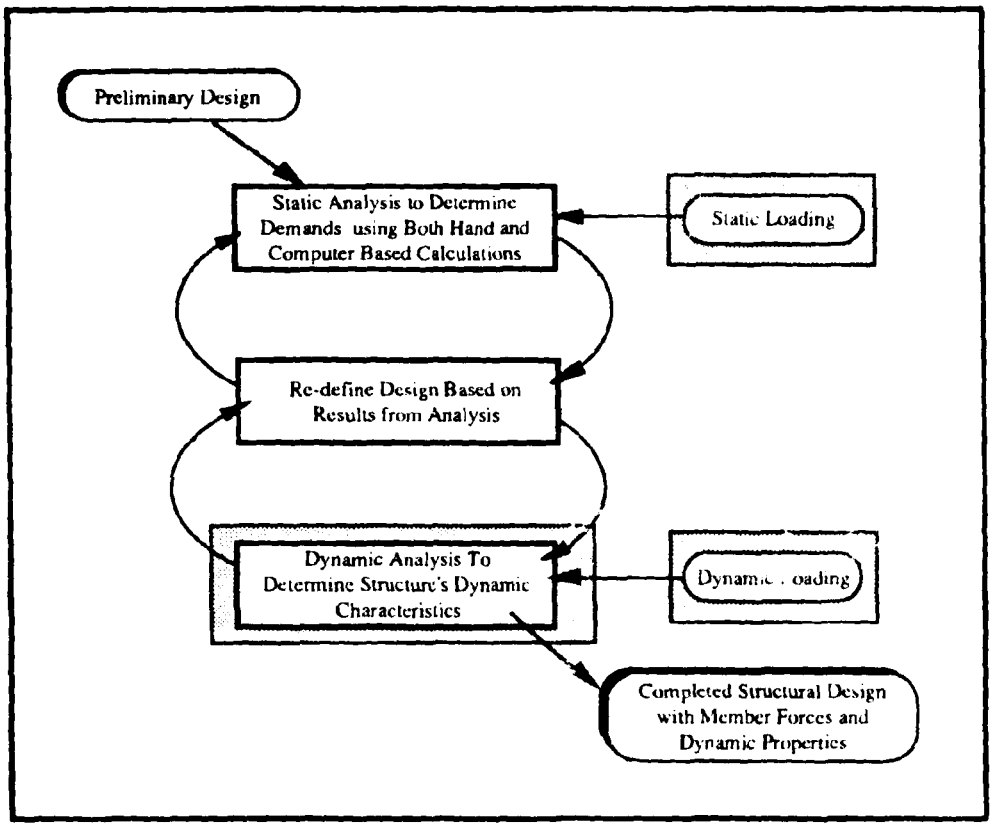

Figure 1.2: The iterative design procedure and sources of uncertainty.

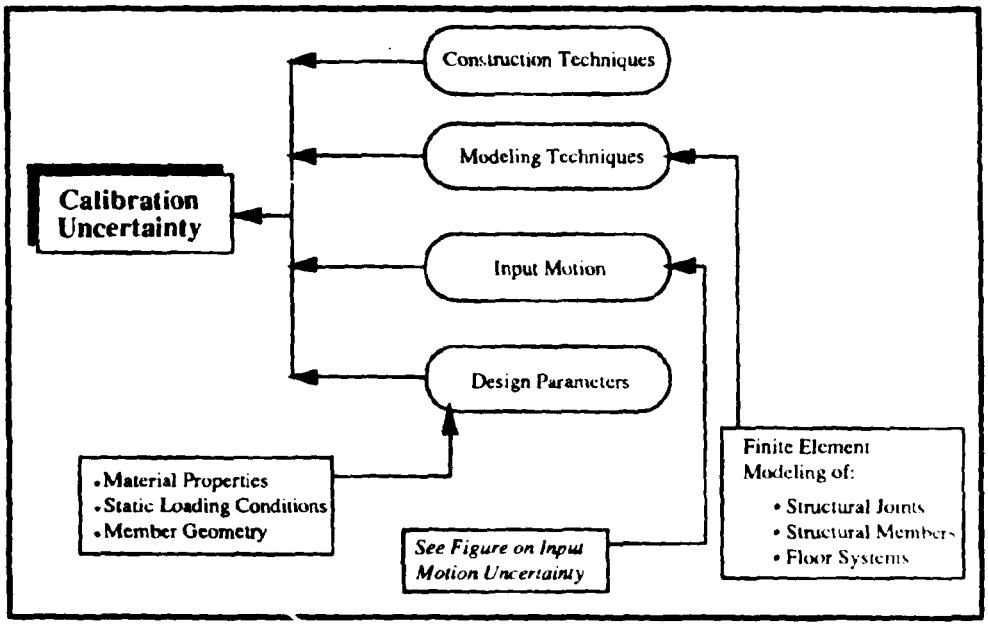

Figure 1.3: Possible sources of uncertainty contributing to calibration error.

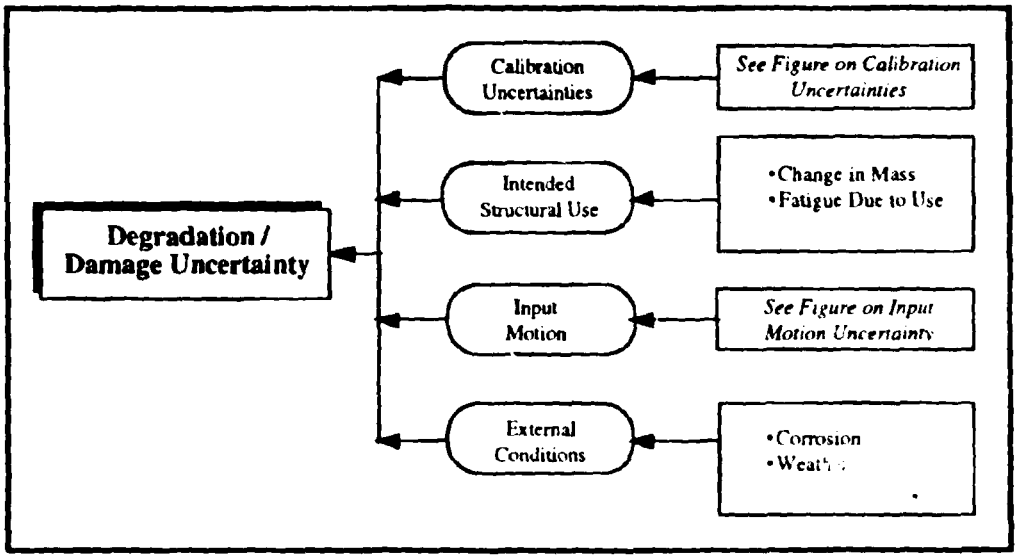

Figure 1.4: Possible sources of uncertainty contributing to degradation and damage errors.

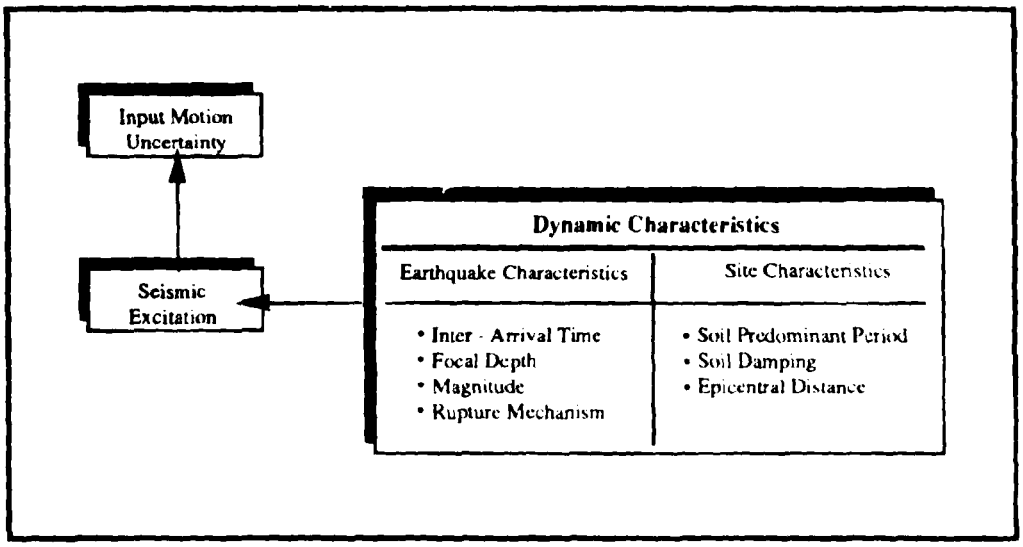

Figure 1.5: Sources of uncertainty associated with seismic input motion.

These three parameters (frequency, frequency ratio, and response) are dependent on fundamental errors, associated with building mass, stiffness properties, damping, etc; therefore, these errors must also be quantified. The three error models are developed in a conceptual framework. In this thesis, the errors for the three parameters presented are quantified at the calibration and degradation stages; thus, giving the engineer the tools necessary to make decisions required of them in practice.

To predict the uncertainty in the structural response, it is necessary to quantify the uncertainty associated with the input to the structure. The dynamic input motion in this scope is an earthquake time history. Uncertainty is quantified for the possible earthquake ground motion through the development of fuzzy spectra. These fuzzy spectra, which quantify the uncertainty associated with the input motion, are then used in the analysis models to predict the uncertainty in the structural response.

The adaptive analysis processes described in this thesis are broad and can consider a large number and different types of uncertainties. For the purposes of research and development, the scope of the project must be "narrow" enough to consider and

develop a thorough and concise process. Figure 1.6 shows the sources of uncertainty considered for this thesis.

Prediction of earthquake inter-arrival time and magnitude is necessary in the reduction of earthquake hazard mitigation and the prediction of damage as a function of a structure's lifespan. However, such predictions are very complicated and are not fully understood. For these reasons, the damage model will be conceptually formulated but not completely developed. This model is discussed briefly in Section 7.2 which is devoted to the presentation of future research areas. Additionally, the calibration and degradation models are developed without considering the inter-arrival time of earthquakes and their potential magnitudes. The fundamental errors considered in the calibration model are: the modulus of elasticity, joint rigidities, static loading conditions, stiffness of the floor system, and input motion based on the method developed in this thesis. These fundamental errors are modified to include a dependency in time and are used in the development of the degradation model.

1.3 Thesis Organization

An overview of uncertainty methods in structural engineering is presented in Chapter 2. Uncertainty and information processing methods are reviewed. A motivation for the use of fuzzy mathematics in the development of the adaptive analysis models is provided, and the fundamentals of fuzzy mathematics is presented.

Chapter 3 presents the theoretical development of the calibration model. Solution methods based on the uncertainty analysis for both free-vibration and forced-vibration analysis are presented. The development of the fundamental errors contributing to the dynamic uncertainty of the structural model also is presented.

In addition to the uncertainty in the model and its fundamental uncertainties, the structural response is dependent also on the input motion to the structural system. Development of the input motion uncertainties as fuzzy response spectra is presented in Chapter 4. Included in this chapter is a complete explanation pertaining to the development of fuzzy spectra for the Loma Prieta earthquake and a discussion of the results.

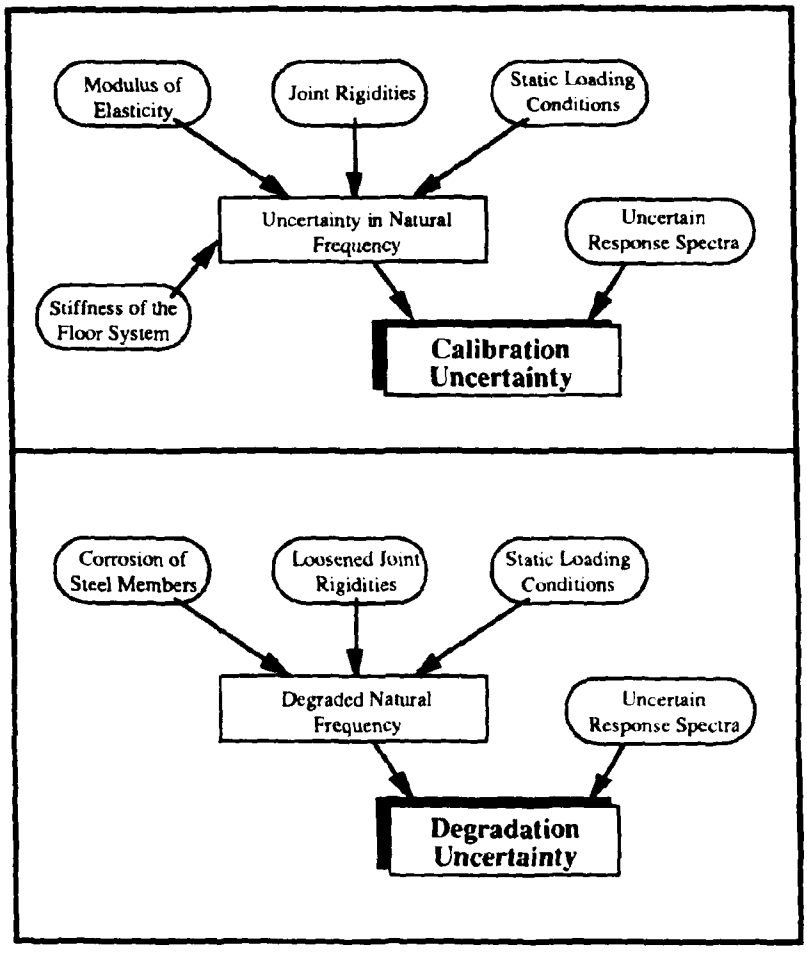

Figure 1.6: Sources of uncertainty considered in this thesis.

The proposed methodology is implemented in Chapter 5 in two illustrative examples. The first example is a two dimensional plane frame. A case study is used to validate the calibration model on the Santa Clara County Office Building which is located in San Jose, California. Quantification of the uncertainties based on fuzzy mathematics is compared to a probabilistic method demonstrating the efficiency of the proposed methodology. Monte Carlo simulation is used to simulate the dynamic response based on a probabilistic representation of the fundamental uncertainties. The probabilistic and fuzzy methods produce histograms and fuzzy sets, respectively, to represent the resulting uncertainty. The chapter concludes with a discussion comparing the two methods.

Chapter 6 presents the theoretical development of the degradation model. This chapter discusses both the solution of the dynamic equations of motion and the quantification of the fundamental errors as a function of time. Examples are presented with demonstrate the implementation of the degradation model based on initial (pre-calibrated) uncertainties and uncertainty in the rate of degradation for the structure's fundamental properties.

This work is concluded with recommendations for future work in Chapter 7.

CHAPTER 2

Uncertainty Analysis Methods

The purpose of this chapter is to present an overview of the uncertainties typically inherent in structural engineering applications. Section 2.1 contains a discussion motivating the study of uncertainty analysis techniques. Methods typically used to model uncertainties are presented in Section 2.2. Arguments towards the use of fuzzy mathematics for the approach presented in this thesis are presented in Section 2.3. The fundamentals of fuzzy mathematics are reviewed in Section 2.4, the conclusion of this chapter.

2.1 Uncertainty in Structural Engineering

Uncertainty exists in every aspect of structural engineering problems. The uncertainty inherent in such a problem can be evaluated with respect to the following aspects: (1) the analytical *model*, (2) the *loads* applied to the system (both static and dynamic), (3) the ability for the structure to *resist* the loads, and (4) the *response* of the structure due to the combination of the first three aspects.

In general, models used to analyze processes in structural engineering can be analytical, empirical, or a combination of the two. Analytical models are derived from first principles and are assumed to be deterministic. For example, the stresses within a beam can be solved relatively accurately if the analytical model truly represents the real system. However, in most cases, assumptions must be made to facilitate the solution process. These assumptions, such as the modeling of end conditions, contribute to the inexactness of the problem solution. Many analytical modeling tools, such as the finite element method, are derived based on approximations.

Empirical models are developed from historical data. Since these models are based

almost completely on past behavior, appropriate use of these models must be constrained to the same systems used in its development. However, use of other models can provide an independent assessment of the empirical model's validity. Often in engineering applications, empirical and analytical models are combined. For example, the structural response can be determined analytically, however, the representation of the dynamic input motion may be obtained from an empirical model.

Loads applied to a structural system can be divided into three general categories: dead, live, and dynamic. Representation of each of these three types of loads involve approximations where the dynamic loads are the most uncertain. Typically, (in LRFD) for the purposes of structural design, the uncertainty in the loads has been considered in terms of load factors. Thus, the loads are increased by a factor permitting the problem to be solved conservatively. Although conservative for the purposes of design, the use of such factors contribute greatly to the misrepresentation of the structural system's dynamic response.

The ability for the structural system to resist loads is based on knowledge about the material and connection properties of the structure. Information about these properties is typically determined through repeated experimentation. To compensate for the uncertainty in the resistance capability of the structure, resistance factors are used to reduce the structure's strength capacity. Although these factors are appropriate for the purposes of design, they can provide misleading values for the response of the system.

It is well acknowledged that the uncertainty which exists in each of the three aspects mentioned above contributes greatly to the inaccuracy inherent in the structural response. Therefore, models capable of handling uncertainties are needed to quantify the uncertainty in the response. In the uncertainty analysis, it is important to understand the sources of uncertainty for each of the contributing factors.

Boissonnade [Boi85] and Chiang [Chi88] have considered the uncertainty in the engineering problem to consist of the stimulus, physical entity, and response. The loads which act as a stimulus onto the structure, or physical entity, create a structural response. Figure 2.1, adapted from Boissonnade's and Chiang's works, depicts how uncertain information frequently available in the framework of an engineering

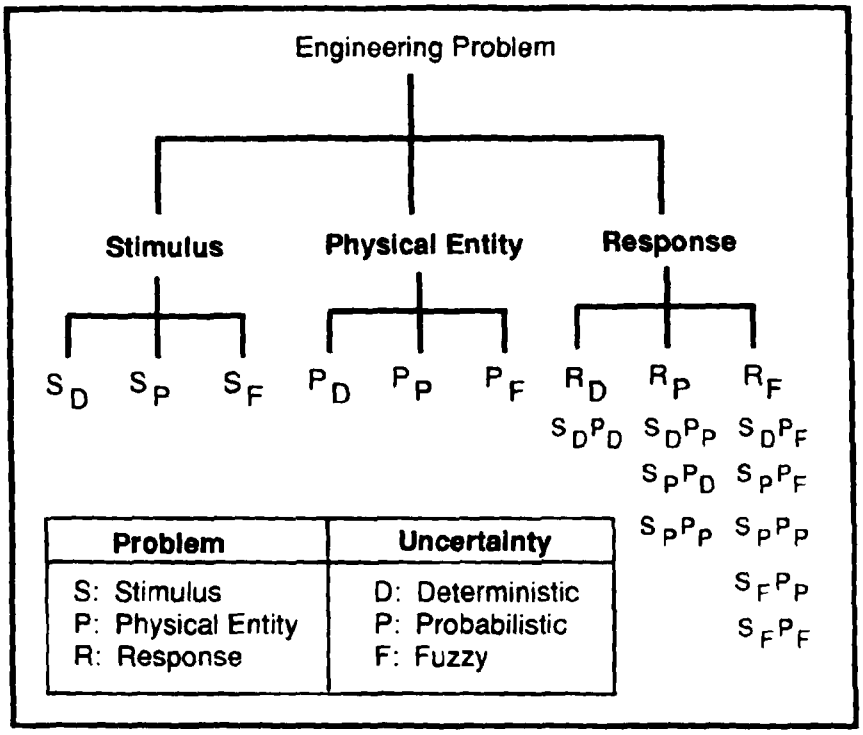

Figure 2.1: Representation of uncertainty in an engineering system (adapted from Boissonnade and Chiang).

problem can influence the resulting uncertainty. The stimulus, physical entity, and response are represented by either deterministic, probabilistic, or fuzzy models. If all of the information in the problem is deterministic, the resulting response will be deterministic. However, if the problem contains uncertain information, then appropriate models must be used to describe the uncertainty. The uncertain information can be represented by fuzzy sets, probabilities, or by ignoring them all together (a deterministic representation). For example, if the problem is dependent on parameters which can be best modeled as both deterministic and probabilistic, the response will be uncertain and, in general, best modeled probabilistically. Furthermore, if the problem is based on which are described best by both probabilistic and fuzzy models,

in addition to the deterministic values, the uncertainty in the result will be representative of fuzzy information. This presentation considers equally contributing factors of uncertainty. However, in most cases, there will be many varying contributions to the uncertainty of the stimulus. In such a case, tracking the various types of uncertainty through the problem is more difficult. Additionally, it is also important to understand the sensitivity of the result to the individual contributing uncertainties.

2.2 Methods Used to Model Uncertainties

The primary focus of this thesis pertains to the quantification of uncertainties in the application of structural dynamic problems. Therefore, deterministic systems will not be discussed further. The following is a discussion about methods used to model both probabilistic and fuzzy uncertainties. Traditionally, uncertainties in structural model parameters have been studied probabilistically using stochastic processes. Probabilistic methods will be presented first, where a tremendous amount of research has been done in this field. Only relevant information is presented to demonstrate typical probability based techniques.

2.2.1 Probabilistic Techniques

Aside from the fact that information must often be inferred from similar (or even different) circumstances or derived through modeling, and thus may be in various degrees of imperfection, many problems in engineering involve natural processes and phenomena that are inherently random; the state of such phenomena are naturally indeterminate and thus cannot be described with definiteness. - Ang & Tang (pg. 1) [AT75a]

Probabilistic methods have been widely used in engineering fields. More specifically, in the field of structural engineering, probability has been used to better understand loading conditions and to establish the reliability of structures against failure. Reliability methods have been used to develop factors of safety currently used in the engineering codes. Additionally, probability has been used to better understand and design a structure for unknown loads such as earthquakes, winds, live loads, snow loads, etc. There have been a large number of probabilistic methods applied

to structural engineering applications which consider the statistical properties of the structural system and the randomness of the loads (static and dynamic) applied to the system. Research in this area is overwhelming; consequently, the work presented here represents relevant research pertaining directly to the objectives of this thesis. The two types of methods presented, moment and simulation techniques, were originally considered as optional solution techniques for the adaptive analysis models developed through this research.

The use of first and second order moment techniques give estimations for the mean and variance of the resulting distributions for the parameter in question. The first order approximations based on a Taylor series expansion [AT75a] are shown for a function of a single random variable in Eqs. 2.1 and 2.2.

$$E(Y) \simeq g(\mu_X) \tag{2.1}$$

$$VAR(Y) \simeq VAR(X - \mu_X)\left(\frac{dg}{dX}\right)^2 \tag{2.2}$$

where,

Y = $g(X)$;
$E(Y)$ = first-order approximate mean of Y;
X = dependent variable;
μ = mean; and
VAR = variance.

Estimates for the variance of a general function requires solution of the function's derivatives with respect to each random variable. This quickly becomes computationally intensive in the case of nonlinear and matrix equations.

Liu et al. [LBM86] recognized the complexity involved with solving the most simple (a single degree-of-freedom) dynamics problem probabilistically. Their work has focused on the development of a probabilistic finite element method which considers uncertainty in the material properties only, while the mass of the system is assumed to be constant. The proposed solution is performed in the time domain and is based on implicit time integrations for unconditional stability. This success of the solution

method is demonstrated with two examples. The authors have provided a computationally efficient solution technique for the dynamic equations of motion based on uncertain parameters; however, it does not incorporate the uncertainty in the dynamic input motion and has difficulty when the method considers structural damping.

Pai and Chamis have studied the probabilistic approach to structural dynamics [Pai90, PC91] in their work at NASA Lewis. Their probabilistic models include uncertainties in primitive variables such as nodal coordinates, material stiffness, and external loads. Definition of these primitive variables requires knowledge about their distributions including type, mean, and variance. Results consist of cumulative density functions for nodal displacement, member forces, and structural frequency. Additionally, a solution is formulated to determine the ultimate load for a structural truss based on probabilistic analysis and repeated member failures.

In the 1950's and 1960's quite a bit of work was devoted to the solution of the probabilistic free vibration problem. A few examples of this work are given as reference here [CT69, HH72, HS71]. In each of the papers, the authors address different issues associated with the probabilistic solution. However, to solve for the variance of the eigenvalue problem's free vibration properties, it is necessary to solve for the derivative of the eigenvalues with respect to the random variants. Thus, for larger structural systems the solution process can become intense.

Monte Carlo simulation techniques have been a popular solution to the statistical finite element problem. These techniques require the simulation of the dependent random variables based on their individual statistical properties. The solution process is then performed deterministically based on the simulated variables. Ultimately, a distribution is obtained from the results of repeated solutions each with simulated variables. Tens of thousands (or more) solutions may be required to obtain an acceptable distribution for the resulting parameter. The number of solutions required increases based on the number random variables in the problem. Techniques have been employed (such as Latin Hypercube [AL89]) to reduce the required number of solutions. Regardless, there remains a high amount of computational intensity required for a typical multi degree-of-freedom structural dynamics problem.

Udwadia [Udw86, Udw87a, Udw87b] investigated the dynamic response of linear

systems with uncertain parameters using probability theory. Closed form expressions for the probability density functions were developed for natural frequency, percentage of critical damping, and damped natural frequency under the assumptions that only the upper and lower bounds of mass, stiffness, and damping values are available. It was shown in these studies that the stochastically modeled mean response of the system with uncertain parameters differs from the response of the system with stochastically modeled mean parameters. Furthermore, these studies were performed for single degree-of-freedom systems with deterministic dynamic loads.

Determination of structural reliability is one of the most popular applications of these probabilistic techniques. These techniques are typically computationally expensive and are used in the most critical circumstances such as the design of a nuclear power plant or aeronautical structures. Reliability of a structure against failure is determined either through the solution of the first and second order methods or simulations, both of which are computationally expensive.

Dong et al. [DCW87] investigated the propagation of uncertainties through a deterministic system using three different methodologies: interval, fuzzy, and random. The authors conclude that the selection of an uncertainty method is dependent upon the type of information available (i.e., is it random or does it contain ignorance?). Selection of an uncertainty method must be based on the intended use of the results.

2.2.2 Fuzzy Uncertainty Analysis

As the complexity of a system increases, our ability to make precise and yet significant statements about its behaviour diminishes until a threshold is reached beyond which precision and significance (or relevance) become almost mutually exclusive characteristics. - Zadeh, 1973 [Zad73]

The literature summarized above presents methods applicable for quantitatively well understood uncertainties. However, uncertainties may not always be easily measured or quantified and may be better described through the use of an expert. The expert can establish bounds on the uncertainty at various levels of confidence based on his experience. Fuzzy mathematics is capable of handling such uncertainties. In fact, fuzzy mathematics can support uncertain variables which are linguistic or numeric.

Section 2.4 presents a more detailed description of fuzzy mathematics.

A considerable amount of work has been done by Dong et al. [DW86a, DW86b, DW86c], Wong et al. [DR85], and Chiang et al. [CDW87, CDSW88] pertaining to the use of fuzzy set mathematics to model structural uncertainties. In these papers, the authors have motivated the need and application of fuzzy mathematics in the area of structural engineering. They have demonstrated the complexity of simple structural dynamic problems when solved probabilistically. Additionally, they have shown that the probabilistic solution is too descriptive of the structural response, allowing information to be inferred that may not be completely accurate.

Lamarre and Dong [LD86] used a fuzzy algorithm in the evaluation of seismic hazard. They developed a methodology for seismic hazard evaluation based on expert knowledge. Approximate reasoning is used to interpret the expert's opinion about ground shaking, soil conditions, and ground rupture for various sites. This study (although highly confined) proved to be applicable to the evaluation of seismic risk.

Fuzzy sets have been used in a number of applications in civil engineering to approximate the vagueness in linguistic terms. Shibata [Shi85] used fuzzy sets as linguistic variables to model possible human design errors. Souflis and Grivas [SG86] used fuzzy sets to establish a relationship between damage states and earthquake load. Hinkle [Hin85] used fuzzy logic to assess the damage to butt welds due to the complex and uncertain fatigue phenomena.

Shiraishi and Furuta [SF85] used fuzzy set theory to evaluate structural damage and to predict structural deterioration. Damage was evaluated using a fuzzy based multi-criteria analysis and deterioration is predicted using fuzzy logic within an expert system. In a comprehensive evaluation of structural damage, Furuta [Fur93] demonstrates his proposed method by ordering a set of bridges based on the severity of earthquake damage. Due to the high ambiguity in such a process, ordering is suggested to provide the information required in the scheduling of repair. Furuta et al. [FSFY85] use fuzzy reasoning to evaluate the potential annoyance to humans due to vibrations. The authors define fuzzy sets for linguistic variables describing levels of disturbance because of the high variability in human perception of vibrations. Fuzzy reasoning is used to interpret the level of annoyance for vibration due

to the orientation of the person and the free-vibration characteristics of the dynamic motion.

In 1985 the National Science Foundation and the School of Engineering at Purdue University sponsored a workshop pertaining to the use of fuzzy logic in civil engineering applications. This workshop [BCPY85] addressed, in part, future applications and needed work in the application of fuzzy sets to civil engineering problems. Fuzzy set theory often is the appropriate tool to use in many civil engineering problems with vague information. Additionally, there may be applications when fuzzy set theory is a valid alternate to the more rigorous and commonly used probabilistic methods.

2.3 Use of Fuzzy Mathematics for the Adaptive Analysis Models

All uncertainties, whether they are associated with inherent variability or with prediction error, may be assessed in statistical terms, and the evaluation of their significance on engineering design accomplished using concepts and methods that are embodied in the theory of probability. – Ang & Tang (pg. 11) [AT75a]

It is true that all uncertainties can be modeled with the use of probabilistic methods. In the initial development of the adaptive analysis models both probabilistic and fuzzy approaches were considered for the complete model development. The decision to use fuzzy mathematics was made based on the criteria established in Section 1.1. The purpose of this section is to provide the reader with arguments towards the election to use fuzzy mathematics. Since these arguments are made before presenting fuzzy mathematics and the adaptive models in more detail, the points illustrated here will become more evident later in this thesis.

It is possible to implement statistical methods to the adaptive analysis models by using statistical calculus (more specifically first or second order reliability methods) or by simulation methods. Each statistical method requires distributions to be defined for the fundamental uncertain variables (in statistics random variables). Application of statistical calculus becomes cumbersome when solving complex relations such as

the eigenvalue problem which must be solved numerically. Furthermore, the reliability methods produce a probability that a desired value for a higher-level parameter will be exceeded. The process must be repeated a number of times to establish a complete evaluation of the potential values the higher-level parameter may take. For the minimum amount of accuracy, simulation methods require thousands of computer runs to quantify the uncertainty for the desired higher-level parameters.

Fuzzy mathematics does not provide the rigor that comes with statistical methods. However, one of the objectives of this thesis is that the results "contain the accuracy required for the designer's decision making purposes" which, with the exception of hazard analysis, does not require the rigor provided by statistical methods. Additionally, use of fuzzy mathematics lends itself to the other objectives: (1) Both methods can be standardized for use on many structures by applying uncertainty models to the finite element representation of the structural system; (2) Fuzzy mathematics is by far a more intuitive method for the practicing engineer. Quantification of uncertainty using fuzzy mathematics requires the establishment of bounds at various levels of confidence. The practicing engineer already thinks in terms of bounding extreme responses; (3) Since the designer selects the fundamental fuzzy sets, then he is in control of the accuracy in his results. Use of probabilistic methods adds an additional level of complexity to the solution, and the practitioner may not have a complete understanding of the resulting accuracy. Furthermore, there are so many uncertainties involved in the design processes that the application of the fuzzy methods may give the practitioner a more intuitive understanding of the potential dynamic characteristics of the structure; (4) Use of fuzzy mathematics, by far, reduces the number of computations necessary. The problem is solved repetitively with different parameters, but there is no need for linear or nonlinear convolutions. Section 2.4 and Chapter 3, which follow, present a detailed explanation of the solution processes required for the dynamic equations of motion; (5) Use of the fuzzy response spectra developed in this thesis incorporates the uncertainty of the input motion to the structure into the dynamic analyses; (6) Use of the fuzzy methods also permits additional uncertainties to be considered in the analysis with minimal effort on the part of the analyst. The

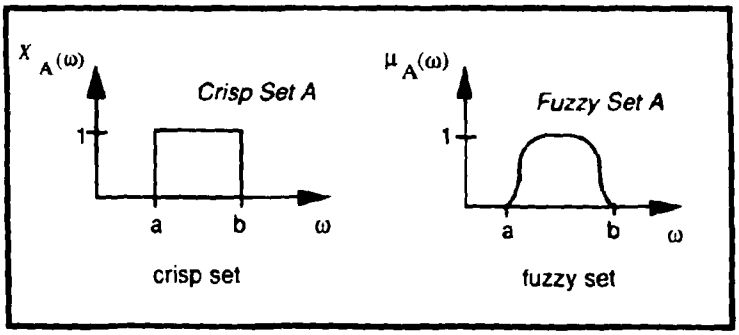

Figure 2.2: Visual comparisons of crisp and fuzzy sets.

only modifications necessary are additional solutions which consider the new uncertain parameters.

A statistician will argue the simplicity of the use of probability in such a problem, and their arguments may be valid; however, use of probability no longer makes the method straight-forward and easily applied in practice. Additionally, if the uncertainties do not warrant a higher-level of accuracy, a method which requires fewer computations is more preferable. Use of fuzzy mathematics gives us a different approach to the types of problems which have been traditionally solved probabilistically.

2.4 Review of Fuzzy Mathematics

This section provides the reader with the theoretical knowledge of fuzzy mathematics used in the development of this thesis. Much of the information presented here is fundamental knowledge within the field of fuzzy mathematics. Several references [TAS92, DP88, KF88, Sch84, Zim91, Don86] were used in the preparation of this section.

Parameter uncertainty in traditional interval analysis requires the expert (engineer) to provide absolute parametric bounds. The characteristic function, $X_A(\omega)$, depicted in Figure 2.2, describes the interval size. In traditional interval analysis the characteristic function defines a crisp set, meaning the interval bounds are sharp, not

incorporating any additional parametric information. In the following calculations all parametric values, regardless of where they lie in the crisp interval, are treated the same. Solutions may result in a larger interval, containing very little relevant information. In many engineering applications, although the engineer may not have enough parametric information to produce a probability density function for use in probabilistic methods, the engineer may be able to provide information about the likelihood of the parameter falling within particular bounds. Fuzzy mathematical modeling is designed to consider such additional information.

In fuzzy mathematics, the parameter (frequency, ω, in this example) is represented as a fuzzy set with the use of a membership function, $\mu_{\mathcal{F}}(\omega)$. The membership function describes the shape of the fuzzy set, shown in Figure 2.2, and represents the likelihood of the parameter falling within specific intervals. The membership function of Equation 2.3,

$$\mu_{\mathcal{F}}(\omega) \in [0, 1] \tag{2.3}$$

where,

μ = the membership function;
$\mathcal{F}$ = the frequency fuzzy set; and
ω = natural circular frequency (uncertain parameter).

was first proposed by Zadeh [Zad65] and must be within the bounds 0 and 1. The alpha-cut, denoted by $\mathcal{F}_\alpha$, is an interval at a level of confidence α which must be between 0 and 1.

In comparing the crisp and fuzzy sets in Figure 2.2 note that the crisp set has abrupt boundaries while the fuzzy set has smoother boundaries representing the variable interval bounds. When a parameter is described as being "about" or "around" a specific value it is useful to describe its behavior with a fuzzy set utilizing variable interval bounds.

As an example, the first fundamental frequency of a structure may be described as a trapezoidal fuzzy set with the membership function in Equation 2.4.

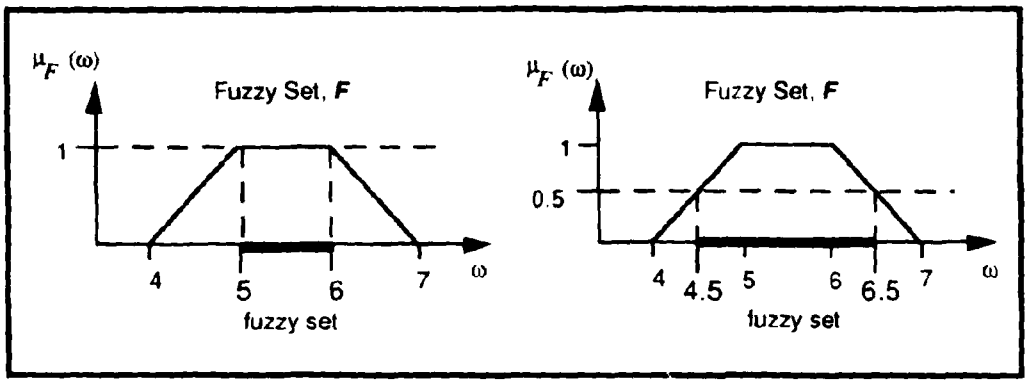

Figure 2.3: Trapezoidal fuzzy set and alpha-cuts.

$$\mu = \begin{cases} \omega - 4 & 4 \leq \omega \leq 5 \\ 1 & 5 \leq \omega \leq 6 \\ -\omega + 7 & 6 \leq \omega \leq 7 \\ 0 & \omega < 4 \text{ and } \omega > 7 \end{cases} \tag{2.4}$$

The graphical representation of the membership function is shown in Figure 2.3. An alternative for mathematically representing the fuzzy set for the fundamental natural frequency is shown in Eq 2.5.

$$\mathcal{F} = \sum_{i=1}^{n} = \frac{\mu_{\mathcal{F}}(\omega_i)}{\omega_i} = \frac{0.1}{4.1} + \frac{0.5}{4.5} + \frac{1.0}{5.0} + \frac{1.0}{6.0} + \frac{0.5}{6.5} + \frac{0.1}{6.9} \tag{2.5}$$

where,

$\mathcal{F}$ = the fuzzy set representing fundamental frequency;

$\mu_{\mathcal{F}}$ = level of membership; and

ω_i = value for the natural frequency.

Although the membership function shown here is symmetric, unsymmetric functions are also possible.

The α-cut represents parametric confidence levels. An α-cut defines a crisp set of

elements which belong to the fuzzy set for the fundamental natural frequency, $\mathcal{F}$, at a membership level α as depicted in Eq. 2.6.

$$\mathcal{F}_\alpha = \{\omega \in \Omega | \mu_{\mathcal{F}}(\omega) \geq \alpha\} \tag{2.6}$$

where,

$\mathcal{F}_\alpha$ = the crisp set of values, ω, from the fuzzy set $\mathcal{F}$ at membership level α.

An α-cut level of 1 denotes a high level of confidence on the part of the expert where, in the case of Fig. 2.3, the parameter will most likely fall within the interval $\omega \in [5,6]$. An α-cut level of 0.5 represents the interval $\omega \in [4.5,6.5]$ as possible frequency values for a proportionally lower level of confidence. The lowest possible level of membership corresponds to an α-cut level of 0. Based on Eq. 2.6 the resulting crisp set contains three intervals of values for the parameter, ω. The first intervals are all values for $\alpha > 0$, corresponding to $\omega \in [4,7]$. Since the α-cut includes values for ω with a level of membership equal to and greater than α, the set contains two additional intervals, $(-\infty,4]$ and $[7,+\infty)$. The support (shown in Eq. 2.7) of $\mathcal{F}$ is a crisp set, $\mathcal{F}_{\alpha=0^+}$, which contains all values of ω in the fuzzy set, $\mathcal{F}$.

$$\mathcal{F}_{0^+} = \{\omega \in \Omega | \mu_{\mathcal{F}}(\omega) > 0\} \tag{2.7}$$

where,

$\mathcal{F}_{0^+}$ = a crisp set denoting all values of ω, with membership greater than 0.

Fuzzy sets do not need to be trapezoidal shapes as denoted in Fig. 2.3. In fact, a crisp set is a specialized fuzzy set where the bounds defined at α-cut 1 and α-cut 0^+ are the same. The shape of a fuzzy set denotes the relationship of the confidence bounds at the different levels of membership. For example, in the case of a triangular or rectangular fuzzy set the rate at which the bounds increase with respect to membership is constant. In other words, the slope of the line connecting the lower bound of α-cut 1 and the lower bound of α-cut 0^+ is constant. Similarly, the slope of the line connecting the upper bounds is constant also, although the slopes of the upper and

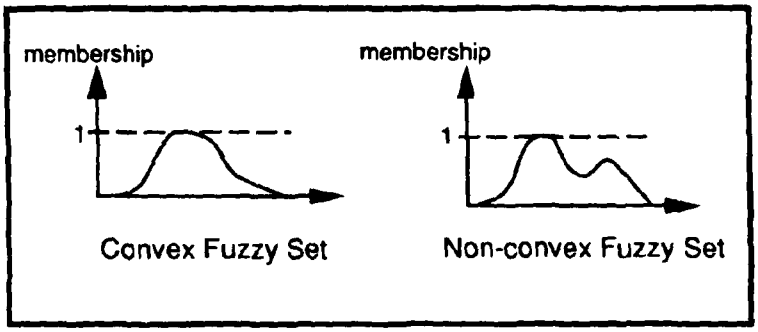

Figure 2.4: Normal convex and nonconvex fuzzy sets.

lower bounds need not be the same. It is important to consider that the lowest level of membership in fuzzy logic represents the most extreme (but realistically) possible values for the fuzzy parameter. Therefore, it is feasible that a fuzzy set represents much higher uncertainty for the lowest levels of membership. This is especially the case when there are a number of factors contributing to the parameter's uncertainty. Figure 2.4 gives examples of two different types of fuzzy sets.

A fuzzy set is *normal* only if the highest level of membership in the set is one. The fuzzy set on the left in Fig. 2.4 is a normal convex fuzzy set, while the set on the right is a normal nonconvex fuzzy set. A fuzzy set is *convex* if the bounds provided by an α-cut at membership level x are contained completely within the bounds given by the α-cut at membership level y where $x > y$. In other words, there must be a single crisp set defined by each α-cut. This states that the crisp set defined by an α-cut will always be a subset of the crisp set defined by an α-cut at a lower level of membership. For example, the extreme bounds (bounds at a membership level slightly greater than 0, $\alpha = 0^+$) for the fundamental frequency of a structure must fully contain the bounds established by the most possible occurrence. This thesis will be confined to the use of convex fuzzy sets, unless otherwise specified.

Typical set operations such as intersection, union, and complement can be performed on the membership functions which define fuzzy sets. Figure 2.5 depicts the resulting fuzzy sets from the intersection, union, and complement of two fuzzy sets.

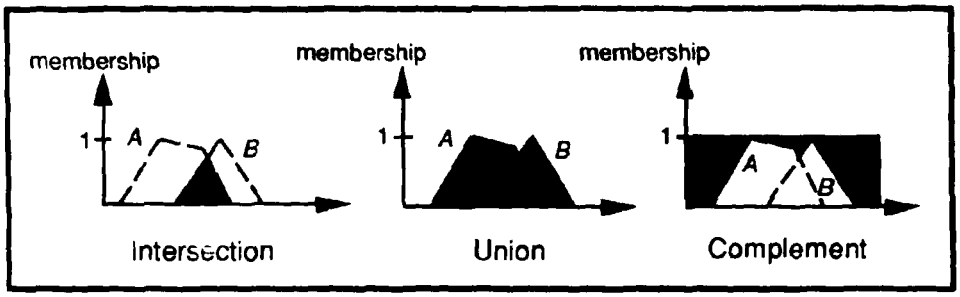

Figure 2.5: Intersection, Union, and Complement of two fuzzy sets, A & B.

The intersection (the logical "and") of two fuzzy sets A and B is a fuzzy set C of values which are in both fuzzy sets A and B. Comparatively, the union (the logical "or") of two fuzzy sets A and B is a fuzzy set D which contains all the values in each of the two fuzzy sets. The complement of two fuzzy sets A and B is a fuzzy set E which contains all values not contained in fuzzy set A. This is analogous to ordinary set theory. However, in addition to the values within the fuzzy sets, it is also important to consider the level of membership for the intersection, union and complement operations. Equations. 2.8, 2.9, and 2.10 define the resulting membership functions for the operations described in Fig. 2.5.

Intersection:

$$\mu_C(x) = \mu_{A \cap B}(x) = min\left\{\mu_A(x), \mu_B(x)\right\}, x \in X \tag{2.8}$$

Union:

$$\mu_D(x) = \mu_{A \cup B}(x) = max\left\{\mu_A(x), \mu_B(x)\right\}, x \in X \tag{2.9}$$

Complement:

$$\mu_E(x) = 1 - max\left\{\mu_A(x), \mu_B(x)\right\}, x \in X \tag{2.10}$$

where,

μ_A = the membership function describing fuzzy set A; and

x = the values contained by the fuzzy set.

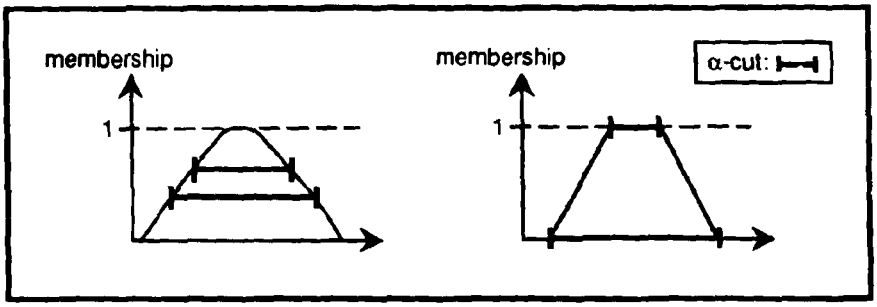

Figure 2.6: Illustration of the Resolution Principle.

Membership functions can be developed based on expert opinion or quantitative data. Whether a fuzzy set is developed based on qualitative or quantitative data, it is necessary to enforce the assignment of membership levels consistently. This is of utmost importance when many fuzzy sets are being used in the same application. The crisp set defined by α-cut 1 bounds the most possible occurrences for the fuzzy set. The crisp set defined at level of membership slightly greater than 0 corresponds to $\alpha = 0^+$ and bounds all possible values (which are realistic) for the fuzzy set. In a similar manner, the crisp set defined by α-cut 0.5 bounds values which are possible proportionately to membership levels 0^+ and 1. This logic must be implemented when using either qualitative or quantitative data in the definition of a fuzzy set.

The resolution principle uses α-cuts to define a membership function. Complete definition of the membership function using the resolution principle requires an infinite number of α-cuts. However, the membership of a fuzzy set can be defined with a finite number of α-cuts. Use of the resolution principle is illustrated in Figure 2.6 in two examples. In the first case, the membership function is defined at two membership levels between 0 and 1. The second case is a less ambiguous result because the two levels of membership used to define the fuzzy set are 0^+ and 1. If more than two levels of membership are used then it is possible to define the curvature of the membership function in more detail.

2.4.1 The Vertex Method

Traditional mathematical operations can be performed on membership functions through function mapping. There are several techniques used for fuzzy and interval mathematics, the vertex method, developed by Dong et al. [DS87, DW87], is used in the adaptive analysis models and is the only method discussed in detail in this thesis. Typical mapping procedures will involve a function of several uncertain parameters which may or may not be associated with membership functions. The objective of function mapping is to produce a fuzzy set or membership function for the resulting parameter. Zadeh [Zad65] first introduced the Extension Principle, which is used for mapping functions and can be equivalent to a nonlinear programming problem [BK77]. The vertex method applies traditional function mapping to uncertain fuzzy parameters while allowing the analysis to be performed deterministically. The mapping procedure is iterative and is repeated at different α-cut values. The resulting membership function resolution is related directly to the number of α-cuts used in the mapping. Typically, mapping is performed at α-cut values of 1.0, 0.5, and 0.0^+. If higher resolution is desired and the integrity of the membership function exists, additional α-cuts may be used.

The number of iterations necessary for each α-cut is 2^n, where n is the number of fuzzy parameters use in the mapping. The function is solved 2^n times representing all possible parametric combinations based on the intervals bounds at an α-cut level. The best way to explain the vertex method is by a numerical example. The following example demonstrates the use of the vertex method to obtain the fuzzy set for γ where:

$$\gamma = \frac{\zeta + \eta}{2\zeta} \tag{2.11}$$

The fundamental fuzzy sets for ζ and η are defined at two α-cut levels and are presented in Table 2.1. Fuzzy sets throughout this thesis will be defined in the same manner in tables. The values used for ζ and η and the resulting γ values are provided in Table 2.2. The last column in Table 2.2 distinguishes whether or not the resulting

Table 2.1: Fuzzy parameters ζ and η.

α-cut	lower Bound ζ	upper Bound ζ	lower Bound η	upper Bound η
0.0^+	2.0	6.0	12.0	20.0
1.0	3.0	5.0	18.0	18.0

Table 2.2: Values for ζ and η used in the vertex method.

α-cut	ζ	η	γ	Resulting Bound
0.0^+	2.0	12.0	3.5	Not a Bound
0.0^+	2.0	20.0	5.5	Upper
0.0^+	6.0	12.0	1.5	Lower
0.0^+	6.0	20.0	2.2	Not a Bound
0.5	2.5	15.0	3.5	Not a Bound
0.5	2.5	19.0	4.3	Upper
0.5	5.5	15.0	1.9	Lower
0.5	5.5	19.0	2.2	Not a Bound
1.0	3.0	18.0	3.5	Upper
1.0	5.0	18.0	2.3	Lower

γ values is a bound in the fuzzy set defining γ. The resulting fuzzy set for γ is given in Table 2.3. Using the vertex method at three α-cut levels ($\alpha = 0.0^+, 0.5, \text{and} 1.0$), the function which defines γ is performed 10 times. Since γ is a function of two parameters, α-cuts 0.0^+ and 0.5 each require the function to be solved 4 times. The function γ only needs to be solved twice at α-cut 1 because η is a triangular fuzzy set.

Table 2.3: Resulting fuzzy number γ.

α-cut	lower Bound γ	upper Bound γ
0.0^+	1.5	5.5
0.5	1.9	4.3
1.0	2.3	3.5

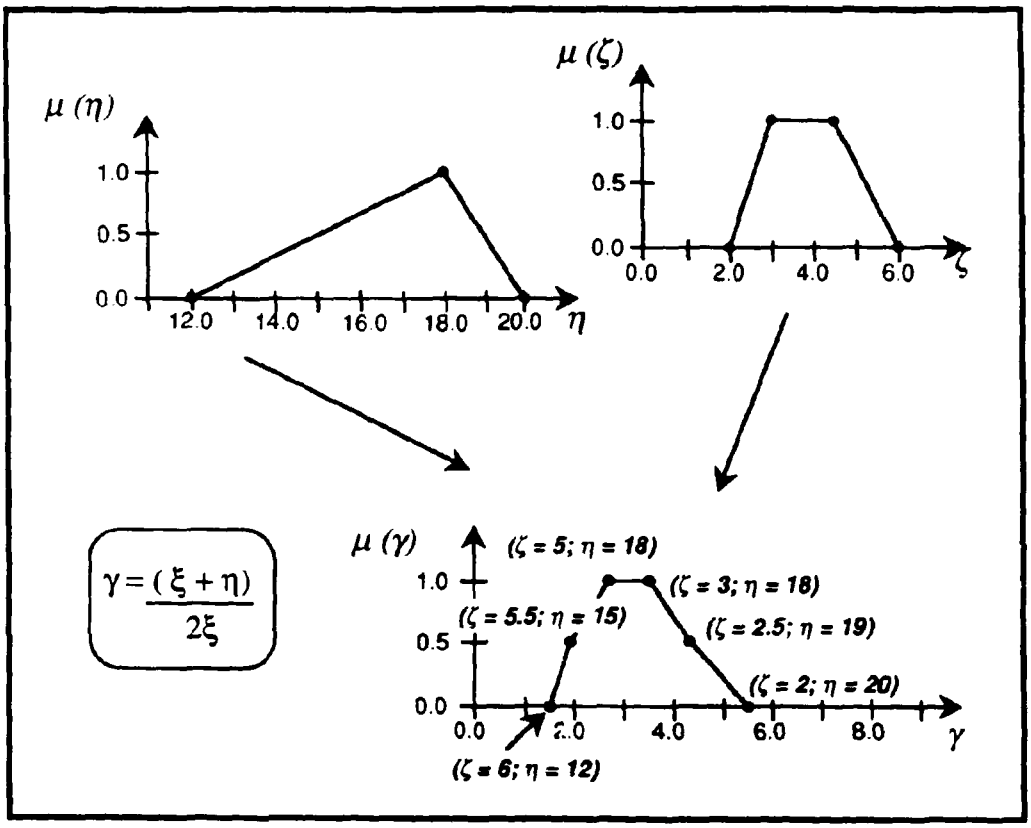

Figure 2.7: Schematic Representation of the Vertex Method.

The results from the 10 solutions are then compared to produce the resulting interval for each α-cut level. The minimum and maximum solutions will be the resulting limits for the interval at the corresponding α-cut. In the case of a nonlinear mapping function, an additional iteration is calculated at the point of extremity. Use of the vertex method is confined to convex fuzzy sets. The vertex method is then repeated at the remaining α-cuts. Realizing that the vertex method is iterative, almost to the point of redundancy, this method is much more efficient than using the alternative method of nonlinear programming. Further explanation of the vertex method can be found in the reference [DS87]. An exhaustive solution using the vertex method, such as the one shown here, may not always be necessary. However, omitting solutions from the application of the method must be done very carefully and requires a thorough understanding of the behavior of the mapping function.

CHAPTER 3

Formulation of the Calibration Model

This chapter contains a detailed presentation of the calibration model which is the first of the three models considering dynamic behavior during the lifespan of a structure. Development of the calibration model requires thorough consideration of the dynamic analysis techniques as well as the sources of uncertainty contributing to the modeling errors. Section 3.1, which follows, presents the formulation of the dynamic equations used in the modeling of calibration errors. The fuzzy representation of the calibration model is presented in Section 3.2. Careful consideration must be made in the establishment of the fundamental errors contributing to the modeling error. Section 3.3 gives a presentation of the development of fundamental uncertainties. Finally, an advantage of the calibration model is its generality and its ability to be applied to almost any structural system, where these aspects are discussed in detail in Section 3.4.

3.1 Dynamic Formulation for the Calibration Model

The calibration model estimates the modeling error that occurs due to the approximations and assumptions inherent in a dynamic finite element model. The parameters considered for calibration are the structural modal properties (natural frequencies, dynamic frequency ratios, and maximum structural response) which are used to calibrate the structural response using modal superposition analysis. The analysis used to establish the calibration model is based on the multi degree-of-freedom (MDOF) equation of motion. The equation of motion governing a linear N degree-of-freedom system takes the form:

$$\mathbf{M}\ddot{\mathbf{v}} + \mathbf{C}\dot{\mathbf{v}} + \mathbf{K}\mathbf{v} = \mathbf{F}(t) \tag{3.1}$$

where,

$\mathbf{M}$ = system (NxN) mass matrix;
$\mathbf{C}$ = system (NxN) damping matrix;
$\mathbf{K}$ = system (NxN) stiffness matrix;
$\mathbf{v}$ = (Nx1) vector containing system displacement (the 1st and 2nd time derivatives denote system velocity and acceleration, respectively); and
$\mathbf{F}(t)$ = (Nx1) vector containing the time dependent forcing function acting on the structure.

The natural frequencies and mode shapes are found by solving the undamped free vibration problem corresponding to the eigenproblem:

$$\omega_n^2 \mathbf{M}\phi_n = \mathbf{K}\phi_n \tag{3.2}$$

where,

ϕ_n = is the nth eigenvector corresponding to the nth system mode shape; and
ω_n = is the ith natural frequency.

Taking advantage of the eigenvectors' orthogonality and assuming proportional damping, Eq. 3.1 can be uncoupled using the eigenvectors found in Eq. 3.2 into a set of N single degree-of-freedom (SDOF) equations. The resulting SDOF equations of motion take the form:

$$\ddot{y}_n + 2\xi_n\omega_n\dot{y}_n + \omega_n^2 y_n = \frac{F_n^*}{M_n^*} \tag{3.3}$$

where,

y = the modal coordinate (or time dependent response);
ξ = the modal critical damping factor;
M^* = the modal mass term, ($\mathbf{\Phi}^T\mathbf{M}\mathbf{\Phi}$), where $\mathbf{\Phi}$ is the (Nxm) modal matrix containing m mode shape vectors, ϕ;
F^* = the modal forcing function, $\mathbf{\Phi}^T F(t)$; and
n = the subscript indicating modal response of the nth mode.

In the calibration model, the solution for the modal coordinate, y_n, in Eq. 3.3 is obtained using fuzzy site-dependent response spectra which are developed in this thesis. Given the frequency and damping properties for an SDOF system, the response spectrum gives the maximum values for the system response. Further explanation of the fuzzy spectra is given in Chapter 4. The results are applicable for the excitation conditions for which the spectrum was developed. The modes are then superimposed to obtain an estimate for the maximum structural response. Use of a response spectrum in modal analysis gives the maximum response for each mode. Therefore, a superposition method which simply sums the maximum modal participation to obtain the maximum response for the structural system is highly conservative because it assumes that the maximum response for each mode will occur at precisely the same time. In reality, the maximum response of one mode will not coincide with the maximum response of the other excited modes. The method of superposition selected for use in this application is SRSS (Square Root of the Sum of Squares) as shown in Eq. 3.4.

$$|\mathbf{V_{max}}| = \sqrt{\sum_{n=1}^{m} (\mathcal{L}_n \phi_n S_v(n))^2} \tag{3.4}$$

where,

$\mathcal{L}_n$ = the earthquake participation factor for mode n where $\mathcal{L}_n = \phi_n \mathbf{M}\{1\}$;

$S_v(n)$ = the maximum velocity obtained from a velocity response spectrum;

m = the number of modes superimposed; and

$\mathbf{V_{max}}$ = the maximum velocity for the structure.

Although SRSS is used here, there are other techniques which can be used in the response spectrum method. These techniques also can be used in the calibration model. For example, in the case of closely spaced modes a solution using CQC (Complete Quadratic Combination) [DK79, WDKB81] may be more appropriate. A solution using CQC is similar to SRSS except two modes are considered in each term of the summation as shown in Eqn. 3.5.

$$|\mathbf{V}_{\max}| = \sqrt{\sum_{i=1}^{m}\sum_{j=1}^{m} \mathcal{L}_i \mathcal{L}_j \phi_i \phi_j S_v(i) S_v(j) \rho_{ij}} \tag{3.5}$$

where,

ρ_{ij} = factor representing the coupling between two modes i and j. For modes with equal damping $\rho_{ij} = \frac{8\zeta^2(1+r)r^{1.5}}{(1-r^2)^2+4\zeta^2 r(1+r)^2}$ where, $r = \frac{\omega_i}{\omega_j}$ for $\omega_j > \omega_i$.

Implementation of CQC with the vertex method is possible; however, it is more complicated due to the combination of the additional variables used in the formulation. Therefore, for this application SRSS is used to illustrate the procedure for the superposition of modal responses.

The frequency ratio is defined by the ratio of the forcing frequencies to the natural frequency for each mode n and is denoted by β_n. A β_n value equal to 1.0 indicates the possibility of a resonance condition for a mode and is to be avoided. When the β_n is close to or equal to 1.0, it is necessary to verify that there is enough damping by examining the dynamic amplification factor for β_n. This is illustrated in Figure 3.1 which shows the graphical relationship of the dynamic amplification factor with respect to frequency ratio, β, and modal damping, ξ. Each line in the figure represents a different amount of damping in the system. There are 11 values of damping where the line with the lowest values for D is obtained from $\xi = 1.0$. The highest values of D occur when there is no damping ($\xi = 0.0$) in the system. The intermediate lines represent values of ξ incremented by 0.1.

$$D_n = \left[\left(1-\beta_n^2\right)^2 + (2\beta_n\xi_n)^2\right]^{-\frac{1}{2}} \tag{3.6}$$

where,

D_n = the dynamic amplification factor for mode n; and

ξ_n = the model damping factor for mode n.

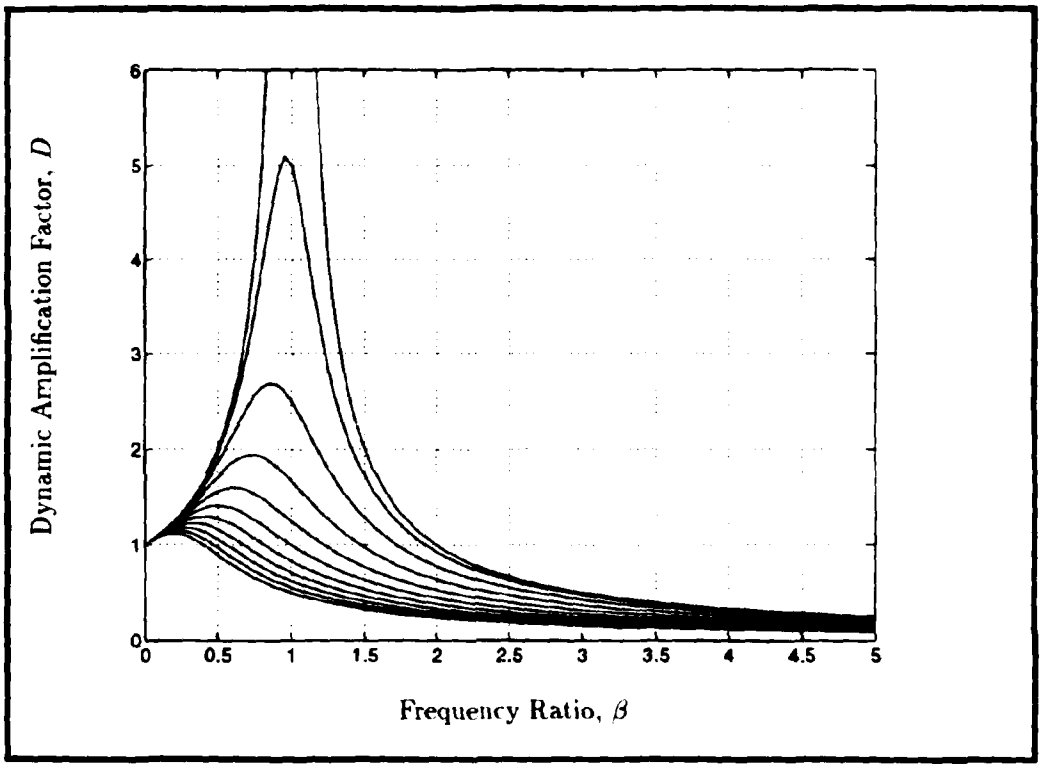

Figure 3.1: Dynamic amplification factor as a function of ξ and β.

The equations presented here give deterministic predictions for the dynamic response of the structure. Calibration error, the difference between the analytical prediction found using the structural model and the experimental measurement taken from the as-built structure, typically has been addressed using system identification techniques. However, these system identification techniques have relied on the use of measured response values to quantify deficiencies in the analytical model. The majority of system identification procedures can be computationally intensive and can suffer from significant drawbacks such as dependence on a good initial analytical model and failure to achieve a unique solution. It has been proven through the use of system identification techniques that dynamic parameters (modal frequencies and shapes) of the as-built structure can differ by 50% from the finite element representation of the structure [TA88]. In addition, because experimental data from the constructed system is required for the analysis, identification techniques cannot be used at the time that they are most needed, i. e., during the design of the system.

The equations presented in this chapter govern the dynamic analysis in the calibration model. Since the uncertainties in the structural model are represented as fuzzy sets, these dynamic equations are solved using the fuzzy (rather than deterministic) parameters. The vertex method allows the dynamic equations to be solved deterministically a number of times based on the fuzzy parameters. Section 3.2 contains the complete development of the calibration model based on fuzzy mathematics.

3.2 Fuzzy Representation of the Calibration Model

Through the use of fuzzy mathematics, bounds are established on the structural parameters found from the original model. Information concerning the a priori knowledge of site conditions, structural design, etc. are used to develop a quantitative basis for determining the potential inaccuracies in the initial pre-calibrated model and to develop the fuzzy set for the structural parameters. A membership function is found for each structural parameter. For the sake of illustration, structural natural frequency is the parameter used for the development of the following adaptive equations.

For natural frequency, the equation governing parametric uncertainty takes the form:

$$\mathcal{F}_\alpha^c = \{[a,b] | a = \omega_o - \mathcal{E}_{cal}^L(\alpha); b = \omega_o + \mathcal{E}_{cal}^U(\alpha)\} \tag{3.7}$$

where,

$\mathcal{F}_\alpha^c$ = uncertainty in calibrated frequency at a membership level, α;

ω_o = original uncalibrated natural frequency based on a deterministic calculation, which is, therefore, constant for all α-cuts;

$\mathcal{E}_{cal}^U$ = calibration error for a membership level equal to α which increases the initial estimate, ω_o;

$\mathcal{E}_{cal}^L$ = calibration error for a membership level equal to α which decreases the initial estimate, ω_o; and

a, b = lower and upper bounds, respectively, for eachα-cut.

Equation 3.7 translates the deterministic value, ω_o, to α-cuts, $\mathcal{F}_\alpha^c$, which represent the calibrated natural frequency. The fuzzyness in the calibrated natural frequency represents the range of possible values for the natural frequency. After the structure has been constructed and a system identification performed, it is possible to reduce the initial uncertainty to include only the uncertainty inherent in the system identification procedure. However, since this calibration procedure is performed before construction, the uncertainty in the actual value for the natural frequency also must include the unknowns in the analytical model for the structural system.

Figure 3.2 shows a possible fuzzy set representing natural frequency for the calibration model. The uncertainty in the initial estimate ω_o is represented with upper and lower bounds for the error, $\mathcal{E}_{cal}$. In theory, an infinite number of estimates for the calibration error, $\mathcal{E}_{cal}$, defines a smooth membership function for the fuzzy set. Since it is virtually impossible to obtain an infinite number of estimates, the fuzzy set will be defined using the resolution principle with errors at membership levels 0^+ and 1. Implementing the vertex method with membership functions defining the parametric uncertainties, it is possible to obtain values for the calibration error at the membership levels of interest.

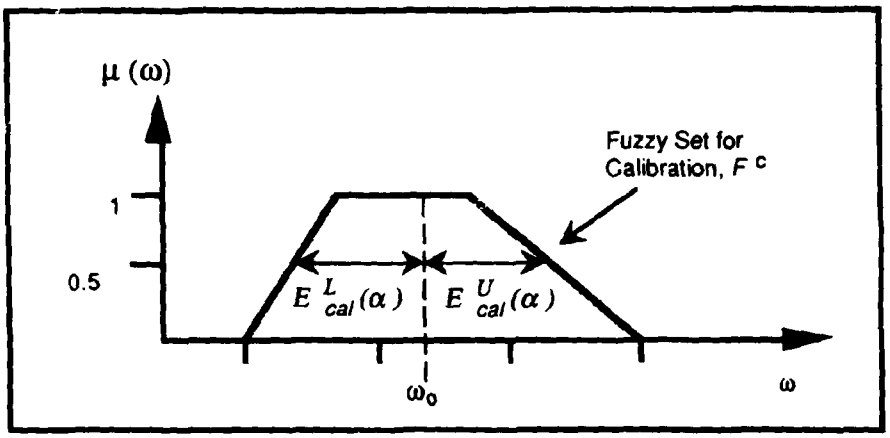

Figure 3.2: Fuzzy set for frequency used in calibration model.

The amount of uncertainty in the result is based directly on the amount of uncertainty in the contributing factors. As shown in Figure 3.3, uncertain fundamental parameters are combined using an eigensolution coupled with the vertex method to solve for fuzzy sets for the natural frequency of the analytical structural model. Therefore, it is of vital importance to develop membership functions for the fundamental parameters based on the best information available to the analyst. This is addressed in more detail in Section 3.3.

Structural response is dependent on both the dynamic characteristics inherent to the building and the characteristics of the applied load. The dynamic characteristics (modal properties and damping capacity) of a building are dependent on the properties of its structural and non-structural elements and, once determined (either by detailed dynamic analysis or system identification), can be assumed to remain unchanged through a short duration of the structure's lifespan. The applied load to the structure is the time history created by the earthquake and is impossible to predict due to the random nature of earthquakes. The ultimate error in the structural response is due to the approximations inherent in the models used to predict the structure's dynamic characteristics and to represent the excitation acting on the structure. The

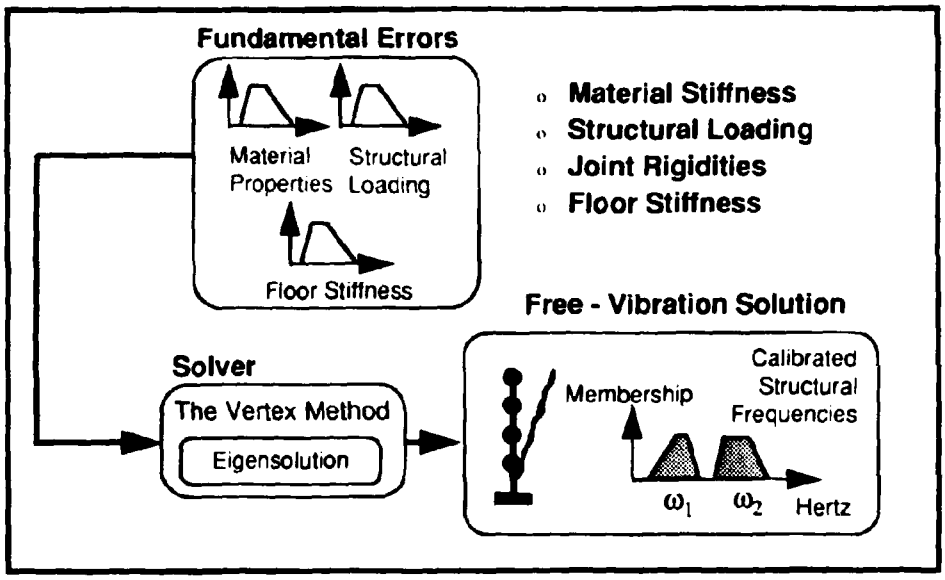

Figure 3.3: Fundamental parametric uncertainty in the calibration model.

error associated with the prediction of the excitation forces is quantified through the formulation of the fuzzy response spectra is given in Chapter 4.

To illustrate the solution of the dynamic equations with fuzzy parameters the natural frequency is obtained for the axial vibrations of the cantilevered beam shown in Figure 3.4. The distributed mass, m, and the stiffness for the spring, κ, at support B for the beam are fuzzy quantities while the other properties for the beam are assumed to be deterministic. Values for the beam's deterministic properties are given in the figure. Table 3.1 gives the values for the fuzzy parameters. These fuzzy parameters may be interpreted as a distributed mass close to 10 and a spring stiffness about equal to the axial stiffness of this continuous system is solved in closed-form [Hum90] based on elementary beam theory assumptions and is given in Eq. 3.8.

$$\omega = \frac{2.03\kappa}{EA}\sqrt{\frac{EA}{m}} \tag{3.8}$$

where,

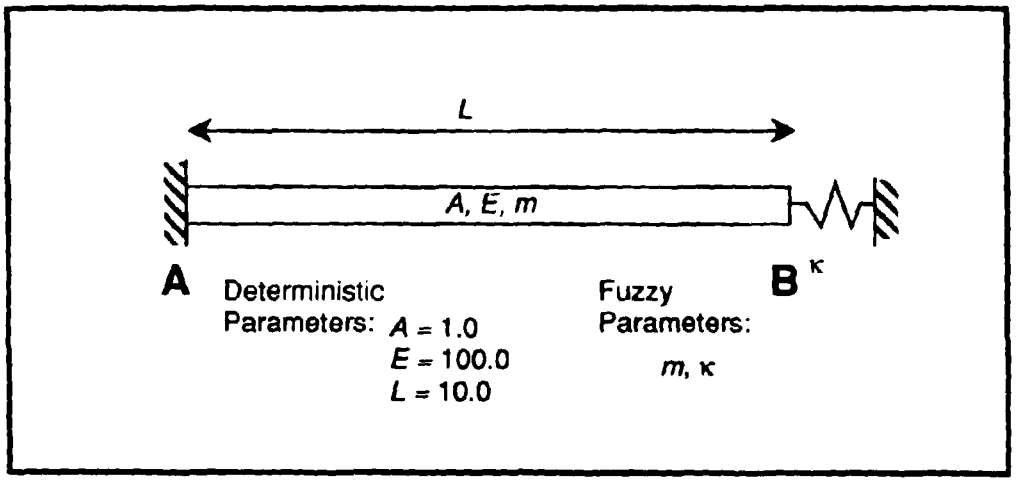

Figure 3.4: Cantilevered beam with a linear spring at support B.

ω = fundamental natural circular frequency (fuzzy);
E = modulus of elasticity for the beam (deterministic);
A = beam's cross-sectional area (deterministic);
m = distributed mass (fuzzy);
κ = linear spring stiffness, where $\kappa = \frac{\gamma EA}{L}$ and L is the beam length; and
γ = dimensionless parameter (fuzzy) used to scale the spring stiffness.

In this example, the vertex method is applied to levels of membership at 0^+ and 1. Since the fundamental fuzzy sets in this example are triangular, one solution is required for membership level 1. An exhaustive implementation of the vertex method requires 4 solutions at membership level 0^+. The natural frequency is highest when the mass is low and the stiffness multiplier is high. Similarly, the natural frequency is lowest when the mass is high and the stiffness multiplier is low. Therefore, the solution at membership level 0^+ can be obtained by performing 2 solutions. Table 3.2 gives the values for the two fuzzy parameters and the frequency obtained from each solution. The extreme values for the fundamental frequency at each level of membership are used to define the fundamental frequency fuzzy set.

Table 3.1: Alpha-cut bounds for the mass and spring stiffness triangular fuzzy sets.

α-cut	**lower bound**	**upper bound**	**lower bound**	**upper bound**
	m, slugs/ft		γ	
1.0	10	10	1.0	1.0
0.0^+	8	14	0.6	1.2

Table 3.2: Parametric values for each solution and the corresponding fundamental frequency.

α-cut	m	γ	Fundamental Frequency	
	slugs/ft		Hz	Bound
1.0	10	1.0	0.64	upper & lower
0.0^+	8	0.6	0.43	none
0.0^+	8	1.2	0.86	upper
0.0^+	14	0.6	0.65	none
0.0^+	14	1.2	0.32	lower

3.3 Quantification of Fundamental Uncertainties for the Free-Vibration Problem

In the calibration model, fundamental fuzzy sets representing uncertainty in structural stiffness and mass values are used in conjunction with the eigenvalue problem of Eq. 3.2 to develop a membership function representing ω. Using the fuzzy set for ω and an additional fuzzy set representing uncertainty in forcing frequency (Ω) defined in Chapter 4, a membership function is developed for β. The vertex method is used in conjunction with solving Eq. 3.3 to determine a membership function for y_n. These modal responses are superimposed using the SRSS in Eq. 3.4 to obtain the higher level fuzzy set for the total maximum building response, **V**max. This section discusses the procedure used to determine the membership functions for the modal properties and the structural response.

There are two types of fundamental fuzzy sets used in the calibration model: normal crisp and normal trapezoidal. The crisp sets are developed when there is a significant lack of knowledge about the parameter's behavior at various levels of confidence where the same extreme parametric values establish the same interval at α-cuts 0^+ and 1. To develop the normal trapezoidal fuzzy set, it is necessary to define two intervals of confidence. This study defines intervals at α-cut 0^+ and α-cut 1, where the interval at α-cut 0^+ defines the most possible values of the parameter and the interval at α-cut 1 defines extreme (but realistically possible) values of the parameter.

3.3.1 Natural Frequency

The natural frequencies of a structural system are found through the solution of the undamped, free vibration eigenvalue problem given in Eq. 3.2. It is assumed that uncertainties inherent in the natural frequencies are due to uncertainties associated with modeling the system stiffness and inaccurate representation of design loads. Uncertainty in the stiffness matrix is a function of uncertainty in the material properties (flexural and axial rigidity) and inaccurate representation of joint rigidities (fixed vs. pinned connections). The skeletal mass of the structure is assumed to be constant for

the purposes of this analysis; however, the uncertainty in design loads (weight of floor, partitions, scaffolding, etc.) is considered. An additional type of uncertainty associated with the finite element model is due to discretization error where exact natural modes and frequencies are obtained only as the number of elements representing the structural system approaches infinity.

As discussed earlier, fundamental membership functions are developed to represent the uncertainty in stiffness, mass, and finite element modeling and the vertex method is used to combine these membership functions into a higher level fuzzy set for the natural frequencies. The result is a membership function which describes the complete behavior of the fundamental frequency due to the contributing errors.

The quantified errors for the free-vibration analysis combined with the quantified error associated with the input motion to the structure are used to determine the resulting error in structural response. This section presents the development of the potential fundamental errors inherent in vibration analysis of steel frame type systems.

Fundamental membership functions, denoting fundamental errors, are developed to represent the uncertainty in stiffness and mass. These uncertainties are fundamental sources to the ultimate errors in the analytical building behavior. The vertex method is used to combine these membership functions into higher level fuzzy sets for the natural frequencies. The result is a membership function for each of the desired natural frequencies which describes the complete behavior of the structure's frequencies due to the contributing errors.

Although these four sources of error are modeled as uncoupled in their effects on natural frequency, the vertex method in conjunction with re-analyses of the eigenvalue problem is used to develop a single fuzzy set which combines the effects of all the uncertainties. The resulting fuzzy set is used by the analyst to determine whether or not the resulting range in natural frequency is acceptable. A discussion devoted to the application and use of the results from the calibration model is presented in Chapter 7.

The natural frequencies of a structure are obtained through the eigensolution of the undamped free-vibration problem originally given in Eq. 3.2. Fundamental uncertainties presented in this section are confined to the structural stiffness and

mass properties, denoted by **K** and **M** respectively. The stiffness matrix, **K**, for the multi degree-of-freedom problem is the assembledge of contributing stiffness elements which have a functional dependence on the individual element properties represented as

$$\mathbf{K} = f(E, \nu, I, A, l) \tag{3.9}$$

where,

E = modulus of elasticity for the structural material;
ν = Poisson's ratio for the structural material;
I = moment of inertia about the strong and weak neutral axes;
A = cross-sectional area; and
l = element length.

The uncertainty in the mass matrix, **M**, is also a result of the uncertainty at the element level. The dependencies for the mass of an element are represented as

$$\mathbf{M} = f(m, L_d, L_l, l) \tag{3.10}$$

where,

m = distributed mass of a structural element;
L_d = dead loads considered in the structural analysis; and
L_l = live loads considered in the structural analysis.

The fundmental uncertainties (errors contributing to analysis uncertainty at the element level) considered in the calibration of the natural frequencies which are quantified in this study are:

- material modulus of elasticity,
- cross-sectional moment of inertia for the consideration of stiffness due to concrete slabs,
- dead loads,
- live loads, and
- joint stiffness (not explicitly addressed above).

The remaining contributions to stiffness and mass (Poisson's ratio, cross-sectional area, length, and distributed mass) are considered to be constant for the purposes of this study. However, the consideration of any uncertainty related to these factors can be implemented in a similar manner to the one presented here. The following subsections present the methodologies used to develop the fundamental fuzzy sets.

3.3.2 Modulus of Elasticity

Uncertainty associated with material properties has been widely published for use in probabilistic analysis. Consequently, the best information available for use in the development of a fuzzy set denoting uncertainty in modulus of elasticity is probabilistic. In this thesis, a mapping function is used to translate a probability density function to a normal trapezoidal fuzzy set, thus quantifying uncertainty in material properties. The modulus of elasticity is the only material property which is considered to vary; Poisson's ratio for the structural members is assumed to remain constant.

The mapping to the normal trapezoidal fuzzy set is performed by defining α-cuts at membership values of 0^+ and 1. The resolution principle is then used to define the fuzzy set's membership function. Since the α-cuts are defined at membership levels of 0^+ and 1, the shape of the resulting membership function will be a trapezoid.

Extensive research has been performed to establish an acceptable mean value and coefficient of variance for the modulus of elasticity for steel [GR78]. For the purposes of the mapping procedure, the distribution is assumed to be lognormal (a reasonable assumption since it is impossible for the modulus of elasticity to have a negative value). The bounds which contain 99% of the area underneath the probability density function translate to the bounds at α-cut 0^+. Although it is assumed that the tail of the probability density function is infinite, it is reasonable to assume that the corresponding α-cut 0^+ will bound all physically and realistically possible values of the modulus of elasticity. Thus, the resulting interval at α-cut 0^+, E_{0^+}, is defined by Eq. 3.11.

$$E_{0^+} \equiv \{E | P(a \leq E \leq b) = 99\%\} \tag{3.11}$$

where,

E = modulus of elasticity;
E_{0^+} = $\{E|\mu(E) > 0\}$;
a = the threshold such that $P(E \geq a) = 99.5\%$; and
b = the threshold such that $P(E \geq b) = 0.5\%$.

Alpha-cut 1 corresponds to the set containing the most likely values for E. Therefore, this α-cut should contain more than half of the possible values for the modulus. A similar procedure defines the interval of confidence for α-cut 1, E_1, by calculating the bounds which contain 51% percent of the area underneath the probability density function. Thus,

$$E_1 \equiv \{E|P(c \leq E \leq d) = 51\%\} \tag{3.12}$$

where,

E_1 = $\{E|\mu(E) \geq 1\}$;
c = the threshold such that $P(E \geq a) = 75.5\%$; and
d = the threshold such that $P(E \geq b) = 24.5\%$.

For steel, the recommended values for mean and coefficient of variance are 29,000 kips per square inch and 0.06, respectively, resulting in a very narrow distribution. Given these statistical properties, Figure 3.5 is a schematic of the mapping procedure and the resulting normal trapezoidal fuzzy set describing the uncertainty inherent in the modulus of elasticity for structural steel. Table 3.3 gives the probability of occurrence for the resulting bounds of α-cuts 0^+ and 1. When possible, all fuzzy sets will be given in tabular form, and the values for the lower bound and upper bounds in the tables can be referenced to the fuzzy set shown in Fig. 3.5.

3.3.3 Structural Mass and other Static Loading Conditions

Uncertainty due to the uncertainty of design loads is estimated with the use of a trapezoidal fuzzy set using the recommended factors of safety in the design code [Int86]. Again, the membership function is obtained through the definition of two α-cut intervals at membership levels of 0^+ and 1. However, in this case, there is little

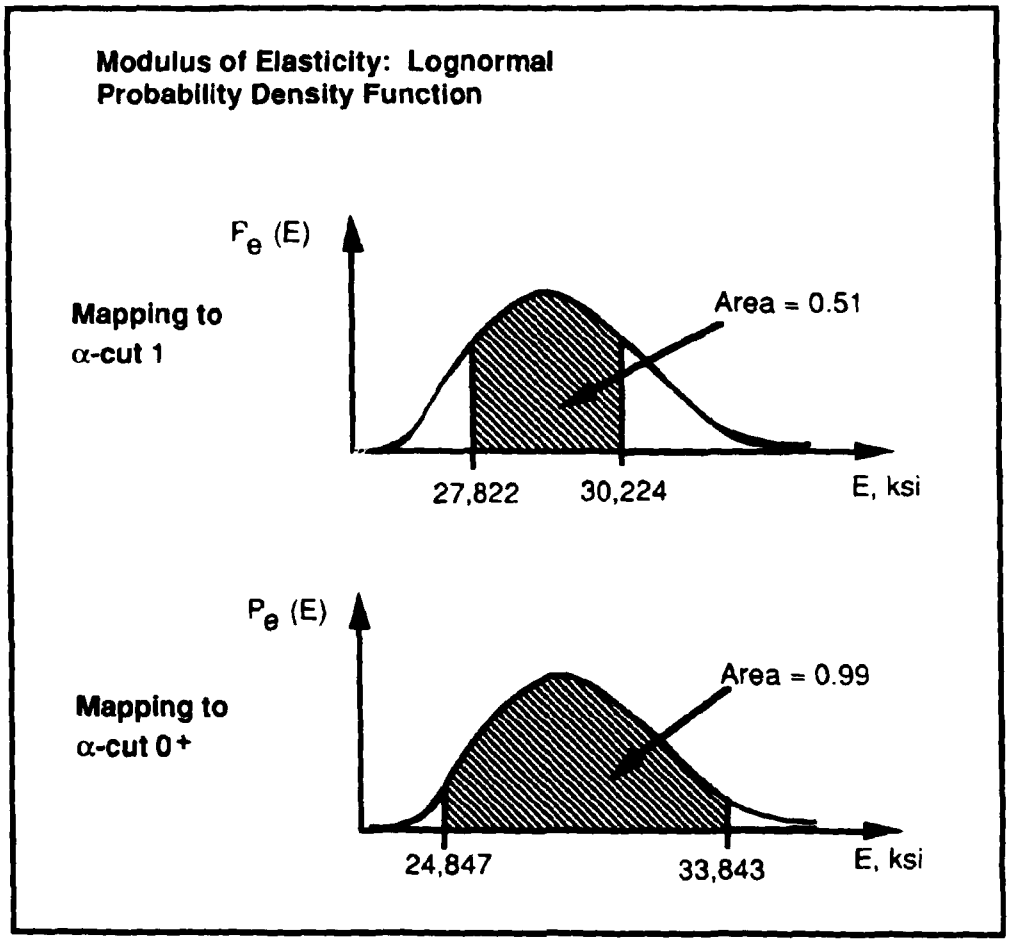

Figure 3.5: Mapping procedure for the development of the membership function which defines the modulus of elasticity fuzzy set.

Table 3.3: Alpha-cut bounds for the elastic modulus fuzzy sets for structural steel.

α-cut	P(a ≤ E ≤ b)	mean	cov	lower bound	upper bound
		ksi		ksi	ksi
0.0^+	99%	29,000	0.06	24,847	33,843
1.0	51%	29,000	0.06	27,822	30,224

information known about the probabilistic behavior in structural loadings (loads due to concrete slabs, furniture, partition walls, etc.) The skeletal mass of the structure is assumed to remain constant due to the small variance in the density of steel; however, there are large amounts of uncertainty associated with the design loads. The uncertainty for these design loads is due to the variability in floor weight, partitions, scaffolding, sheet walls, furniture, etc. For example, the fuzzy set denoting structural mass is defined by calculating the loads for the building and bounding them using a $\mathcal{X}(\alpha)$ factor of $\pm$ 10% for $\alpha = 1$ and $\pm$ 20% for $\alpha = 0^+$ (see Fig. 3.6). Therefore, the intervals for each of the two fuzzy sets are defined best by the analyst. The analyst first estimates the center of mass for the fuzzy set. This center of mass represents the initial mass, M_o, estimated by the engineer to be considered in analysis. Additionally, a factor is used to map the uncertainty in the initial mass estimate to a fuzzy set for the mass loading conditions. The analyst gives a value for this factor based on knowledge of the architect's plans and structural use. In this study, the factors of safety in the LRFD code are used as a guide. The resulting fuzzy set is obtained based on the following equation.

$$M_o \equiv \{[a,b] | a = (1 - \mathcal{X}(\alpha))M_o; b = (1 + \mathcal{X}(\alpha))M_o\} \tag{3.13}$$

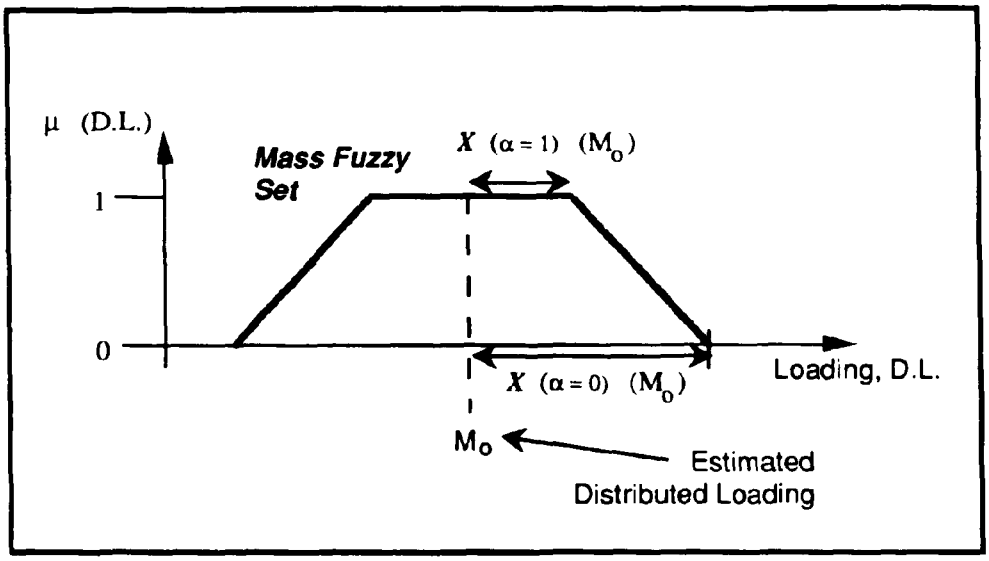

Figure 3.6: Fuzzy set denoting fuzzy mass estimate.

where,

M = structural mass;

M_α = $\{M|\mu(M) \geq \alpha\}$;

M_o = mass value specified by the analyst;

$\mathcal{X}(\alpha)$ = value specified by the analyst for membership α such that $\mathcal{X}(\alpha = 1) \leq \mathcal{X}(\alpha = 0^+)$;

a = the lower bound for the alpha-cut set; and

b = the upper bound for the alpha-cut set.

3.3.4 Joint and Stiffness Uncertainties

The uncertainty in natural frequency resulting from uncertainty in joint rigidities is also described in terms of a normal trapezoidal fuzzy set where four separate cases defining joint rigidity are used to define the two α-cut levels. It is assumed that welded connections are perfectly rigid and that joints which are bolted are semi-rigid. For a membership value of 0^+, the lower bound represents the most flexible possible structure obtained by modeling all semi-rigid joints as perfectly hinged, where the

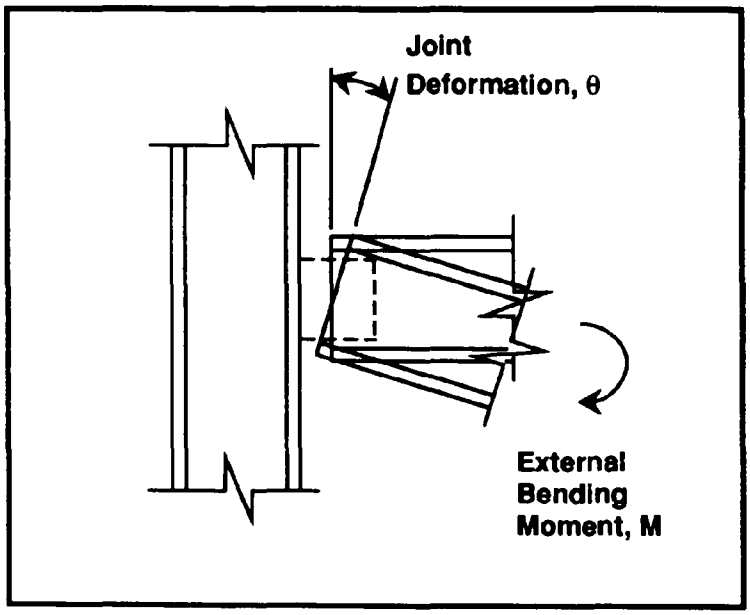

Figure 3.7: Rotational deformation, Θ due to an external bending moment, M.

resulting fundamental frequency is the lower bound of the α-cut 0^+ interval. The upper bound of the α-cut 0^+ interval is determined through analysis of the least flexible structure obtained by modeling all semi-rigid joints as perfectly rigid (a spring with infinite stiffness). The interval at α-cut 1 is obtained by modeling the semi-rigid joints with springs having variable stiffnesses.

Moment-curvature relations of semi-rigid joints have been studied [KC86] and can be used to determine appropriate bounds for specific connection types for α-cut 1. A semi-rigid joint will typically experience a rotation between the column and connecting flange as shown in Fig. 3.7. The shape of a typical moment-curvature relationship for a semi-rigid joint is shown in Fig. 3.8. Due to the nonlinear relationship between moment and curvature, the slope in the figure decreases as the applied bending moment increases. In other words, the rotational stiffness of the joint decreases permitting more joint deformation as the bending moment increases.

The uncertainty in the joint stiffness is based on the uncertain range of internal

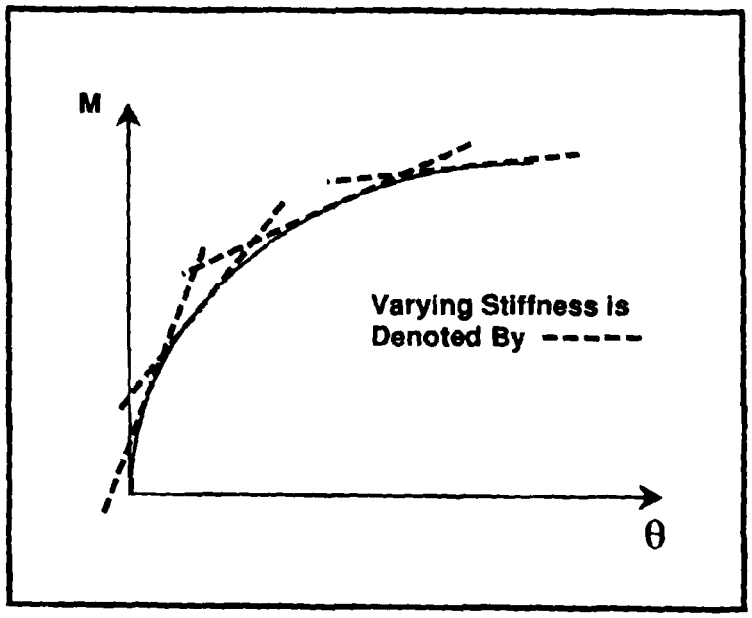

Figure 3.8: Moment-curvature relationship for a semi-rigid connection.

moments that joint must be able to resist. The range in stiffness for the α-cut bounds may be defined by evaluating the changing slope for typical semi-rigid connections. For example, the most possible range of internal moments will correlate to the most possible range of joint stiffness. Table 3.4 gives possible points for α-cuts 0^+ and 1 for two connection types: shear tabs and detailed joints.

3.3.5 Uncertainty of the Floor Rigidity

The rigidity of the floor system is an important consideration in three dimensional dynamic analysis. Floor system rigidity affects the overall stiffness of the structure and is an important consideration when determining the structural frequencies. A fully rigid floor system permits the transfer of all forces from one structural frame to another, as opposed to a flexible diaphragm which inhibits the transferring of forces as illustrated by Figure 3.9. For the purposes of this research, floor rigidity is quantified through the analysis of a composite beam section. The composite beam section

consists of steel decking and concrete used in the slab system. Variance of the width of the concrete slab in the composite section directly affects the analytical stiffness of the floor system. Figure 3.10 shows the composite sections used in this study. The width, w, of the concrete slab and the modulus of elasticity for the concrete are two uncertain variables used in the analysis. Additionally, since the concrete slab is an irregular shape, the slab thickness, t, may also be used in approximating the bending stiffness of the slab. Since the values used to quantify the stiffness of the concrete slab vary significantly based on the slab type, floor plan, and bay width, fuzzy sets denoting their values will not be given here. A case study is presented in Chapter 5 which illustrates the uncertainty of the floor system rigidity and the fuzzy sets for the geometric parameters are given in the example.

3.4 Generality of the Calibration Model

The calibration model presented here is a general methodology which can be applied to almost any analytical finite element model for a structural system provided that the methodology is applied consistently. The error quantified in the calibration analysis is based on estimates of the fundamental contributing errors to the desired solution. With careful definition of the fundamental errors the resulting error obtained from the calibration model will be a realistic representation of the potential values for the parameter of interest.

Table 3.4: α-cut bounds for the connection stiffness.

α-cut	lower bound	upper bound
	$\frac{lbf\,t}{Rad}$	$\frac{lbf\,t}{Rad}$
	Shear Tab	
0.0^+	0.0	∞
1.0	0.0	10^7
	Detailed Joint (no welds)	
0.0^+	0.0	10^7
1.0	10^7	∞

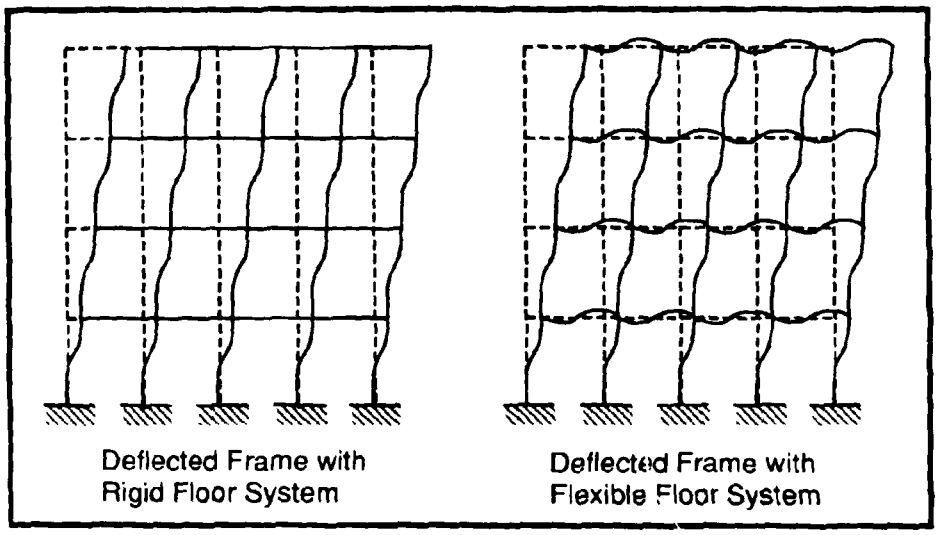

Figure 3.9: Rigid and flexible floor systems.

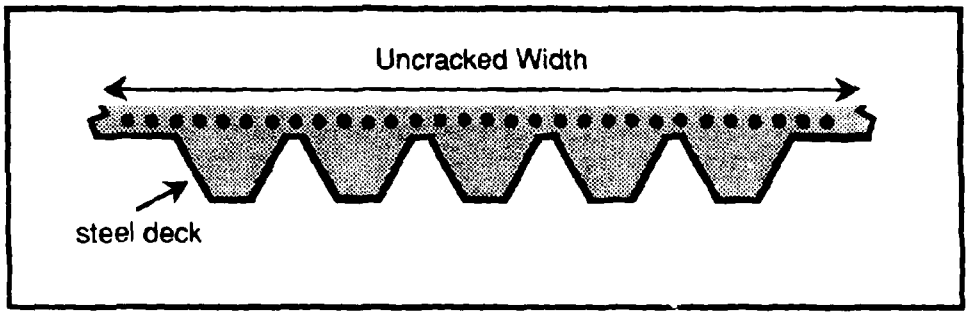

Figure 3.10: Typical cross section for composite elements.

In this thesis, the procedure for the development of fundamental errors pertaining to a civil structural system is established. Most certainly there are additional uncertainties in the analytical structural model which are not considered here that may relevant to the uncertainty in the structural dynamic properties. It is impossible to develop fuzzy sets for every type of fundamental error contributing to the dynamic properties of a structural system. However, the purpose of this chapter has been to present methods that can be used to define the errors. In defining fuzzy sets for additional errors the same logic used here must be maintained. Such that extreme yet realistically possible values must be used to define the bounds at α-cut 0^+. The most possible values (whether that is defined by a frequency of 51%, occurring most of the time, or an expert's opinion) define the bounds at α-cut 1. Membership levels of 0^+ and 1 are used here because it is more intuitive for qualitative data to be extracted at the corresponding levels of logic. If there is enough information or experience about the uncertainty, the fundamental errors can be defined at additional levels of membership. Ultimately, this will increase the integrity and usefulness of the calibration model results.

Application of the calibration model is not confined to civil structural systems. The methodology presented in this thesis can be applied to any structural system which is modeled using the finite element method. The fundamental errors need to be consistently defined to represent the uncertainty specific to the application of interest. For example, in the case of an off-shore oil platform, the uncertainty in the structural mass is not based on scaffolding and dead load approximations, rather the uncertainty is due to the loading of machinery at the platform. Marine growth on the structural members may contribute to the uncertainty in the structural stiffness. Thus, it is critical to give careful consideration of the application in the use of the calibration model.

Regardless of the application, repetitive solutions based on extreme bounds of the contributing fuzzy sets at various levels of membership are required to obtain the final solution. Consistent definitions of uncertainty will provide the analyst with results needed for his future decision making purposes.

CHAPTER 4

Quantification of Input Motion Uncertainty

Uncertainty in the dynamic input motion felt by the structure is quantified for use in the adaptive dynamic analysis models through the development of fuzzy response spectra. The fuzzy response spectra which are developed in this thesis give a fuzzy set for the maximum response of a single degree-of-freedom (SDOF) system. The maximum response fuzzy set is obtained by referencing the deterministic or uncertain frequency of the SDOF system to the spectrum. Additionally, it is possible to obtain a fuzzy set for the system's maximum response based on a fuzzy representation of the system's dynamic properties.

This chapter presents the process established for the definition of the fuzzy velocity response spectra. Section 4.1 contains a detailed discussion pertaining to the objectives and motivation towards the development of the fuzzy spectra. Definition of the response spectra as fuzzy sets requires the organization of selected data from individual deterministic spectra into groups classified by soil types and distances to the rupture zone. Furthermore, fuzzy logic is then used to translate the data obtained from individual spectra into fuzzy response spectra. A detailed presentation of this formulation is given in Section 4.2. Section 4.3 contains the resulting spectra which are used in the adaptive analysis models. The fuzzy spectra developed here are used to demonstrate the capability of the adaptive analysis model to consider input motion uncertainty. Section 4.4 addresses specific issues which need to be considered in the future development of fuzzy spectra.

4.1 Objectives of the Fuzzy Response Spectra

Response spectra which were studied initially by researchers such as Housner [Hou47] enable engineers to better understand the effects an earthquake time history can have on a structure due to the local site conditions. A response spectrum gives the results of the equation of motion for a SDOF system excited by a time history as shown in Eqs. 4.1, 4.2, 4.3, and 4.4.

$$m\ddot{y} + c\dot{y} + ky = -m\ddot{z}(t) \tag{4.1}$$

$$S_d(T,\xi) = max|y(t)| \tag{4.2}$$

$$S_v(T,\xi) = max|\dot{y}(t)| \tag{4.3}$$

$$S_a(T,\xi) = max|\ddot{y}(t)| \tag{4.4}$$

where,

- y = the time dependent modal coordinate displacement response (where 1st and 2nd derivatives with respect to time denote velocity and acceleration, respectively);
- k, c, m = the stiffness, damping, and mass, respectively for the SDOF system ;
- T = system period where, $T = \frac{2\pi}{\omega}$, with $\omega = \sqrt{\frac{k}{m}}$ (for an SDOF system);
- ξ = fraction of critical damping where, c is the viscous damping coefficient and $\xi = \frac{c}{2\sqrt{km}}$;
- $\ddot{z}(t)$ = the time dependent earthquake acceleration input at the system support; and
- $S_{d,v,a}$ = the maximum displacement, velocity or acceleration, respectively obtained from Eq. 4.1.

In general, a response spectrum is a graphical relationship of the maximum response (displacement, velocity, or acceleration) of a SDOF elastic system versus natural frequency (or period) of the system for a particular input motion. Representation of the input motion as response spectra makes it possible to compare the consequences

of a system's response to various system dynamic properties such as damping and natural frequency. It is possible to use a response spectrum to find the maximum response for a multi degree-of-freedom (MDOF) system by first analyzing the m responses of the equivalent, uncoupled SDOF systems. Modal superposition, as described in Section 3.1, superimposes the m responses of the uncoupled SDOF modal coordinates in the time domain to a MDOF response in space and time. Initially, the fuzzy spectra are applied to the calibration model which predicts the response for an undamaged structure. Therefore, the spectra developed here, are elastic spectra which give the maximum response for an elastic system.

Structural response is dependent on both the dynamic characteristics inherent to the building and the characteristics of the applied load. The dynamic characteristics (modal properties and damping capacity) of a building are dependent on the properties of its structural and non-structural elements and, once determined (either by detailed dynamic analysis or system identification), can be assumed to remain unchanged through a short duration of the structure's lifespan. The applied load to the structure is the time history created by the earthquake and is impossible to predict due to the random nature of earthquakes. The ultimate error in the structural response is due to the approximations inherent in the models used to predict the structure's dynamic characteristics and the excitation acting on the structure. Parameters which describe the earthquake's peak ground acceleration (velocity or displacement), duration, frequency, and energy content are difficult to predict. Consequently, it is difficult to select representative earthquake time histories for the purposes of structural design [AB86, Hou90].

The objective of this work is to formulate a methodology which can be used to characterize the uncertainty in the ground motion felt by a structure. The following is a motivation towards the use of response spectra in this uncertainty quantification. The purpose of the fuzzy response spectra is to enable the analyst to bound the potential maximum response a structure may experience; thus, enabling him to make better informed decisions about structural integrity.

4.2 Formulation of Fuzzy Sets

It has been well accepted that the excitation acting on a structure is dependent on the site's proximity to the fault rupture, earthquake magnitude, and local site conditions. Other factors which may also affect the characteristics of the excitation acting on the structure are damping characteristics of the soil and soil-structure interaction.

Earthquake motions are characterized by random vibrations. Although considered random both in time and space earthquakes do have common characteristics. Use of response spectra make it possible to generalize some of the common characteristics of earthquake motions. Spectra were studied by Housner [Hou47] in an attempt to characterize strong motion earthquakes. Housner continued to study response spectra by introducing analytical methods which use the response spectrum to measure earthquake intensity [Hou59]. He recommends the use of such analytical measures in comparing the strength of earthquakes rather than the empirically based Modified Mercalli Intensity (MMI) scale.

A number of researchers have realized the importance of local site conditions in characterizing ground motion parameters [BG76, Cam85, JB81, MJB83]. The random vibration of the earthquake is filtered as it passes through a soil profile before reaching the earth's surface, creating a smooth surface motion. Consequently, the frequency content of the motion at the earth's surface is similar to the natural frequencies of the soil profile. This filtering process in some cases can add randomness of their own making the surface motion even more complex. Additionally, amplification is generally greater for soft soil as compared to rock sites. Dorby et al. [DOU76] compares closed-form solutions to approximate methods used to estimate the fundamental period of a soil profile. The shear wave velocities at various depths are used to determine the natural frequency of the soil column.

Atkinson and Boore [AB90] have noted that the difference in earthquake characteristics between the eastern and western regions of North America is primarily due to the different properties in the earth's crust. Typically, earthquakes in the East have significantly lower attenuation rates than in the Western regions. Thus, response spectra represent characteristics which are specific to the local site conditions and

the more global characteristics of the earth's composition in addition to that of the earthquake itself. Boore and Joyner have developed attenuation relationships based on statistical regression analyses to empirically predict ground motion [BJ82, BJF93]. Based on values for magnitude and distance to the rupture zone, these attenuation relationships predict peak ground acceleration (velocity and displacement) as well as formulate response spectra which further describe the frequency characteristics of an earthquake.

Currently in the design code, design spectra are selected according to the local soil conditions. However, after determining the local site conditions, the spectrum used in the analysis is deterministic. Although the spectra provided in the design code is developed from many earthquake time histories, the result is a single relation because it would be difficult if not impossible to design for several spectra. In design, a single spectra is used based on an expected peak ground acceleration for the region and local soil conditions. This single relation does not consider the uncertainty inherent in the soil and other potential ground motion characteristics. The design spectra, in general, define the criteria for which a structure should be built [NL93, App74]. A design based on the response spectra approach does not consider the duration of the earthquake [App74]. Furthermore, since the design spectrum is normalized the spectrum's shape is an important characteristic for design [Sei90]. This shape highlights the response specific to the structural system's natural frequencies. Since the local soil conditions have one of the greatest influences in the surface motion, further analyses can benefit from the consideration of the uncertainties inherent to the local site conditions. Furthermore, in the case of a detailed forced-vibration dynamic analysis, there is difficulty in selecting applicable time histories to represent accurately the next unknown earthquake. A response spectrum inherently represents the local site conditions because it is obtained using free-field data.

By developing a fuzzy response spectrum which denotes uncertainty in frequency and amplitude it is possible to anticipate characteristics of future earthquakes at a particular site. Use of a fuzzy spectrum provides the analyst with bounded ranges of values for possible structural response. The idea of bounding a response spectrum is not new. Seed (in a number of papers [SI69, SUL76, SMLI76]) has statistically

bounded response spectra grouped by soil types and distance categories with a mean response and an upper bound of one standard deviation.

4.2.1 Theoretical Development of Fuzzy Response Spectra

The theoretical development of the fuzzy response spectra is performed in four steps: (1) The shape is characterized for individual site-dependent spectra; (2) Data is organized; (3) Data is mapped from the site-dependent spectra to the fuzzy spectrum; and (4) Results from any of the above steps are refined as needed. These steps are described in greater detail in the remainder of this chapter.

In this thesis, fuzzy velocity response spectra are developed considering uncertainties in distance from the fault rupture, local soil conditions, and the random ground motion felt by the structure. The velocity response is selected for the fuzzy response spectra because it is, in general, the smoothest of the three response parameters. The uncertainty of the earthquake is determined by the location of the two corner points of a site-dependent velocity response spectrum, "Corner A" and "Corner B" (shown in Fig. 4.1). Identification of these two points helps to approximate the trapezoidal shape typical of the velocity spectrum [NH82] and describe both the velocity amplification and frequency content specific to the site from which the spectrum is developed. The trapezoid outlines the shape of the site-dependent velocity response spectrum using corner points A and B and two additional points, C and D (also shown in the Figure). In this development, points C and D will always have the same location regardless of the shape of the site-dependent response spectrum. The purpose of these deterministic points (C & D) is to fix the two sloped lines of the trapezoidal shaped curve.

A response spectrum which is obtained from a real discretized earthquake record is generally rough due to the randomness of the earthquake. Peaks which occur across the spectrum of frequencies represent the frequency content of the earthquake. Depending on the local site conditions, the range in frequency content in a spectrum may vary greatly in breadth. It is difficult to define the exact points for each of the corners A and B, because of the variable shape of typical site-dependent spectra. However, it is possible to locate points A and B such that the line connecting the two

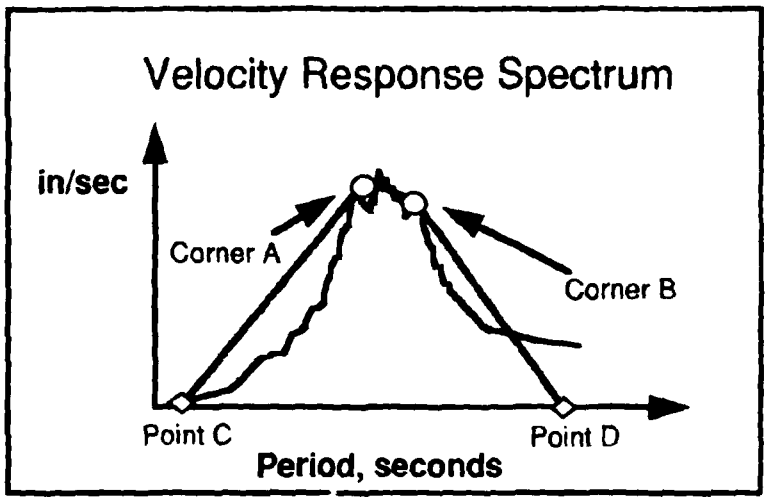

Figure 4.1: Corner points A & B for site a dependent spectrum.

points generally follows the spectrum. It is not important to capture every peak in the spectrum; however, it is important to locate the average amplitude height across the range of frequencies. The corners are located at frequencies where the amplitude has a distinctive and continuous drop-off.

4.2.2 Organization of Data

The data used to derive the representative fuzzy response spectrum are: (1) location of the two corner points from site specific velocity response spectra; (2) local site conditions (a soil type); and (3) the distance from the site to the fault rupture. These characteristics are selected based on the best information available to the analyst during the design stage. Additional factors which affect the amplitude of the spectra are the magnitude and rupture mechanism of the event. Magnitude is not considered in the initial establishment of the fuzzy spectra presented here. The example which is presented at the conclusion of this chapter uses data from the Loma Prieta earthquake only. Therefore, data organization with respect to magnitude will not be considered in more detail. Uncertainty in the response due to the magnitude or rupture mechanism can certainly be added to this formulation, but it is imperative that

careful consideration be made as to the amount of data available in each data group such that enough information is available to effectively represent each spectrum.

During the design of a structure, the location and general soil conditions are typically known for the potential site. Data is, therefore, separated into two general soil type groups: rock and alluvium. By separating these two soil types, it is possible to characterize the fuzzy spectra based on the frequency content of the soil profile. The distance from the site to the next earthquake is generally unknown, although assumptions may be made by studying the proximity to fault zones and earthquake recurrence relationships. In the example which follows, three response spectra are developed for each local site condition based on distance (x) to the fault rupture zone: $x < 30$ km, $30 < x < 60$ km, and $x > 60$ km. Application of the fuzzy response spectra requires the analyst to use the spectra best-representing the local site conditions and denoting each of the three distance groups.

4.2.3 Development of Fuzzy Sets for Earthquake Spectra

Fuzzy set development for the period and maximum velocity amplitude is performed separately based on the data obtained from the corner point locations. Four fuzzy sets (one each for the period and amplitude at corners A and B) are developed which provide the information necessary to define the "fuzzy location" of the two corner points in the resulting fuzzy spectrum. The α-cut 0^+ is established such that all data points within a distance group are bounded, and α-cut 1 is defined by crisp set bounds denoting the most-possible values of occurrence. Regions representing the most-possible values of occurrence are generally where data is clustered and where more than half of the available data is contained. Four fuzzy sets (shown in Figure 4.2), two each for period and amplitude, are used to define a fuzzy spectrum by specifying the fuzzy location for corners A & B.

Once period and amplitude fuzzy sets have been defined for each corner, set theory is used to define the resulting fuzzy velocity response spectrum. The union of the period fuzzy sets for corners A and B define the membership for period content in the resulting fuzzy response spectrum. The resulting fuzzy set for period content must be convex, and modifications may be necessary. Alpha-cuts taken at higher

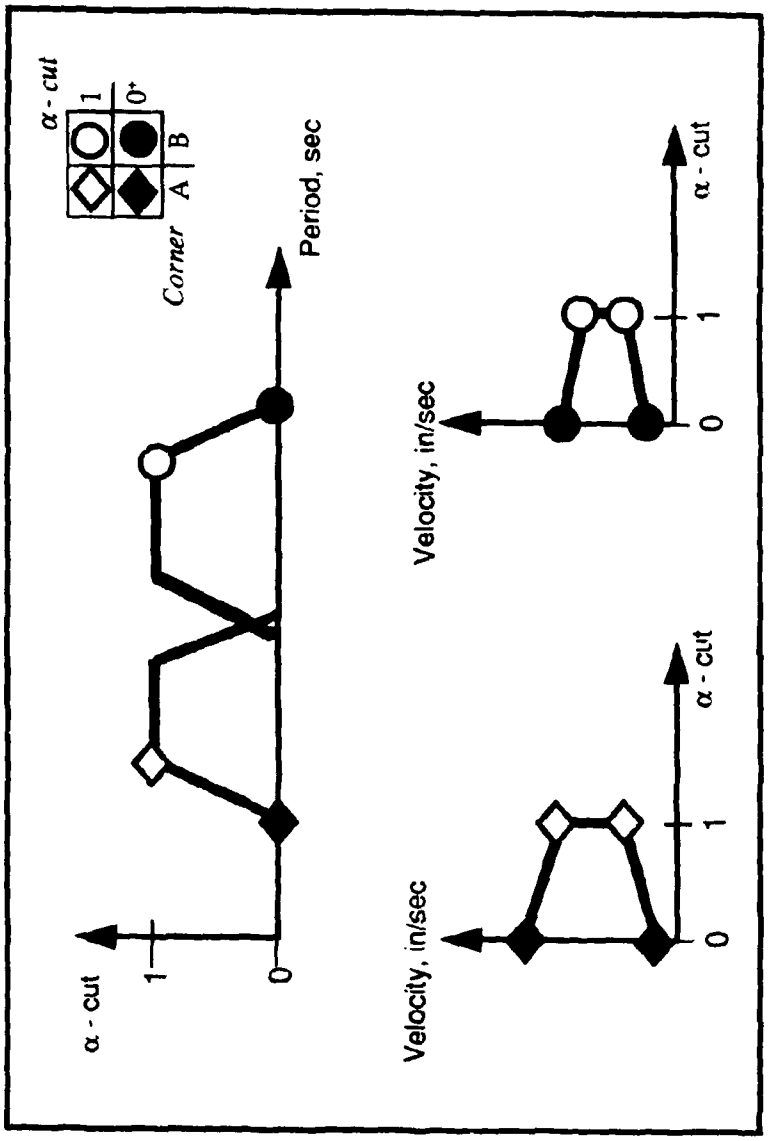

Figure 4.2: Fuzzy sets for period and frequency of corners A & B.

levels of memberships for this resulting period content fuzzy set may produce two crisps sets. The α-cut bounds which produce two crisp sets are modified such that the new bounds consist of the minimum of the two original minimum bounds and the maximum of the two original maximum bounds. Repeating this procedure for all the affected α-cuts creates a convex fuzzy set. The intersection is then taken of the newly defined membership for period content and the amplification fuzzy sets for each corner point. This results in fuzzy locations for corners A and B.

In addition to the two fuzzy corners A and B, two additional points are required to define the shape of the response spectrum and are labeled "Point C" and "Point D" as shown in Fig. 4.1. These points are taken to be deterministic and, as stated earlier, are used as constraints to create the general trapezoidal shape typical of the velocity spectra. Point C is located at a period of 0.01 sec. and a velocity of 0.1 in/sec., and point D is located at a period of 60.0 sec. and a velocity of 0.1 in/sec. The placement of the two fuzzy corners and the two deterministic points define the fuzzy velocity response spectrum. The fuzzy velocity response spectrum now is defined fully by two crisp sets at α-cut 0^+ and α-cut 1 for the two fuzzy parameters (velocity amplitude and period), where the bounds for each α-cut are established by the placement of six points representing the vertices of the trapezoidal shaped velocity response spectrum. This procedure is illustrated in Figure 4.3 which shows the mapping from the fuzzy sets in Figure 4.2 to the fuzzy spectrum.

It may be necessary to refine the fuzzy sets at two stages of their development. First, the amount of data available for a particular earthquake may suggest slight modifications to the distance categories to make the best use of the data. Secondly, if the analyst wishes to enforce a particular shape to the fuzzy spectra (such as the trapezoidal shape used in this study), there may be instances when α-cut 1 is not completely contained within α-cut 0^+, which is contradictory to the requirements of fuzzy logic. This problem occurs because the slopes of the lines representing the α-cuts forming the membership function act as a constraint on the development of the fuzzy spectra. To eliminate this problem the α-cut 0^+ bounds can be altered to be the same as the α-cut 1 bounds. This modification does not corrupt the validity of the fuzzy spectra because it does not affect the region of primary importance to

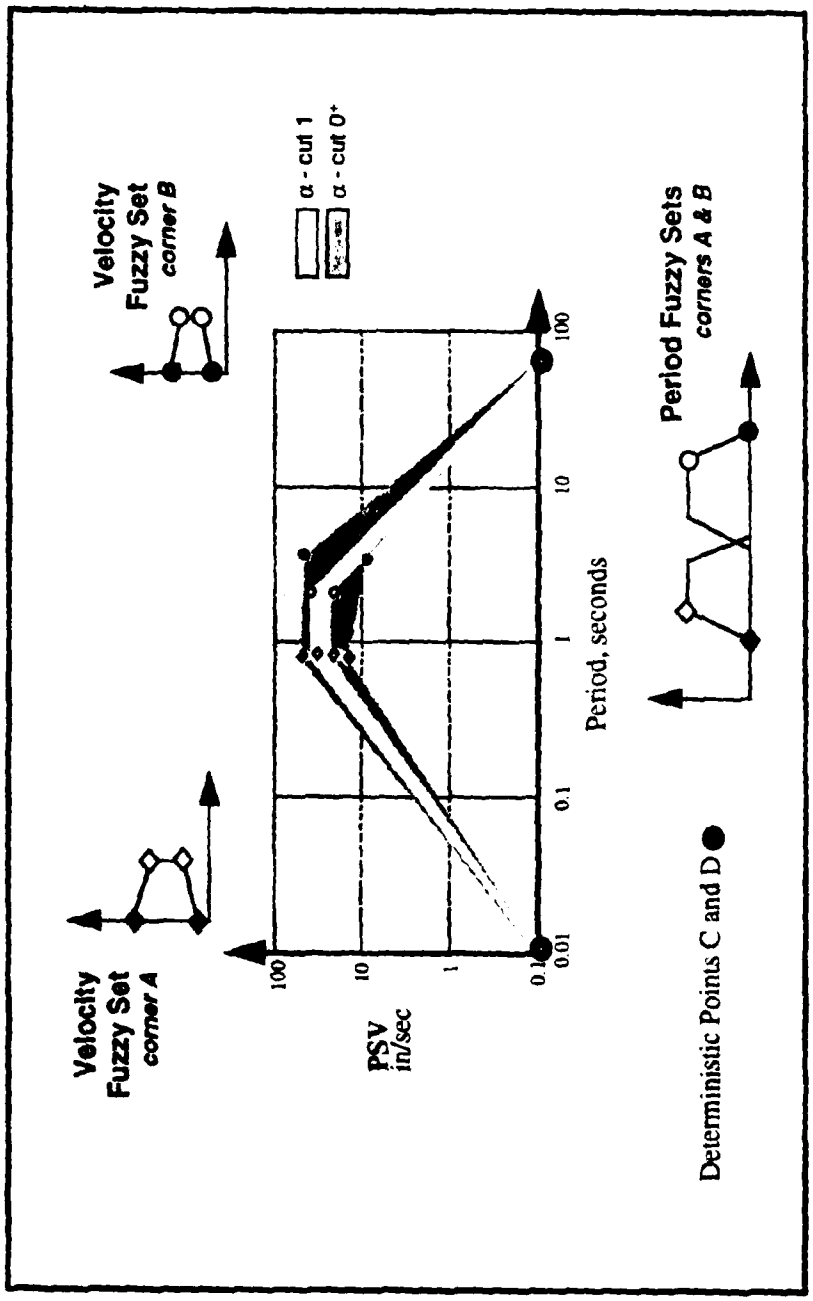

Figure 4.3: Establishment of a fuzzy velocity response spectrum.

the analyst, i.e., the points defining α-cut 1 between corners A and B. However, the bounds for α-cut 0 are broadened by this modification.

The flowchart in Fig. 4.4 is a schematic representation of the procedure used in the development of fuzzy response spectra. The resulting spectra are in three dimensions, with axes denoting period, velocity, and membership level. In the figure, the fuzzy spectrum is viewed in two dimensions with the membership, denoted by α-cuts 1 and 0^+, representing slices from the third dimensional view. The following is an example further describing the implementation of this method.

4.3 Fuzzy Velocity Spectra for the Loma Prieta Earthquake

The methodology proposed here is applied to data from the Loma Prieta earthquake of October 17, 1989. The thirty-nine records used in this development were obtained from the California Strong Motion Instrumentation Program (CSMIP) [csm91]. Two orthogonal horizontal channels were used from each site and considered to be independent thus doubling the data available. Fuzzy velocity response spectra are developed at the three distance categories for two soil types (alluvium and rock). Appendix A contains the soil type, distance to the rupture zone for each site, and the coordinates for the corners A and B for each horizontal channel at each site. The data is organized by separating the data into six groups for analysis. Tables 4.1 and 4.2 give the tabular representation of the four two-dimensional fuzzy sets for the six groups used.

Fuzzy response spectra are developed for each of the six groups of data through the processes of fuzzy set theory as described in the previous section. Figure 4.3 highlights the placement of the 6 points used to establish the α-cut 0^+ bounds in the fuzzy spectrum. The points in Fig. 4.5 represent the data for rock sites located less than 30 km from the fault rupture zone and can be referenced to Table 4.1. Figures 4.6, 4.7, and 4.8 are spectra developed at the three distance categories for rock sites, and Figs. 4.9, 4.10, and 4.11 are spectra developed for alluvium sites at the three distance categories.

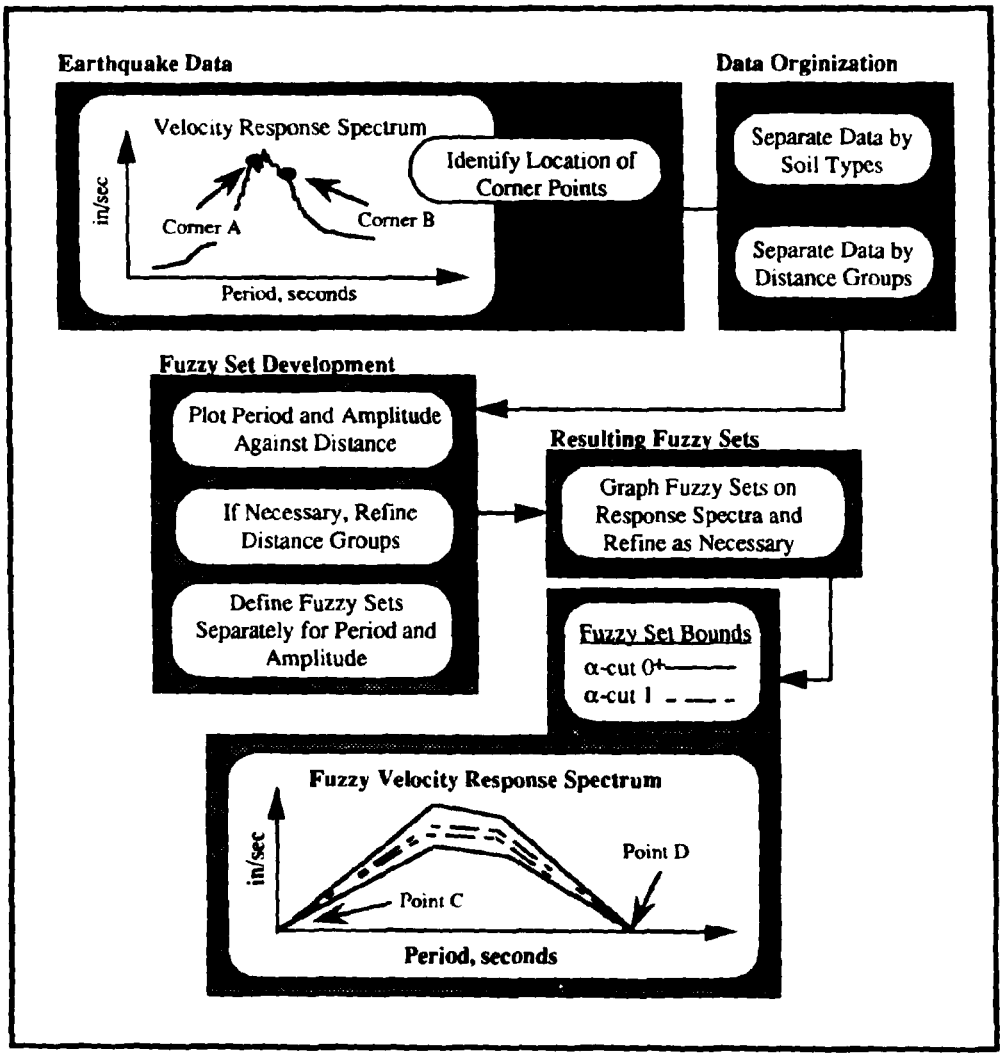

Figure 4.4: Schematic representation of the fuzzy response spectra development.

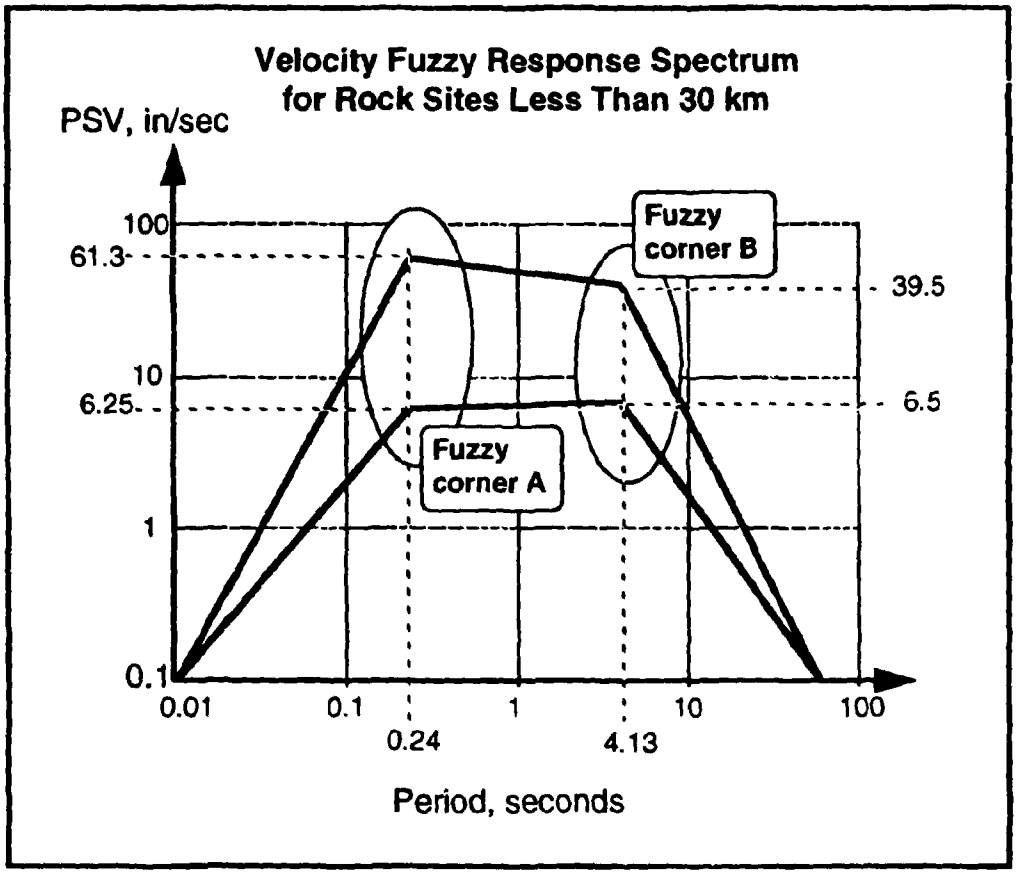

Figure 4.5: Fuzzy velocity response spectrum for rock sites less than 30 km from the rupture zone at α-cut 0^+.

Table 4.1: Corner location fuzzy sets for rock sites.

Distance	Corner A Bounds		Corner B Bounds	
	α-cut 0^+	α-cut 1	α-cut 0^+	α-cut 1
km	seconds	seconds	seconds	seconds
less than 30	0.24 - 1.02	0.38 - 0.8	1.0 - 4.13	1.5 - 3.25
between 30 & 60	0.16 - 1.02	0.32 - 0.62	0.88 - 7.13	2.63 - 5.25
greater than 60	0.18 - 1.42	0.38 - 0.90	1.63 - 6.13	2.25 - 4.13
km	in/sec	in/sec	in/sec	in/sec
less than 30	6.25 - 61.3	18.75 - 32.5	6.5 - 39.5	10.0 - 22.0
between 30 & 60	2.5 - 15	7.4 - 12.5	3.0 - 17.0	4.0 - 13.0
greater than 60	1.0 - 22.5	2.5 - 8.75	0.5 - 20.0	3.5 - 9.0

Table 4.2: Corner location fuzzy sets for alluvium sites.

Distance	Corner A Bounds		Corner B Bounds	
	α-cut 0^+	α-cut 1	α-cut 0^+	α-cut 1
km	seconds	seconds	seconds	seconds
less than 30	0.2 - 0.61	0.35 - 0.48	0.4 - 6.3	1.5 - 2.75
between 30 & 60	0.2 - 1.2	0.44 - 0.67	1.5 - 5.3	2.4 - 3.8
greater than 60	0.77 - 1.13	0.77 - 0.91	0.9 - 3.4	0.9 - 2.0
km	in/sec	in/sec	in/sec	in/sec
less than 30	6.3 - 51.3	13.3 - 33.3	6.3 - 59	14 - 32.5
between 30 & 60	5.0 - 62	7.5 - 21	4.3 - 36.3	7.5 - 16
greater than 60	11.0 - 32	17.5 - 27.5	7.3 - 31	17.5 - 27.5

It is difficult to make generalizations for the α-cut 0^+ bounds since these bounds must contain extreme points to remain valid in fuzzy set theory. However, it is possible to make generalizations for α-cut 1 bounds which represent the most possible values for the velocity response spectra. In general, the resulting period bounds for the rock sites are broader than the alluvium sites representing the wide range in shear wave velocity for rock in the San Francisco Bay Area. The maximum velocity bounds are broad for both the rock and alluvium sites because of the selection of the distance categories. These distance categories were broad due to the lack of data points in finer categories. The bounds for α-cut 1 become tighter at farther distances, representing an overall attenuation of the maximum velocity. In Fig. 4.7 the bounds for α-cut 0^+ were modified, because the original bounds did not fully contain α-cut 1.

Based on the results for the Loma Prieta example, further developments of the fuzzy response spectra should consider soil types by shear wave velocities rather than the general classifications of rock and alluvium. Introducing more earthquakes to the data set will make it possible to further refine the distance categories. Thus, the bounds for both the maximum velocity and the period will be tighter. The spectra developed here give conservative, but high results for low and high periods (periods which do not fall between fuzzy corners A and B). Placement of two additional fuzzy corners between the deterministic points and the fuzzy corners will give the analyst more realistic results for low and high structural periods.

4.4 Discussion

In this study earthquake response spectra are formulated using fuzzy mathematics to represent uncertainties inherent in the local soil conditions, distance from the fault rupture, and the random nature of the earthquake. Fuzzy velocity response spectra were developed based on data from the Loma Prieta earthquake for both alluvium and rock sites. These fuzzy spectra can provide the analyst with more insight into the most likely response, quantified to consider the uncertainties associated with the site conditions and the earthquake parameters. The fuzzy response spectra developed here for velocity are valid for earthquakes due to a combined right lateral fault and

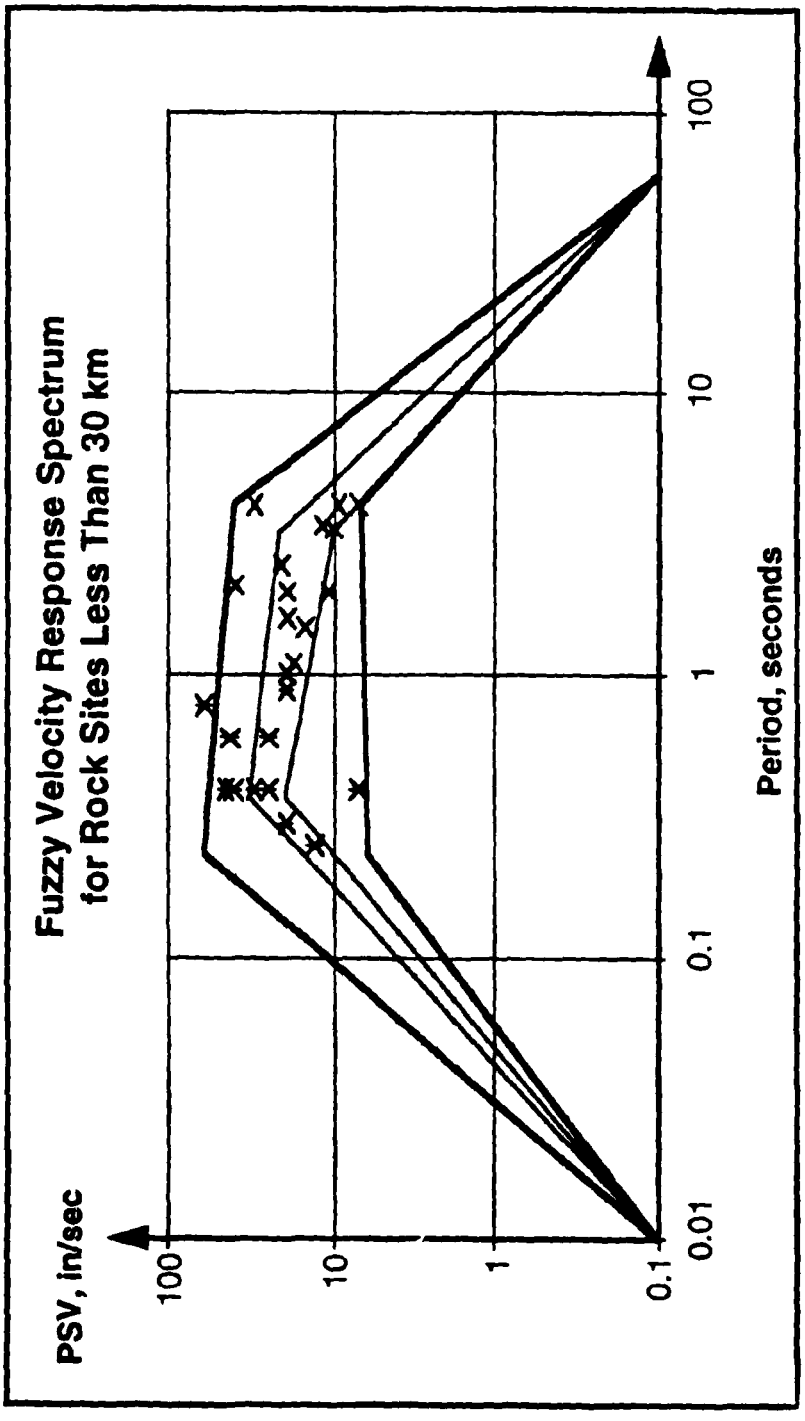

Figure 4.6: Fuzzy velocity spectrum for rock sites ($x < 30$ km).

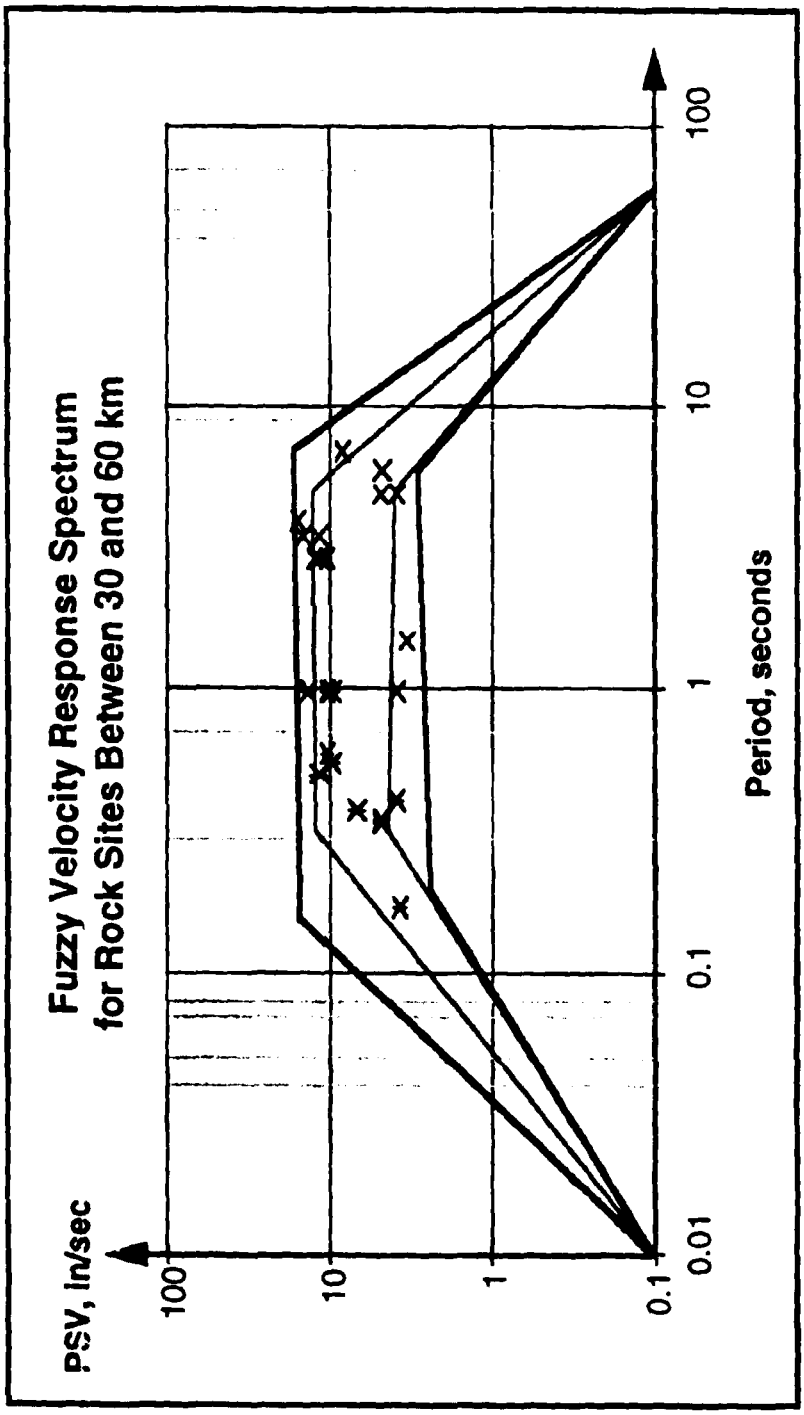

Figure 4.7: Fuzzy velocity spectrum for rock sites ($30 < x < 60$ km).

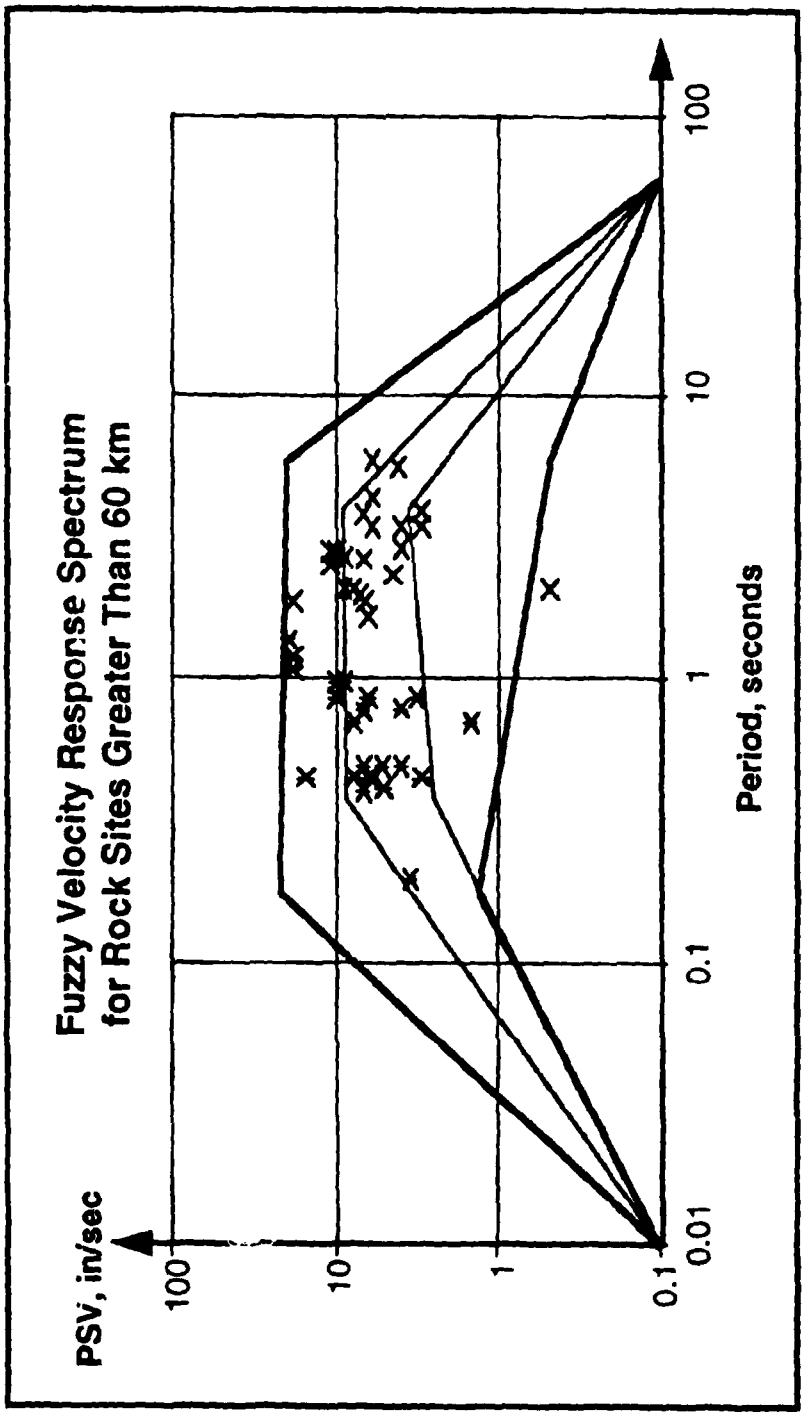

Figure 4.8: Fuzzy velocity spectrum for rock sites (x >60 km).

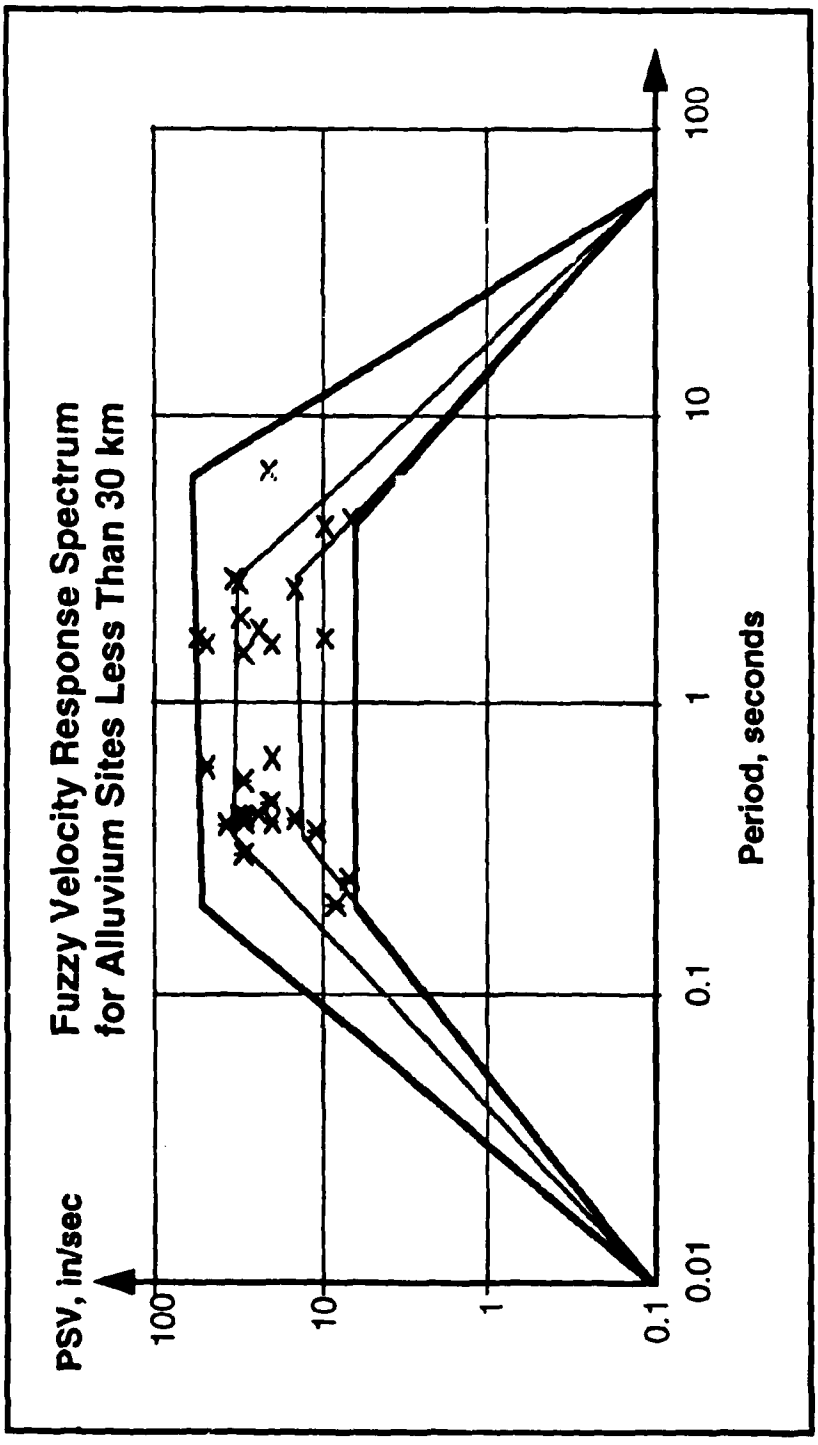

Figure 4.9: Fuzzy velocity spectrum for alluvium sites ($x < 30$ km).

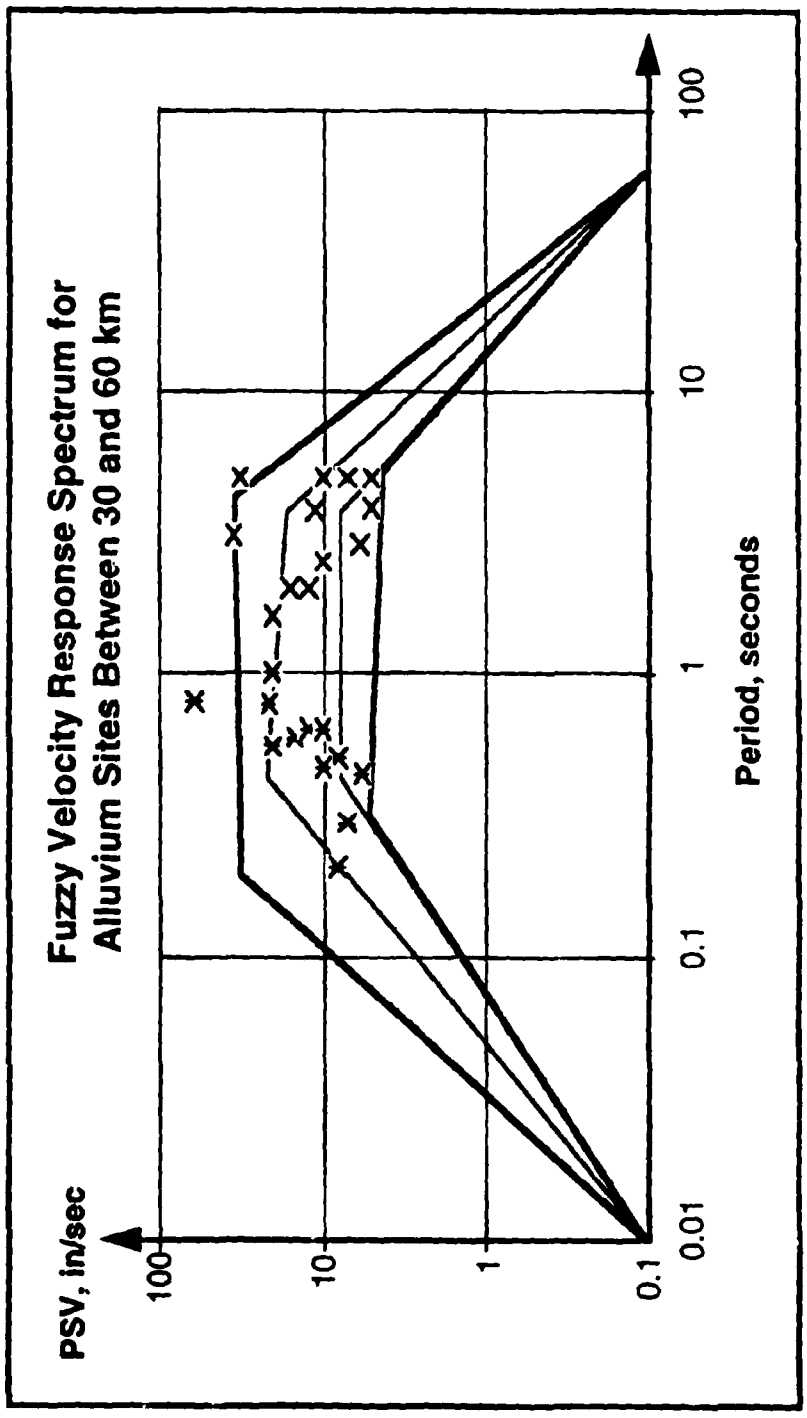

Figure 4.10: Fuzzy velocity spectrum for alluvium sites ($30 < x < 60$ km).

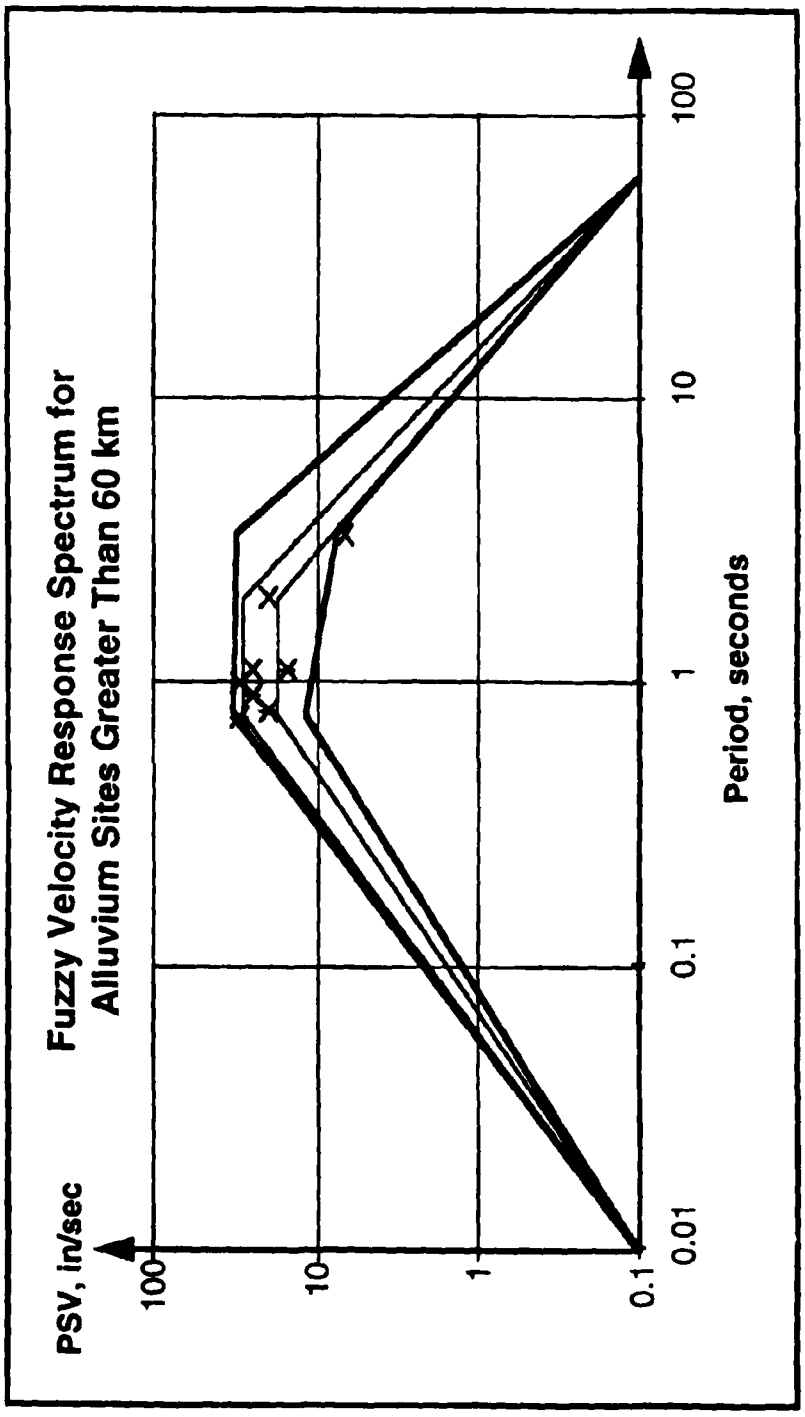

Figure 4.11: Fuzzy velocity spectrum for alluvium sites (x >60 km).

subduction mechanism of magnitudes similar to 7.1. Fuzzy sets are developed for two types of general soil conditions, rock and alluvium, at three distance categories. Use of the fuzzy response spectra helps the analyst to gain a better understanding of the potential maximum responses for the structure resulting in a fuzzy set for the maximum structural response.

The spectra developed in this chapter motivate further work in this area. In anticipation of future building codes, prediction of ground motion parameters [BJF93, Bor94] is moving towards the classification of soils into groups by shear wave velocity, rather than "rock" or "soil". Due to the broad range in frequency content and the new grouping of soil types, future refinements for this methodology include dividing the soil types into four categories based on shear wave velocities. In addition, other earthquakes of a similar magnitude can be added to the database. Ultimately, fuzzy response spectra should be developed for categories of soil type, distance, and earthquake magnitude providing the analyst with uncertainty information for different types of potential earthquakes.

CHAPTER 5

Illustrative Examples

This chapter presents two examples which illustrate the implementation of the calibration model. The first example is a two-dimensional plane frame structure with uncertainties in mass, material stiffness, and input motion. The second example is a three-dimensional structural model of the Santa Clara County Office Building located in San Jose, California, U.S.A. This structure has been instrumented since its construction in 1976, and information has been collected from several earthquakes since that time. In addition, system identification techniques have been used to evaluate structural parameters using the collected response data, and the results of these studies are available for comparison with the calibration model results. The fundamental uncertainties considered in this example are static loading conditions, material stiffness for steel, the stiffness contributions of the floor slab system, and input motion.

5.1 Small Scale Building – Example

The small scale example is a two-dimensional representation of a steel three story shear building with two wings on the first floor. This building is modeled based on uncertainties in the static loading conditions, material stiffness, and the input motion felt by the structure.

The building, shown in Fig. 5.1, has story heights of 10 feet and bay widths of 20 feet. The masses for the columns and beams are modeled as distributed loads of 4 slugs/ft and 8 slugs/ft, respectively. For the simplification of this example, the structure is assumed to have special moment resisting joints which are capable of fully transferring a moment; thus, the joints are assumed to be fully rigid with complete

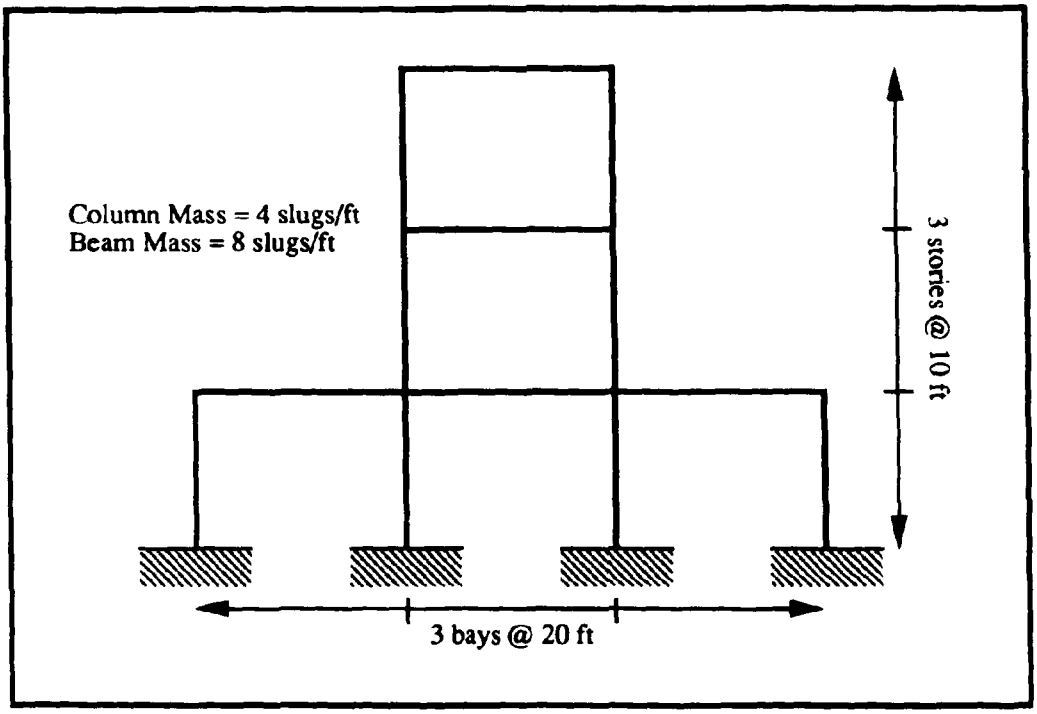

Figure 5.1: Three story shear building.

certainty. A finite element model is used to represent the structure using 13 Bernouli-Euler beam elements. The finite element method is a well accepted approximation in structural analysis; however, theoretically, an infinite number of elements is required for exact representation of structural members. In addition, the elements which assume pure beam theory (i.e., typically Bernoulli-Euler) represent the true physical system. The errors associated with the loading conditions (static and dynamic) and the uncertainty with the structure's stiffness properties are far greater than those introduced by a lack of discretization in the finite element model. Furthermore, in the analysis of a full-scale building it is rarely feasible to model the structure with more than one finite element per structural member. Therefore, this example will not be discretized further.

The fundamental fuzzy sets used for the analysis are given in Figure 5.2. Column mass, denoted by the crisp set, considers the uncertainty in the weight of the fire proofing material and architectual components, for example. Due to the few contributing uncertainties, the bounds created by α-cut 0^+ for this fuzzy set are tight; consequently, the same bounds are used to define α-cut 1. There is much more uncertainty associated with the mass of the beam elements. Beam element mass, in addition to the uncertainty of the element mass itself, include the masses which each element must support. Determination of the beam mass requires an estimate of the mass over the floor area and a calculation of the tributary area supported by the beam element. The trapezoidal fuzzy set quantifies the uncertainty associated with these mass estimates and bounds the initial mass estimate, M_o. The material stiffness fuzzy set is also given and has been established based on the methods presented in Chapter 3. The final uncertainty considered in this example is the input motion acting on the structure which is represented by the fuzzy velocity response spectra developed in Chapter 4.

5.1.1 Free-Vibration Analysis

The free-vibrational analysis is performed for this structure through repetitive solutions of the eigenvalue problem using the input parameters given in Figure 5.2. As the vertex method specifies, a solution procedure is performed at each α-cut level

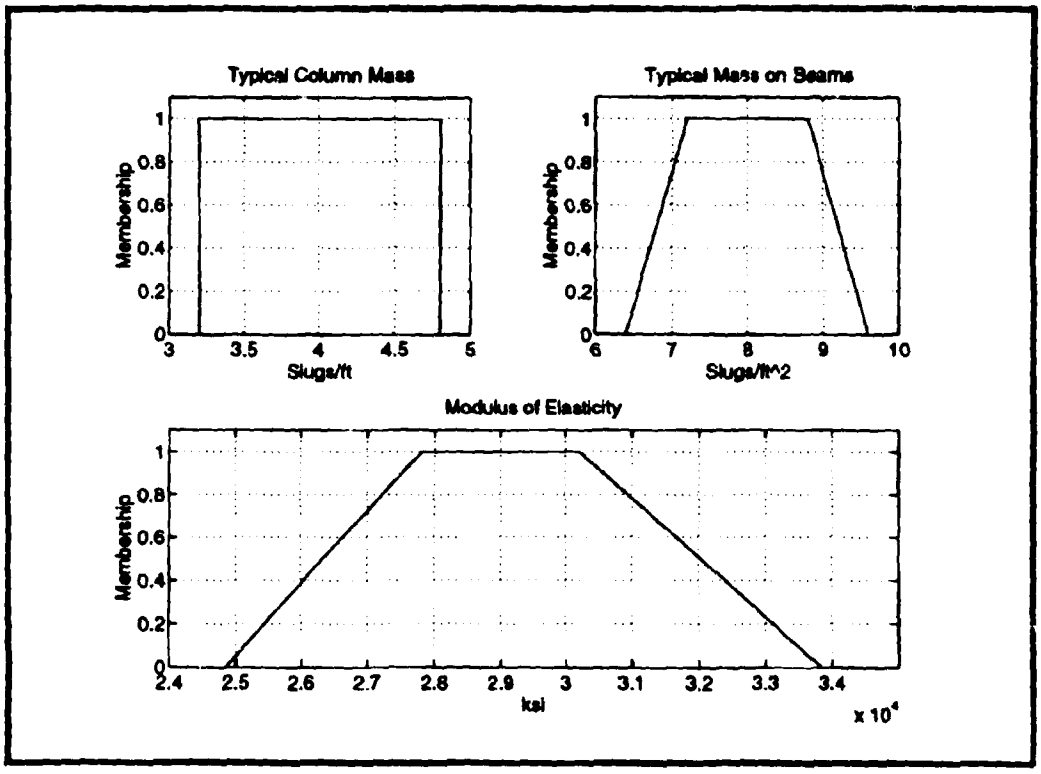

Figure 5.2: Fundamental uncertainty fuzzy sets for Example - I. Clockwise from the top left corner: (1) column mass; (2) beam mass; (3) modulus of elasticity for steel.

ensuring that the extreme bounds have been obtained for the resulting parameter. Care must be taken when applying the vertex method to a finite element model to keep track of the changing parameters. For example, one possible case for the mass conditions in the structure may be a maximum load at the top of the structure and minimum loads at the lower levels. Such a situation may cause the structure to be extremely flexible. This loading condition may occur during the construction of a facility when there is a considerable amount of construction equipment on the roof, and very little activity at the other levels. For the purposes of this thesis, it will be assumed that the extreme parameter conditions will occur together. In other words, all elements will have minimum or maximum mass simultaneously. This ensures that the eigenvalue problem will produce the extreme solutions of interest. It is important to realize, however, that by approaching the solution in this way, the torsional modes (which are often excited by eccentricities in mass and geometry) may not be represented realistically.

The four eigenvalue solutions (shown in Table 5.1) bound the potential values for the natural frequencies by strategically simulating values for the uncertain parameters. If there are lumped masses in the finite element model, then the high and low masses will follow the procedure established in Table 5.1.

The free-vibration solution is presented graphically in Figure 5.3. The natural frequencies (given in the top graph) for the structure have been converted to structural periods in the second graph. In these graphs, the first and second modes of vibration are denoted by solid lines. These resulting fuzzy sets give the potential range for uncertainty in the actual built structure by representing the the potential values

Table 5.1: Extreme values for mass and stiffness to obtain the frequency fuzzy set.

Solution	column mass	beam mass	steel modulus	frequency
1	high α-cut 1	high α-cut 1	low α-cut 1	low α-cut 1
2	low α-cut 1	low α-cut 1	high α-cut 1	high α-cut 1
3	high α-cut 0^+	high α-cut 0^+	low α-cut 0^+	low α-cut 0^+
4	low α-cut 0^+	low α-cut 0^+	high α-cut 0^+	high α-cut 0^+

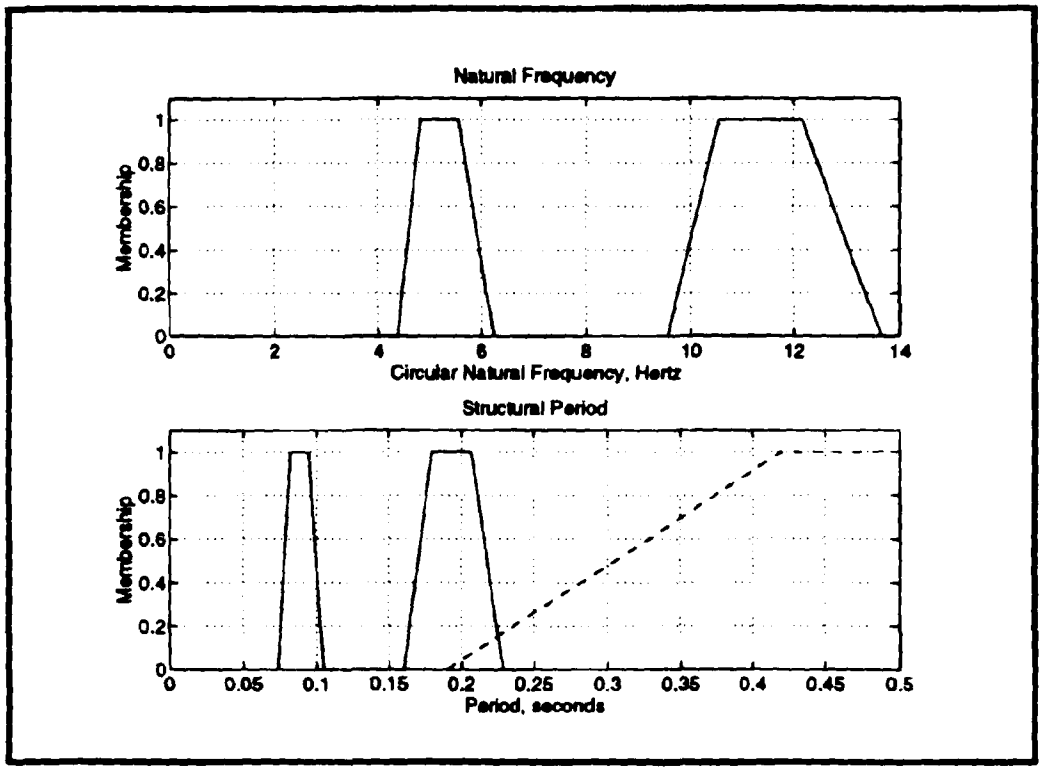

Figure 5.3: Top: Fuzzy sets for the first two natural frequencies (the fundamental fuzzy set is the lowest frequency corresponding to the first mode of vibration). Bottom: Corresponding fuzzy sets for the associated periods T, where $T = \frac{2\pi}{\omega}$ (here, the highest mode corresponds to the first mode of vibration). The dashed line denotes the predominant period fuzzy set for the input motion.

that the natural frequencies can have given uncertain fundamental parameters. Since calculation of structural modal properties is the first step in dynamic analysis, the uncertainty obtained here is an essential piece of information in the quantification of the uncertainty in structural response.

Two frequencies are given here, because the first two modes are superimposed to determine structural response. As the next step in analysis the frequency ratio is determined by comparing the ratio of the forcing frequency to the natural frequencies of the structure. Since each of these frequencies (in this case there are 3 frequencies; 2 natural frequencies and 1 forcing frequency) is a fuzzy set, the vertex method is again used to develop the resulting ratios.

5.1.2 Spectrum Analysis

The first step in evaluating the structural response due to an earthquake motion is to compare the dynamic characteristics of the structure to those of the site. This comparison can inform the analyst of the possibility of resonant conditions. A frequency ratio of 1.0 suggests severe response. If the dynamic characteristics (the dynamic frequencies) of the structure are similiar it is necessary to provide ample damping into the system to reduce the chances of extreme responses, as shown in Eq. 3.6. An excitation applied to the structure due to an earthquake is filtered by the soil column between the structure and bedrock. This filtering process is dependent on the dynamic properties of the soil. There are a number of analytical techniques used to quantify the dynamic properties of a soil column. Here, the fuzzy response spectra (presented in Chapter 4) are used to characterize the dynamic properties of the soil. For this reason, the uncertainty in frequency content of the surface motion is taken from the site dependent response spectrum for velocity. In this example, the fuzzy velocity response spectrum developed for soil sites between 30 and 60 km from the epicentral zone is used to develop the uncertainty in the frequency of the forcing function.

The uncertainty in period content of the input motion obtained from a fuzzy spectrum (depicted by the dashed line) is given in the second graph in Fig. 5.3. In this case, the input motion period fuzzy set extends beyond the graph. However,

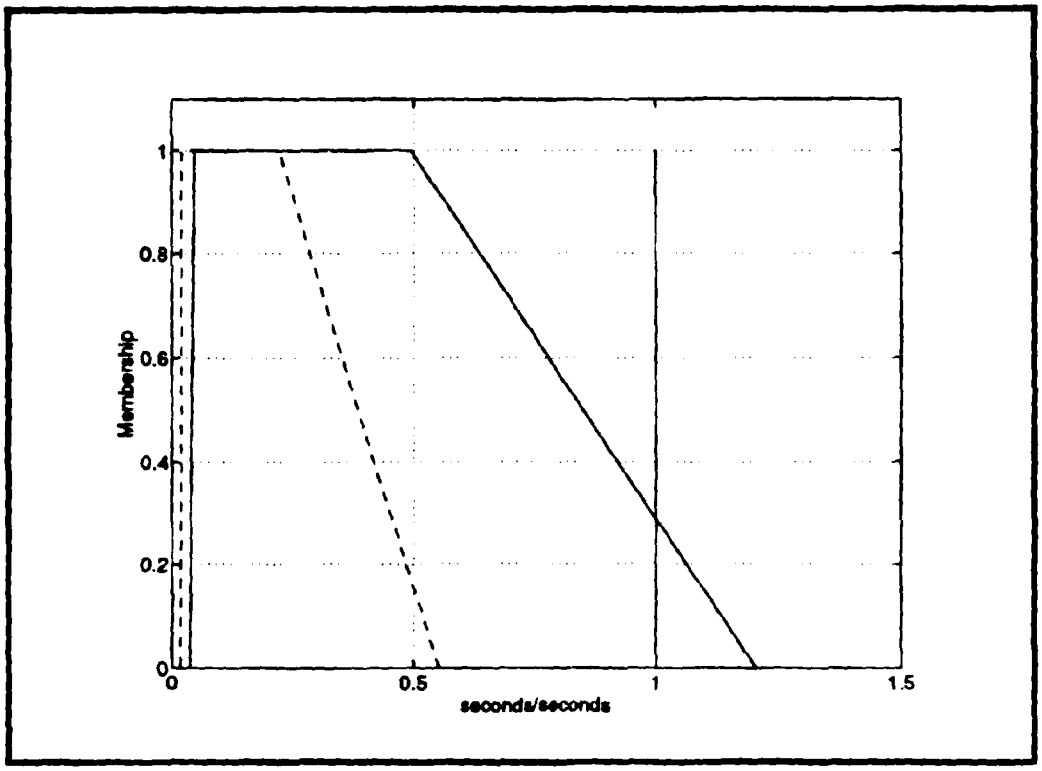

Figure 5.4: The frequency ratios, β_n, for $n = 1, 2$.

since this structure has relatively low periods, the higher periods are not relevant to this analysis. A fuzzy set is determined (shown in Fig. 5.4) for β_1 and β_2 where $\beta_n = \frac{T_n}{T}$ and T denotes the period of the input motion to the structure. The vertex method is used to find the uncertainty in the frequency ratio using the same iterative methods used to find the natural frequencies. Ratios for the first and second modes of vibration are depicted by the solid and dashed lines, respectively. The vertical line which crosses the horizontal axis at 1.0 highlights the region of frequency ratios which indicate the structure may be prone to resonant response. Here, it is found that only the first mode may exhibit resonant response. However, this is unlikely because only α-cuts taken below 0.3 produce bounds which cross 1.0. The second mode of vibration is well out of the range of resonant response. These results suggest

that not only will the first mode of vibration contribute significantly to the overall structural response for the fuzzy spectrum considered, but that the participation of the first mode is dominant to that of the second modal participation.

The possible maximum response for the structure is obtained by performing repetitive modal analyses for each α-cut level. Four values for S_v are used in the analysis which are obtained from the curves defining α-cut 1 on the fuzzy response spectrum. The two bounding period values at α-cut 1 from the free-vibration solution are used to obtain the S_v values. The vertex method requires that all possible iterations be performed for the analysis at each α-cut level. To accomplish this, every possible parametric combination is used at a particular α-cut level with the constraint that the earthquake participation factor and eigenvector must always be used with the same value for frequency. This is because the earthquake participation factor is dependent on the normalization of the eigenvectors, and for each eigenvector there is a corresponding eigenvalue (the resulting frequency values).

Modal superposition is performed four times using SRSS (Eq. 3.4), and the maximum and minimum values from these analyses bound the resulting fuzzy sets for maximum response. Repeating this procedure at α-cut 0^+ gives the bounds at the lowest level of membership. This procedure is explained in full detail in Appendix B. These fuzzy sets give both upper and lower bounds for the possible maximum response. Theoretically, the actual maximum response for a structure should fall within the lower and upper bounds for the fuzzy set denoting a range in maximum structural response. Since this process predicts the maximum response it does not make sense to represent a lower bound estimate. Consequently, the maximum response fuzzy sets are defined by a single sloped line from $\mu = 1$ to $\mu = 0$ which bound the maximum response for all levels of confidence. Furthermore, these results are only valid for the Loma Prieta earthquake from which the spectra were developed.

The resulting possible maximum response fuzzy sets for the displacement and acceleration of the roof are given in Fig. 5.5. Displacement spectral response can be found from the velocity response spectrum using the following equation.

$$S_d(n) = \frac{S_v(n)T_n}{2\pi} \tag{5.1}$$

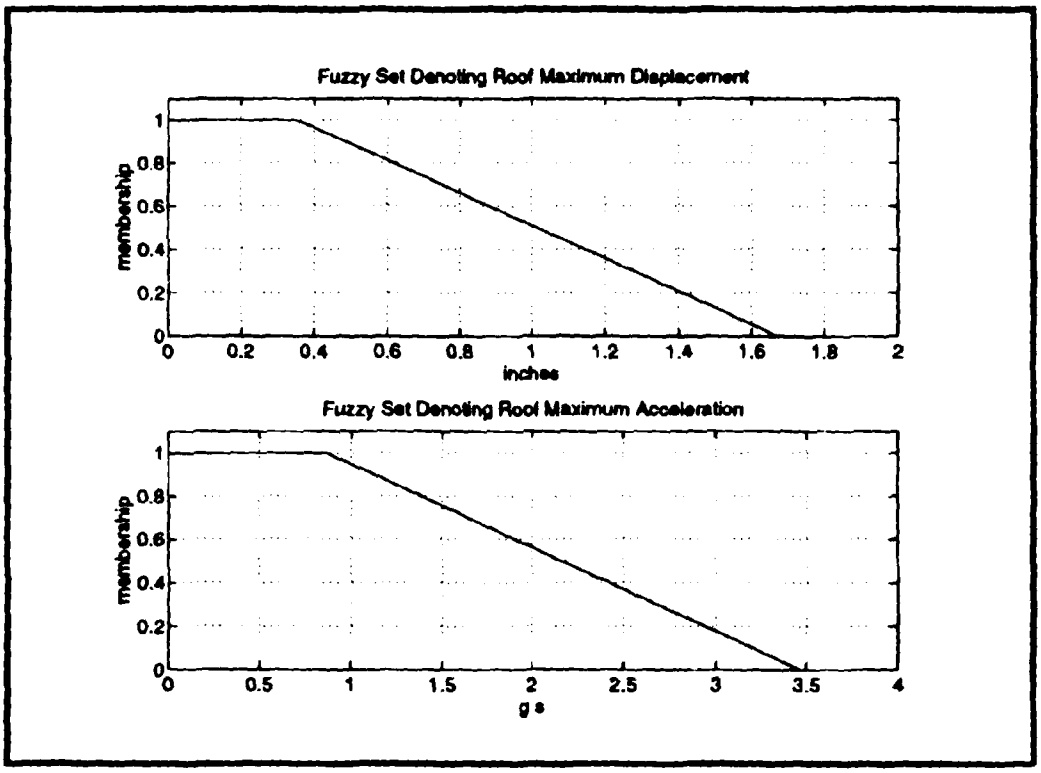

Figure 5.5: Maximum response fuzzy sets for roof displacement and acceleration.

where,

S_d = maximum displacement;

T = dynamic period of vibration; and

n = mode of vibration.

Since the displacement is proportional to the structural period and the periods are, in general, small (< 1) the resulting displacements are small. Similarly, acceleration is inversely proportional to the velocity response spectrum as shown in Eq. 5.2.

$$S_a(n) = \frac{S_v(n)2\pi}{T_n} \tag{5.2}$$

where,

S_a = maximum acceleration.

Therefore, the accelerations are higher for low structural dynamic periods. These characteristics are reflected in Fig. 5.5. The predicted acceleration and displacements for the structure are conservatively high because the structural periods fall between deterministic point C and fuzzy corner A. As discussed in Chapter 4, the resulting spectral values in these regions are high due to the placement of the two corner points.

5.2 Santa Clara County Office Building – Case Study

The following is a numerical example to demonstrate the application of the calibration model to an actual building. The Santa Clara County Office Building, located in San Jose, has been instrumented since construction to record earthquakes and has been well studied through the processes of system identification. This building, designed in 1972 and constructed by 1976, is a nearly square thirteen story structure consisting of a steel moment resisting frame with members encased in fire proofing and plaster. The building stands 188 feet in height with sides each measuring 147.5 feet. Refer to the elevation and plan views in Figs. 5.6 and 5.7.

The building was designed using the seventh edition of the *Manual of Steel Construction (1970)* by the American Institute of Steel Construction and consists of seven

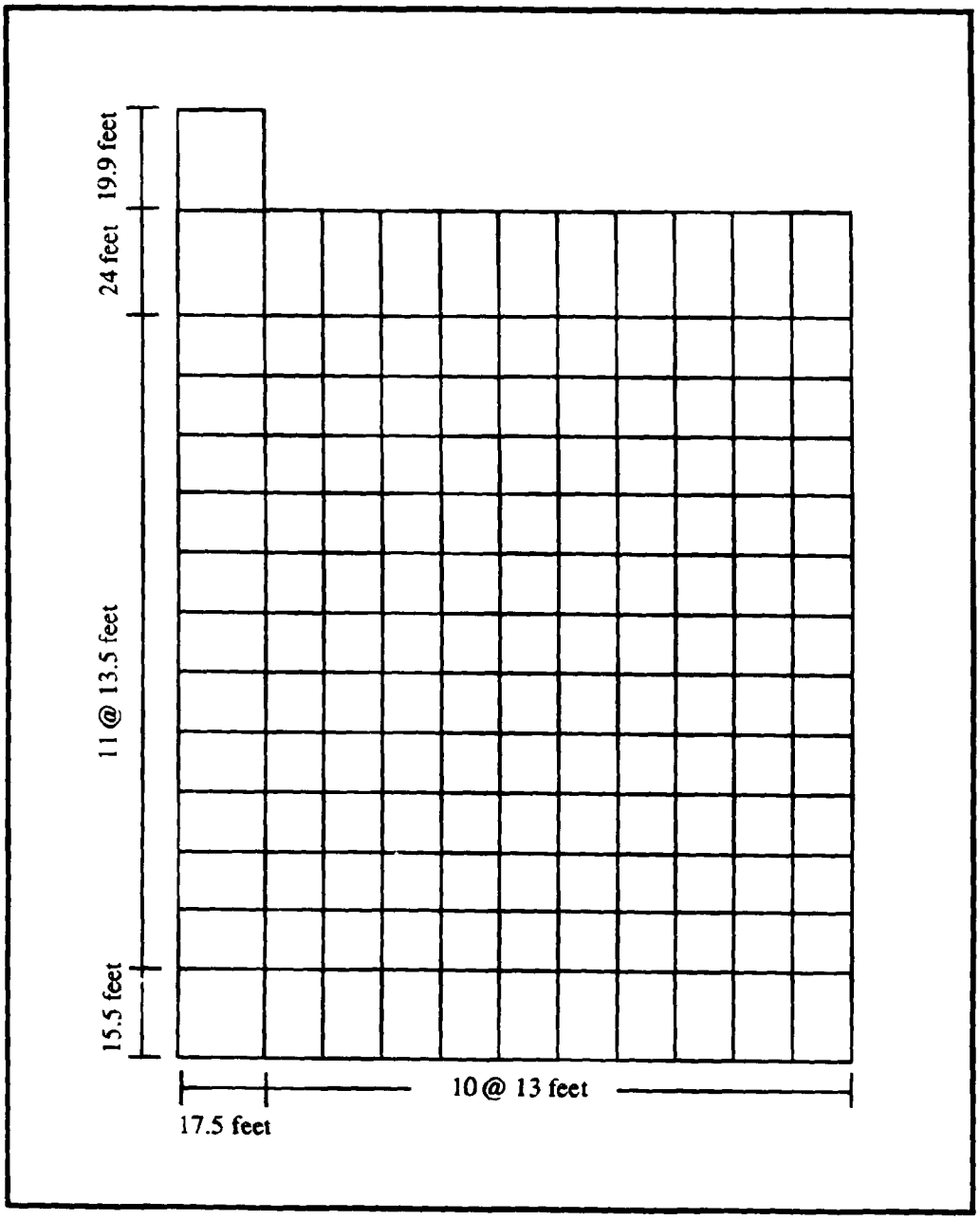

Figure 5.6: Elevation view of the Santa Clara Co. office building.

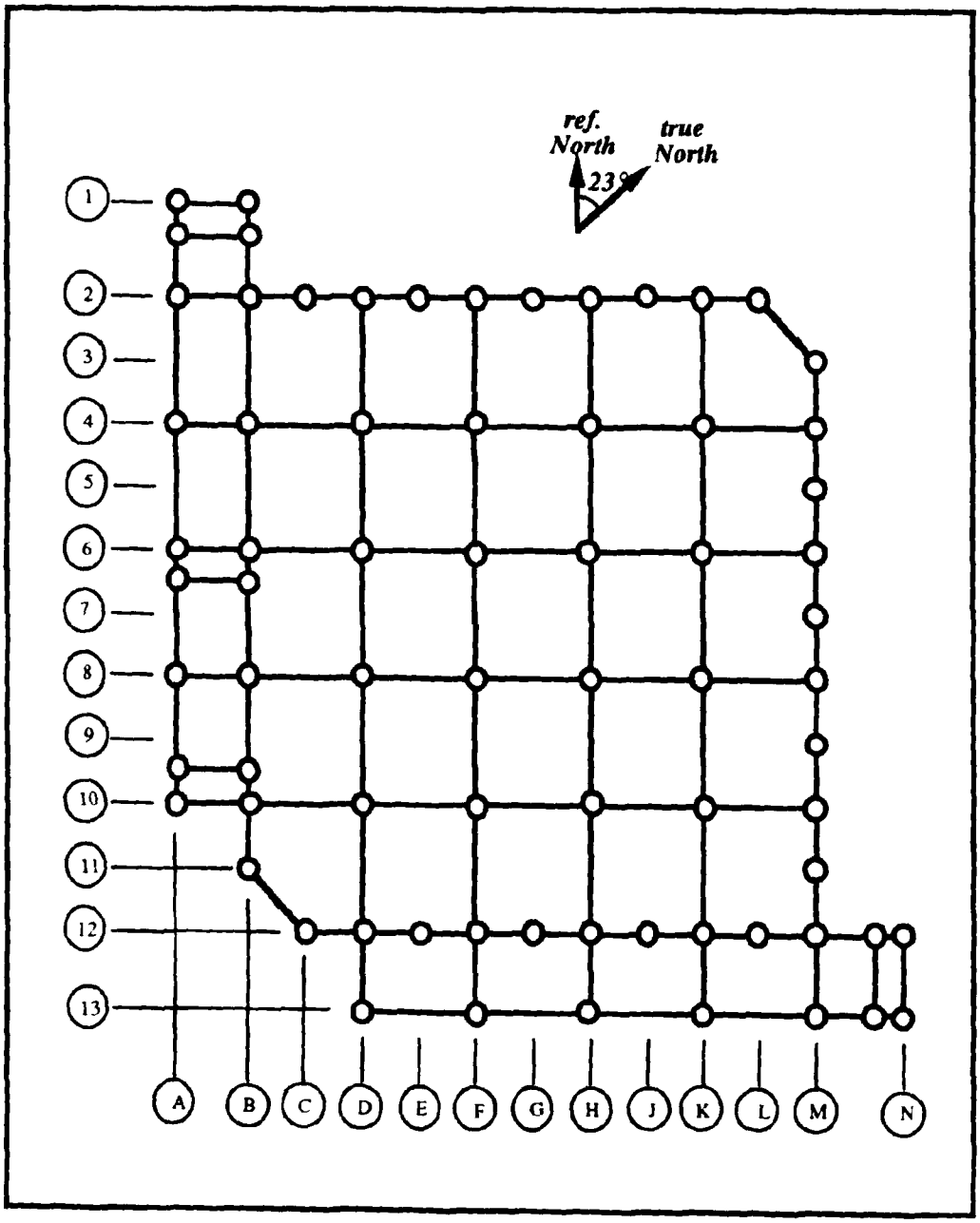

Figure 5.7: Plan view of the Santa Clara Co. office building.

frames spaced 26 feet apart in both the East-West and North-South directions. The columns are spaced 26 feet apart except on the perimeter where the spacing is only 13 feet (see Figure 5.7). The steel moment resisting frames are designed to carry the lateral loads of the structure and are located primarily on the perimeter of the structure. Vertically, the frames of the building are supported by box columns and wide flange columns with attached steel plates. Steel girders and wide flange beams make up the floor plan of the building.

On the south and west side of the central supporting structure are wings (17.5 feet wide) used to house the elevators and stairwells. The frames that compose these external walls are not moment resisting frames, but carry gravity loads only. These sides of the building have walls made of corrugated steel; whereas, the other two faces of the building are comprised mostly of glass. This building has been studied by a number of researchers, and the results from some of this prior research are summarized in the following subsection.

The objective of this case study is to demonstrate the use of the calibration model on a full scale realistic example. Blueprints for the structural design were obtained from the County of Santa Clara. In this case study, the potential values for the structural frequency are obtained through a free-vibration analysis. The maximum responses also are predicted using the fuzzy response spectra developed for the Loma Prieta earthquake. Results obtained from the calibration model are compared to those obtained through system identification methods. For verification of the calibration model, the building's identified dynamic characteristics need to be within the fuzzy sets developed.

5.2.1 Results Obtained from System Identification

There are 22 instruments, distributed among four floors and the basement level, used to record acceleration. Through conventional system identification techniques the building's natural modes of vibration have been identified from its response to several earthquakes. The lowest two modes are predominantly translational with periods of 2.2 seconds (along the East-West axis) and 2.1 seconds (along the North-South axis) the corresponding frequencies are 0.45 Hz and 0.48 Hz, respectively. The third

mode, which is predominately torsional, with a period of 1.72 seconds (a frequency of 0.58 Hertz). The fourth and fifth modes are again translational corresponding to the East-West and North-South directions, respectively. The periods of both these modes are identified to be within the range of 0.60 and 0.70 seconds (1.43 and 1.67 Hz.). These values were identified by Boroschek and Mahin [BM91]. The response of this structure was recorded during the Morgan Hill earthquake of 1984 (M = 6.2), the Mt. Lewis earthquake of 1986 (M = 5.8), and the Loma Prieta earthquake of 1989 (M = 7.1). During each of these earthquakes, the building response was classified as severe. The maximum displacement at the South West corner of the structure on the twelfth floor was 45 cm and 39 cm for the North-South and East-West directions, respectively. The maximum acceleration at this corner was recorded as 0.34 g's in the North-South direction.

5.2.2 Free-Vibration Results from the Calibration Model

This subsection gives the results obtained from the calibration model for the free-vibration analysis. An analytical finite element model is developed to study the modal properties of the structure. The calibration model is performed based on the finite element model coupled with estimates of the contributing fundamental uncertainties. The result includes bounded ranges for the structural natural frequencies.

Due to the large size of the full three dimensional model (N > 10,000 degrees-of-freedom), preliminary tests were performed on two-dimensional frames representative of the structure's predominant behavior. From these tests natural frequency fuzzy sets for the four lowest bending modes (1st, 2nd, 4th, and 5th modes) of vibration were obtained. The results highlighted the similarity between the frequencies in the North-South and East-West directions for the structure. However, the analytical model was stiffer than the actual structure due to its inability to capture the torsional response of the building. The results obtained from the two-dimensional modeling were encouraging enough to consider more detailed analysis of the structure. Due to the significant response of the torsional mode in the building's dynamic behavior, analysis of a three dimensional model is mandatory. The building was modeled in three dimensions using skeletal beam finite elements. The CRAY C90 located at the

San Diego Supercomputing Center was used to perform the free-vibrational analysis for the structure.

The calibration of the three dimensional model considered uncertainty in the modulus of elasticity for steel, the static loading conditions, and the stiffness contributions from the floor system. Material property uncertainty is the same as described in Section 5.1. Uncertainty in the static loading conditions is estimated using Eq. 3.13 with initial mass estimates, M_o, $\mathcal{X}(\alpha = 1) = .4$, and $\mathcal{X}(\alpha = 0^+) = .6$. The estimated mass, M_o, is 60 psf for the typical floors and 90 psf for the twelfth floor and roof (atypical floors) and is primarily due to mechanical equipment in the building. The stiffness of the floor system is the final fundamental uncertainty considered in this analysis. These fundamental uncertainties are displayed graphically in Fig. 5.8.

The gravity loads on the floor systems produce moments which cause the surface of the floor system to be in tension near the column supports. In this case study, it is assumed that the concrete is fully cracked in these regions. Consequently, these cracked regions will not be able to contribute stiffness to the structural system. At α-cut 0^+ the contributions of the floor system stiffness are taken to be extremes with bounds ranging from zero stiffness contribution to full stiffness contribution. The floor system is analyzed as a continuous beam over roller supports. The gravity loads on the floor systems produce moments which cause the surface of the floor system to be in tension near the column supports. In this case study, it is assumed that the concrete is fully cracked in these regions. Consequently, these cracked regions will not be capable of contributing stiffness to the structural system. The upper bound for α-cut 1 considers 100% of the floor length contributing to the floor stiffness (i.e., no concrete has cracked). The lower bound for α-cut 1 is calculated by determining the length of the floor system where the concrete is in compression (i.e. not cracked). In this case study the rigidity of the floor system for this bound is taken to be 66% of the full floor span.

The first three modes are shown in the form of fuzzy sets for the structural natural frequencies and the corresponding periods in Fig. 5.9. The fundamental frequency (a translation mode in the EW direction) is denoted by the solid line, while the second (translational mode in the NS direction) and third (predominantly a torsional mode)

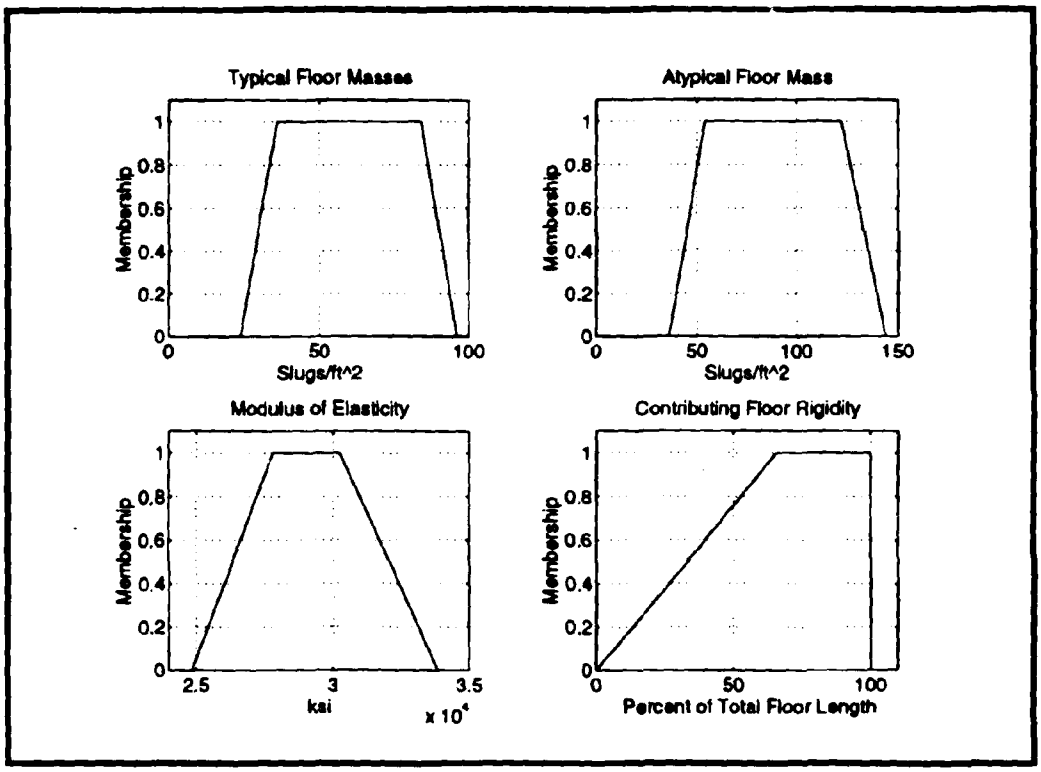

Figure 5.8: Fundamental uncertainties used in the calibration of the Santa Clara County Office Building.

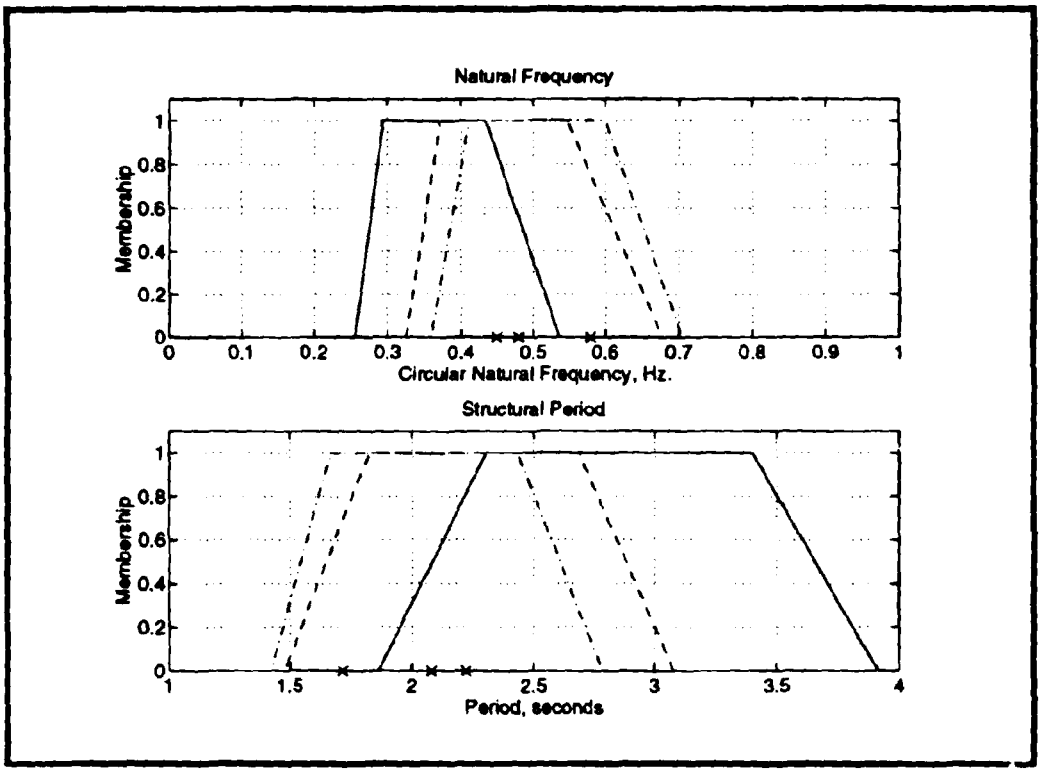

Figure 5.9: First three natural frequencies and the corresponding structural periods.

modes are depicted by the dashed and dash-dotted lines, respectively. The 'X' marks on the horizontal axis in the graphs denote the buildings first three modal frequencies which were obtained through system identification. Uncertainty in the structural periods is obtained through a conversion from the natural frequency. This structure is considered to be a dynamic building since its natural frequencies fall well within the range of frequency content of most earthquakes.

5.2.3 Structural Response Results Obtained from the Calibration Model

This subsection presents the resulting upper bound for structural response obtained from the calibration model. Free-vibration results from the calibration model with the fuzzy spectra, developed in Chapter 4, are used to determine the potential maximum response for analytical degrees of freedom. The resulting maximum response is presented for the displacement and acceleration of the South West corner on the twelfth floor.

The site for the Santa Clara County Office Building is primarily stiff clay. The structure is located at a distance of 35km from the Loma Prieta earthquake rupture zone. Consequently, the fuzzy response spectrum (Fig. 4.10) developed for alluvium sites between 30 and 60 km of the rupture zone is used for this analysis. Estimates for the maximum structural response are shown in Fig. 5.10.

5.2.4 Discussion of the Case Study

The Santa Clara County Office Building has suffered severe responses during each of the three earthquakes (Mt. Lewis, Morgan Hill, and Loma Prieta). This has been primarily due to the similarity in natural frequency between the translational modes in the North-South and East-West directions. Furthermore, the dynamic characteristics of the local site conditions are similar to that of the structure which promotes resonant response. Boroschek [BM91] determined from Fourier analysis that the natural periods of the site are approximately 2 and 1 seconds for the first and second modes of vibration, respectively. Low damping within the structure, which is due to

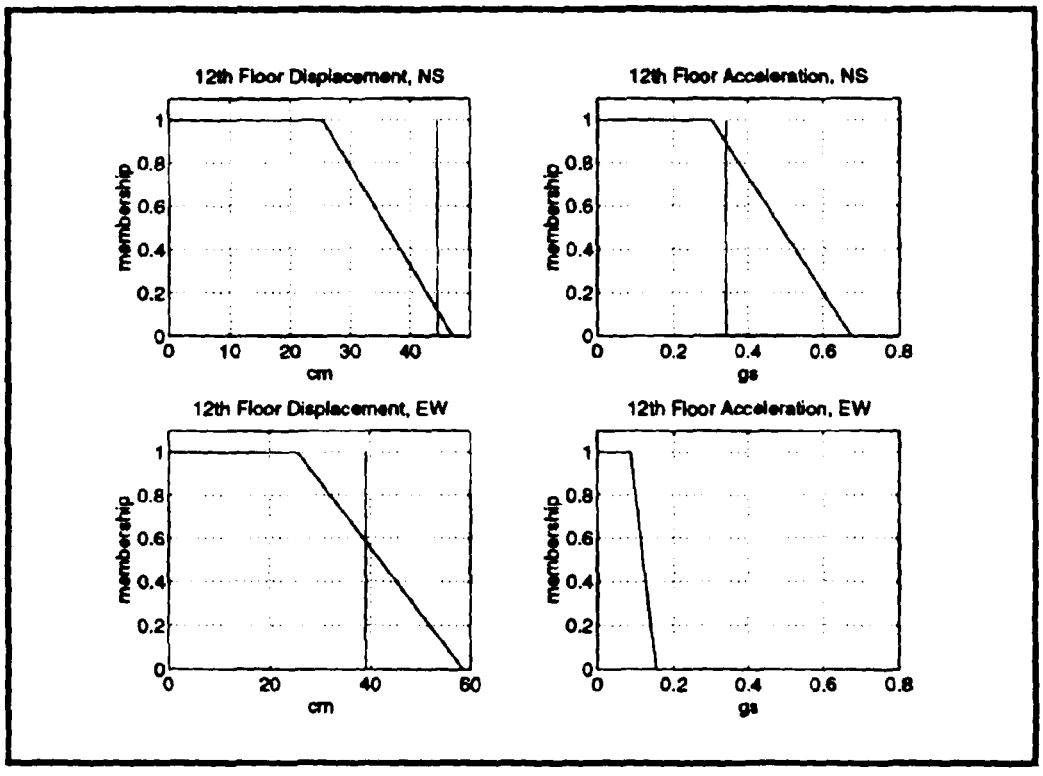

Figure 5.10: Potential maximum response for the North-South and East-West directions at the twelfth floor.

Table 5.2: Natural periods and damping obtained from system identification.

Predominant Direction	Mode	Period (sec.)	Damping (%)
EW	First	2.15 - 2.20	2-3
NS	Second	2.05 - 2.10	2-4
Torsion	Third	1.70	-
EW	Fourth	0.65-0.75	-
NS	Fifth	0.60-0.70	-

the bare interior architectual characteristics, does not sufficiently suppress the large responses. Dynamic response of the structure has been as long as 80 seconds. In an effort to alleviate these problems, viscous dampers have recently been added to the structure since the Loma Prieta earthquake in 1989. System identification using the earthquake input motions and the structure's dynamic characteristics have given the results shown in Table 5.2 which is adapted from Boroschek [BM91].

The calibration model is capable of predicting the dynamic characteristics for the Santa Clara County Office building. The frequency fuzzy sets, in general, contained the actual frequencies of the structure. Both the second and third natural frequency fuzzy sets contained the actual frequencies within the bounds given by α-cut 1. The fundamental frequency fuzzy set contained the actual fundamental frequency within the bounds given by α-cut 0.8. Due to large "overlap" in the membership functions representing frequency, this structure may experience significant modal beating.

Conclusions made from results of this case study are itemized below:

- The calibration model captured the frequencies for the actual structure, where, the 1st frequency falls within α-cut 0.8 bounds and the 2nd & 3rd fall within α-cut 1 bounds.
- The calibrated frequencies are well within the range of the natural frequencies for the site suggesting the possibility of severe structural response.
- The maximum response fuzzy sets, in general, captured the actual response.
- Predicted displacement response is lower than the actual response because the

spectra were developed for 5% critical damping, which is high compared to the identified damping in the structure.

- Maximum acceleration also was captured in the fuzzy sets.
- The actual displacement of 44 cm (relative from the 12th floor to the ground) fell within α-cut 0.1 bounds. Although this large displacement may appear to be discouraging, it can be explained. First, the structure is very lightly damped (only 1-2% critical damping per mode). The response spectrum used in this analysis was obtained based on 5% damping from the site dependent spectra. Therefore, it is not surprising that the response predicted with the calibration model is low compared to actual response. Second, the modal beating phenomena has been used as an explanation to the structure's severe displacements.
- The actual responses are higher than those predicted by full membership in the predicted fuzzy response. This is due to the modal beating of the structure. Spectral analyses only predict the maximum response not the actual time history. Therefore, these methods cannot predict the modal beating phenomena or the duration of the structural response. The long response of the building can contribute to the higher accelerations and displacements.

The comparison between the actual structural response and the results obtained from the calibration model validates the quality of the proposed model. It is proposed that the calibration model can be used at the design stage to inform the analyst of potential problems associated with the structural dynamic response. Therefore, with proper application of the calibration model the analyst or designer can make modifications to the design based on the resulting fuzzy sets. Thus, reducing the possibility of inappropriate structural response.

Given the overlap of the membership functions for the natural frequencies and the membership function for the frequency content of the potential earthquake motion an analyst will suspect the likelyhood of severe resonant response. As shown in Eq. 3.6 the dynamic amplification factor (which represents the amplification of response for an SDOF system) is maximum when the system natural frequency and the frequency

of the input motion are close. However, the amplification decreases as the damping in the system increases. The potential for severe response should alert the analyst to investigate the structure's potential to dissipate energy through damping. Therefore, in the case of the Santa Clara County Office building where there is evidence of potential resonant response, a designer may choose to add more damping to the structural system. This can be done by adding floor to ceiling nonstructural partition walls into the workspace of the building or cladding (which is capable of dissipating energy) to the exterior of the structure. In this application of the calibration model, the *low damping characteristics of the building were not predicted.*

5.3 Assessment of Fuzzy Methodology to Probabilistic

Implementation of the adaptive analysis methodology requires an analyst to bound contributing errors at the design stage of a project in order to obtain a prediction of the potential range in the higher-level dynamic parameters. The ultimate uncertainty in the dynamic parameters is based on the initial uncertainty estimate for the fundamental parameters made by the analyst. Thus, the selection of the initial uncertainty estimates must be made carefully. An advantage to using fuzzy mathematics for uncertainty analysis is that only a few calculations are needed to quantify a higher-level fuzzy set.

Probabilistic techniques which already have been established are arguably more rigorous. The purpose of the following example is to compare the results obtained from the approach proposed in this thesis and those obtained from Monte Carlo simulation. Uncertainty in the stiffness and mass in the analytical model are considered in the analysis.

Free-vibration analyses are performed for the two-dimension frame used in Section 5.1 (shown in Fig. 5.1). The uncertainty in the fundamental parameters for the stiffness and mass properties of the structural system is represented in terms of both fuzzy sets and probability density functions. Here fundamental fuzzy sets are given for beam and column masses as well as material stiffness.

To compare the two techniques it is necessary to produce probability density

functions which represent the uncertainty defined by the fuzzy sets. The following section describes the mapping procedure used to convert the fuzzy sets to probability density functions. Immediately following is a description of the simulation technique used in the analysis.

5.3.1 Monte Carlo Simulation

Monte Carlo simulation is used in this example to represent a sample of experimental observations for the mass and stiffness properties of the structural system shown in Fig. 5.1. The simulation is performed by generating random values for the mass and stiffness properties of the structure based on parameters which describe the probability density function. The dynamic equations of motion are solved using simulated random values to obtain a representative sample of the structure's dynamic properties. This process is repeated to obtain a smooth histogram which gives the number of occurrences for various values of a structure's natural frequency.

The simulation process is performed by first generating random numbers in a uniform distribution between 0 and 1.0. These standard uniform variates are then transformed to random numbers representative of a specified probability distribution [AT75b]. In the following example, random numbers are generated for lognormal distributions. Equations 5.3 and 5.4 give a relationship between two independent standard uniform variates and two independent normal variates for the normal distribution, $N(\mu, \sigma)$ [BM58].

$$x_1' = \mu + \sigma\sqrt{-2\ln U_1}\cos(2\pi U_2) \tag{5.3}$$

$$x_2' = \mu + \sigma\sqrt{-2\ln U_1}\sin(2\pi U_2) \tag{5.4}$$

where,

μ = the mean of the normal distribution;

σ = the standard deviation of the normal distribution;

$U_{1,2}$ = two independent standard uniform variates; and

$x'_{1,2}$ = two independent normal variates.

A random number, x, from a lognormal distribution, $N(\lambda, \zeta,)$, with parameters,

$\lambda = \ln \mu - \frac{1}{2}\zeta^2$ and $\zeta^2 = \ln\left(1 + \frac{\sigma^2}{\mu^2}\right)$ is related to the normal variate, x' where

$$x = e^{x'} \tag{5.5}$$

In this example, three parameters are simulated to obtain an uncertainty prediction for the structure's natural frequency. These parameters are: the mass distribution on the beams; the mass distribution on the columns; and the modulus of elasticity for the steel members. Fuzzy sets are typically defined for parameters when there is not enough quantifiable information available to adequately define a probabilistic distribution. Therefore, it is difficult to develop a clear relationship between a fuzzy set and a probability density function. However, because this example compares the uncertainty obtained from the proposed fuzzy approach and that obtained from the more traditionally used probabilistic approach, fundamental uncertainties must be established such that the fuzzy sets and probability density functions are comparable. Lognormal probability density functions are used to model the uncertainty represented as fuzzy sets in Section 5.1. Lognormal functions are selected for use in this example to guarantee that all occurrences of the random variables are greater than zero.

This example uses the probabilistic uncertainty for the modulus of elasticity for steel which is presented in Section 3.3.2. The modulus is a random variable represented by a lognormal distribution with mean and coefficient of variance, 29,000 ksi and 0.06, respectively. To perform the simulation, lognormal distributions described by mean and coefficient of variance parameters are developed to quantify the uncertainty described by the mass fuzzy sets. The mean and coefficient of variance are defined such that α-cut 1 bounds 51% of the area beneath the lognormal distribution and α-cut 0^+ bounds 99% of the area, as explained in Section 3.3.2. Two α-cuts are used to define the two unknown lognormal distribution parameters, (λ and ζ, which represent the probabilistic occurrence for the mass variables; however, the curvature of the lognormal distribution makes it difficult to select a mean and coefficient of variance which correspond to the bounds established by the fuzzy sets. Consequently, the

Table 5.3: Alpha-cut bounds, mean and coefficient of variance for the modulus and mass fuzzy sets.

α-cut	P(a ≤ E ≤ b)	mean	cov	lower bound	upper bound
		Modulus of Elasticity			
		ksi		ksi	ksi
0.0^+	99%	29,000	0.06	24,847	33,843
1.0	51%	29,000	0.06	27,822	30,224
		Distributed Beam Masses			
		slugs/ft		slugs/ft	slugs/ft
0.0^+	99%	8	0.112	6.4	9.6
1.0	51%	8	0.112	7.2	8.8
		Distributed Column Masses			
		slugs/ft		slugs/ft	slugs/ft
0.0^+	99%	4	0.106	3.2	4.8
1.0	51%	4	0.106	3.6	4.4

final selection for the distribution parameters are made such that the standard deviations required for α-cut 1 and for α-cut 0^+ are averaged. Table 5.3 gives the fuzzy sets used in this comparative example and the corresponding distribution parameters used in the simulation.

The simulations are performed with three independent random variables. Three seeds are used to generate three independent series of random numbers, one for each of the three random variables. Each structural member has the same stiffness properties, each column member has the same mass, and each beam member has the same mass (which may or may not be the same as the columns). In reality, there will be some dependence between the properties in the structural members. However, it is unlikely that each of the member types will have the same mass and stiffness as described here. Implementation of the calibration model requires that each solution must be based on extreme values given by the fundamental fuzzy sets. This approach is conservative because it assumes that all masses will be low, for example, rather than the mass in a particular area of the structure. From a probabilistic standpoint, analyses can be performed such that each of the masses is independent of the others. For the

purposes of comparison, the probabilistic simulation is performed such that each beam or column has the same mass and stiffness properties as the other beams and columns.

5.3.2 Discussion and Assessment of the Two Methods

Figure 5.11 shows the resulting fuzzy sets and histograms for the two lowest natural frequencies. The vertical axis in the figure gives the number of occurrences for the resulting frequencies. Three thousand simulations were performed to obtain relatively smooth histograms for the two frequencies. The trapezoidal fuzzy sets give bounds for the most possible range of frequencies (membership level of 1) and the most extreme range of frequencies (membership level of 0). Although not denoted on the axes, the highest level of confidence for these fuzzy sets is 1.0. It can be seen in the figure that α-cut 1 bounds most of the occurrences and α-cut 0 bounds essentially all of the occurrences.

Four eigensolutions are performed to obtain the fuzzy sets shown in the figure. The fuzzy sets obtained from the four solutions using the calibration model is compared to the histogram based on three thousand samples. Three thousand samples were used to produce smooth histograms. There are procedures available such as Latin Hypercube sampling which reduce the number of simulations required for a smooth result. If such a method is used, the number of samples typically needed is greatly reduced, decreasing the computational intensity of this probabilistic approach.

This example has compared the computational intensity required for the calibration model and the more traditionally used probabilistic simulation. Probabilistic simulations are based on fundamental uncertainties represented as probability distributions. A probability distribution is fully defined by selecting the type of distribution (i.e. lognormal, beta, etc.) and its parameters. The parameters, mean and standard deviation, need to be defined for the lognormal distributions used in this example. These parameters are based on measurable quantities for the uncertain parameter. The calibration model requires uncertain fundamental parameters represented as fuzzy sets. Fuzzy sets can be established for an uncertain parameter based on measured quantities or expert opinion. Thus, fuzzy sets can be obtained from

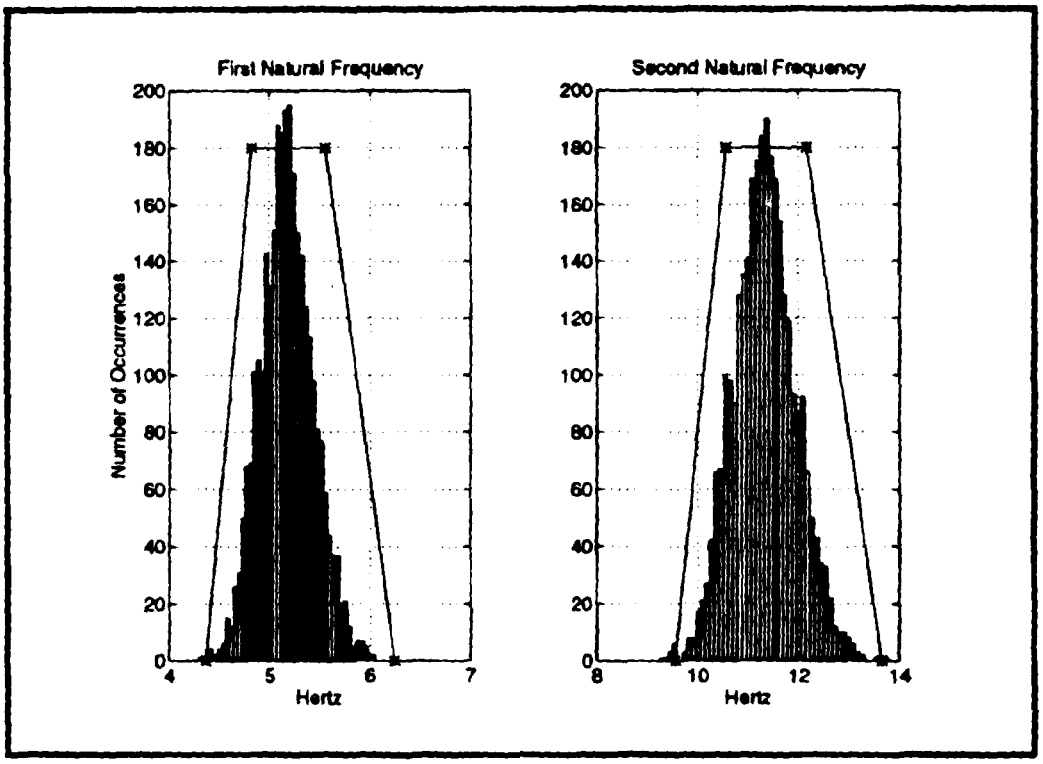

Figure 5.11: Fuzzy sets with levels of membership from 0^+ to 1 are overlaid on histograms for the first and second natural frequencies.

probabilistic information; however, it is difficult to determine the value of probabilistic parameters from fuzzy sets.

This example was structured to demonstrate the solution process required for both the fuzzy and probabilistic approaches. Although the frequency of occurrence for parametric values can be inferred from both approaches, the probabilistic technique gives a more rigorous result. Results from the calibration model can increase the analyst's understanding about potential parametric behavior with a minimal amount of computations. Thus, when an analyst needs to understand the consequence in dynamic behavior due to a design change, the calibration model is a useful and appropriate tool.

CHAPTER 6

Formulation of the Degradation Model

Prediction of the potential degradation of structural properties' makes it possible to design a structure considering the change in its fundamental characteristics. In the proposed adaptive analysis models, fuzzy mathematics is used to quantify the initial error in a structure's dynamic parameters and the error in the dynamic parameters as the structure ages. The purpose of this chapter is to formulate the framework for the degradation model which gives a prediction of the error in dynamic properties as a function of time. As in the calibration model, the calculation of uncertainty in dynamic parameters is based on the solution of the equation of motion. Section 6.1, which follows, presents the fuzzy representation of the degradation errors which are considered in the solution of the dynamic equations of motion. The development of degradation errors for fundamental parameters is discussed in Section 6.2. Implementation of the degradation model is demonstrated in Section 6.3 through the use of a small example. Finally, Section 6.4 gives a short discussion pertaining to the application and limitations of the degradation model.

6.1 Fuzzy Representation of the Degradation Model

A degradation model is added to the calibration model to predict the gradual degradation of structural properties as the structure ages. This model is time dependent and can be used to estimate the structural characteristics at any point during the structure's lifespan. Fuzzy sets with time dependent membership functions are developed to represent the deterioration of structural integrity and the changes in the structural parameters. This time dependent function takes the following form for natural

frequency, assuming that frequency will decrease as the structural stiffness degrades:

$$\mathcal{F}_{\alpha}^{dg} = \left\{[c,d] | c = \omega_o - \left[\mathcal{E}_{cal}^{L}(\alpha) + b^{L}(\alpha)t\right]; d = \omega_o + \left[\mathcal{E}_{cal}^{U}(\alpha) + b^{U}(\alpha)t\right]\right\} \qquad (6.1)$$

where,

$\mathcal{F}_{\alpha}^{dg}$ = uncertainty in degraded frequency at a membership level, α;

$b^{U,L}$ = slope for the upper and lower bounds, respectively of the degradation function;

t = time; and

c, d = lower and upper bounds, respectively, for each α-cut.

The estimation of the extent of structural degradation over time and the slope, b, of the degradation function is found from the properties of the construction materials, typical loading and unloading patterns on the structure, and structural maintenance needs. As with the calibration model, multiple analyses of the structural model are performed to establish the membership function of the fuzzy set representing degradation.

The degradation model consists of a calibration fuzzy set superimposed with two additional fuzzy boundaries to represent the changing error bounds over time. The degradation fuzzy set supporting this model is developed from the calibration fuzzy set which is shown in Fig. 6.1. The increasing error bounds in time are modeled with the use of two additional fuzzy boundaries, represented by the shaded areas in the figure. These fuzzy sets vary over time to model the long term structural degradation.

Equation 6.1 represents the change in frequency and the corresponding error in frequency prediction as a function of time. The dynamic properties of a structural system are dependent on the fundamental parameters as shown in Eqs. 3.9 and 3.10. The mass and stiffness properties of the structure are used in the solution of the eigenvalue problem (Eq. 3.2) to obtain the structure's free-vibration characteristics. Therefore, to predict the degradation characteristics of the frequency for the structure, it is necessary to model the degradation characteristics of the fundamental contributing parameters. The eigensolution is then solved discretely with bounding values for the fundamental parameters at different instances in time.

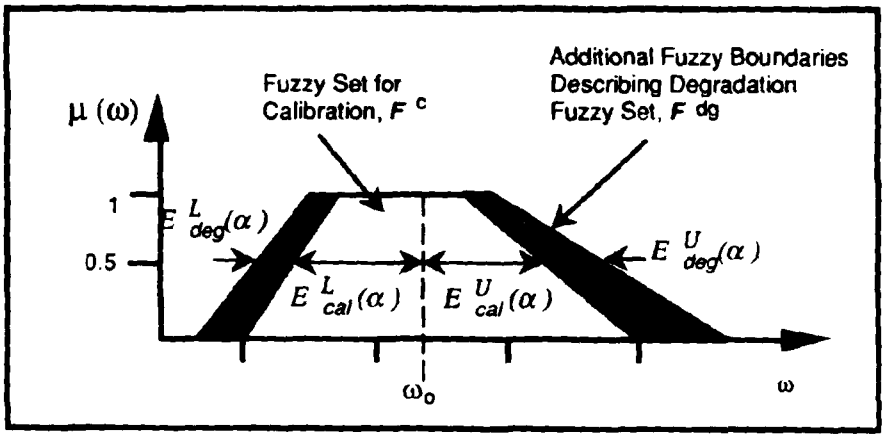

Figure 6.1: Fuzzy set representation of frequency degradation.

Since the natural frequency as a function of time is dependent on the degradation properties of the fundamental parameters, Eq. 6.1 is rewritten in more specific terms as:

$$\mathcal{F}_{\alpha}^{dg} = \left\{[a,b] | a = \omega_o - \mathcal{E}_{deg}^{L}(\alpha,t); b = \omega_o + \mathcal{E}_{deg}^{U}(\alpha,t)\right\} \tag{6.2}$$

where,

$\mathcal{E}_{deg}^{U}$ = the upper bound which describes degradation error for a membership level equal to α which is determined from the initial fuzzy estimate, $\mathcal{F}^c$, as a function of time, t;

$\mathcal{E}_{deg}^{L}$ = the lower bound which describes degradation error for a membership level equal to α which is determined from the initial fuzzy estimate, $\mathcal{F}^c$, as a function of time, t; and

a, b = lower and upper bounds, respectively, for each α-cut.

In this formulation, the degradation error, $\mathcal{E}_{deg}$, is quantified from the combined errors in the fundamental parameters. After the degradation model has been completed, it is possible to analytically determine the parameter b which describes the

overall degradation of the frequency parameter. The parameter b is dependent on the combined degradation of the fundamental parameters.

6.2 Fundamental Uncertainties in the Degradation Process

By quantifying the potential degradation of the fundamental parameters it is possible to determine the change in the higher-level dynamic parameters. Initial estimates of the error for the fundamental parameters, obtained from the calibration model, coupled with fuzzy estimates for the parameter's degradation as a function of time give the information required in the degradation model.

The framework for the degradation model is shown schematically in Fig. 6.2. Implementation of the degradation model begins with the initial errors obtained from the calibration model. Then estimates for the degradation potential for fundamental parameters are used to predict errors as a function of time. The solver consists of repeated eigensolutions using extreme bounds at each α-cut level as specified by the vertex method. As in the calibration model, solutions for each point in time require extreme values for the contributing fundamental parameters. The degradation model can be applied at any time increment to obtain an estimate of the parametric behavior in the time domain.

As shown in Fig. 6.2 the results of the degradation model can be interpreted either as a function of time or at a particular point in time. The free-vibration results are then superimposed with the fuzzy representation of the input motion to obtain a prediction of the maximum structural response.

The most important information needed for the implementation of the degradation model is an understanding of fundamental parameter degradation characteristics. Degradation can be due to a number of factors, thus adding to the complexity of the problem. Studies have been performed to determine the degradation of the modal properties of a structural system. The dynamic properties of an existing structure are obtained by performing system identification on data obtained from an excited structure. Typically, the data consists of acceleration recordings at discrete points in time at select degrees-of-freedom. By performing system identification with data

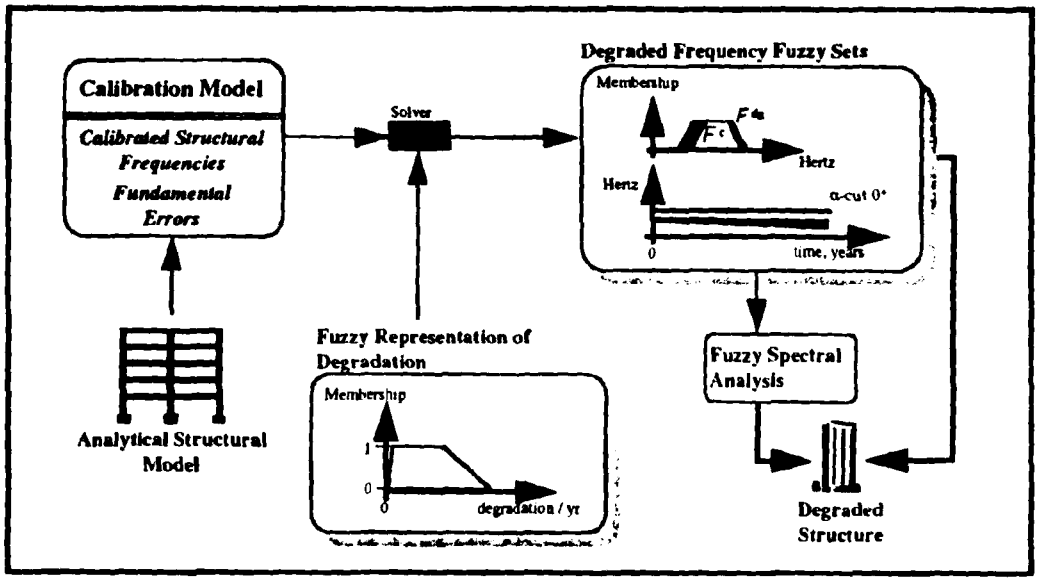

Figure 6.2: Schematic of the degradation model.

obtained over a period of time, it is possible to study the degradation of the structural frequencies. Such studies which have been performed in the Las Vegas area with structures which were excited dynamically due to blasting in the region [Cza94].

System identification also can be performed in the time domain. Such identification procedures identify the coefficients needed in the mass and stiffness matrices to obtain the recorded dynamic response. Constraints can be added to the process to ensure that the modal properties obtained from the newly identified mass and stiffness matrices match those of the actual structural response. Although the change in the coefficients of the mass and stiffness matrices represent changes in fundamental parameters, it is extremely difficult if not impossible to determine which structural elements and which parameters are affected. It is impossible to use the data to locate the potential damage or degradation in the structure. Consequently, information obtained from these system identification methods is not useful in predicting a priori degradation of fundamental material properties.

Due to the lack of quantifiable knowledge about the degradation of the fundamental material properties, expert opinion is the best information available for use in the adaptive analysis models. The analyst develops fuzzy sets to represent his best knowledge of the potential degradation in time for fundamental parameters. Currently, there is an increasing amount of interest in obtaining the degradation properties of the fundamental parameters [Hop93, Ver93, Joh93, Sch90]. As more data becomes available, these procedures and fuzzy sets can be updated to incorporate the new information.

The analyst defines the fuzzy sets for degradation prediction for the fundamental parameters based on his knowledge of the structure's environment and future use. Corrosion, fatigue due to minor dynamic loadings, loosening of joints, and appropriate maintenance are all factors which can possibly contribute to damage that an analyst may wish to consider when applying the degradation model. Proper maintenance of structures on a regular basis can reduce the effects of structural aging. Although not considered here, maintenance procedures should be included as a fundamental uncertainty. Membership functions for degradation rate fuzzy sets can be assigned by the analyst based on his experience or expert knowledge about aged structures. If possible, the expert opinion should be supported by analytical calculations.

For example, it is expected that an exposed steel bridge spanning over water will experience corrosion, while a steel frame building with fire proofing will not. Based on his knowledge, the analyst may wish to define a fuzzy set for corrosion (such as the one shown in Fig. 6.3) which can be defined as either a fuzzy set with crisp boundaries or a trapezoidal fuzzy set. Corrosion is a complex process and is dependent on a number of variables [Sch88, Kno75]. In an application the fuzzy set for the rate of corrosion must be established such that the most influential factors are considered. In addition to the removal of structural material, corrosion also can promote crack growth in structural materials.

The resulting uncertainty for the degrading area of the steel member is based on the change in geometry as a function of time. Equation 6.3 gives the relationship for

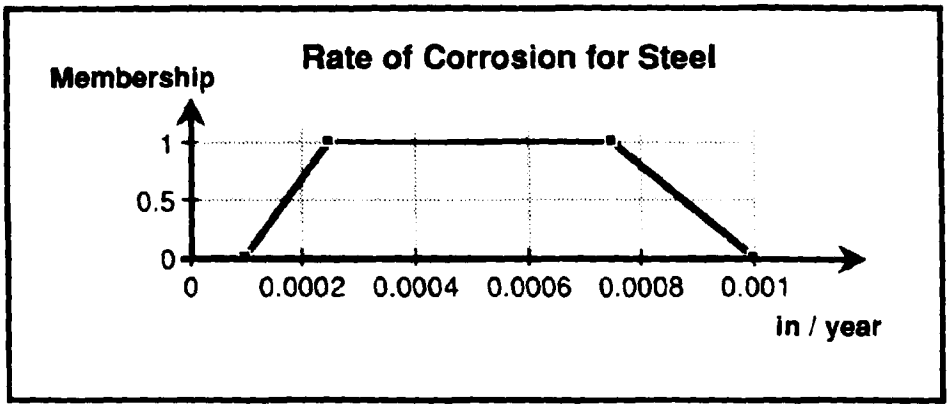

Figure 6.3: Fuzzy set for inches of steel corroded per year.

the area of a rectangular member as a function of time.

$$A(t) = (a - 2vt)(b - 2vt) \tag{6.3}$$

where,

A = cross-sectional area;

a, b = the length of the two sides for the rectangle;

v = the rate of corrosion per year for an exposed surface; and

t = time in years.

The potential degradation rate due to the corrosion of an exposed member is given here as an example. Degradation estimates can be made for a structural system based on the analyst's best judgment. Another example of potential degradation is the loosening of bolted connections which can result in a stiffness reduction. Gradual changes in mass, loosening of nonstructural elements from the main load-bearing structural system are other fundamental parameters which may be considered. Each of these cases is highly specific to the structural system and environment and must be carefully determined based on the individual application. However, there is very little

information available pertaining to the degradation of such fundamental parameters. Until such information is available, estimates for these degradation properties must be applied by the engineer on a case-specific basis. As more knowledge is obtained about the degradation behavior due to these fundamental contributions, the fuzzy estimates can be refined and updated; thus, the model is adaptive.

6.3 Degradation Examples

To illustrate the incorporation of the fundamental degradation rate into the adaptive models the example presented in Section 3.2 is used. The fuzzy set for the fundamental natural frequency for the axial vibration of the cantilevered bar with a spring support at the right side is determined as a function in time. This system is shown in Fig. 3.4. Degradation for this system is due to the corrosion which is represented by the fuzzy set of Fig. 6.3. In this example, the fundamental errors are represented as triangular fuzzy sets given in Table 3.1. The cross-sectional area (considered deterministic in the previous example) will now degrade due to corrosion.

To determine the fundamental frequency in the time domain, analyses are performed at four 25-year increments. Table 6.1 gives the parametric values for the mass, stiffness factor (denoted by γ, a dimensionless parameter), and the cross-sectional area, A. The functional dependence for A is based on Eq. 6.3 where the a and b are initially both equal to 1.0. In 100 years, based on the fuzzy set used here for corrosion, the area can decrease 4% to 36% from its original value. A 36% reduction in area may be considered unreasonably large; however, it is a result of the most extreme conditions corresponding to α-cut 0^+. The resulting frequencies as a function of time are presented in Fig. 6.4.

A second example is presented in this section to demonstrate use of the degradation model to determine the natural frequencies for the lateral vibrations of a fixed-fixed beam with semi-rigid joints near each of the ends. The system (shown in Fig. 6.5) is a beam with stiffness properties denoted as AE and EI equal to 1000 and a constant mass, $m = 1.0$ distributed uniformly along the length of the beam.

The uncertainty considered in this example is the stiffness of the rotational springs

Table 6.1: Parametric values used in the degradation model.

α-cut	Mass	Stiffness	Area	Mass	Stiffness	Area
	m, slugs/ft	γ	A, in^2	m, slugs/ft	γ	A, in^2
	T = 0 years			T = 25 years		
0.0^+	8	0.6	1.0	8	0.6	0.99
1.0	10	1.0	1.0	10	1.0	0.98
1.0	10	1.0	1.0	10	1.0	0.93
0.0^+	14	1.2	1.0	14	1.2	0.90
	T = 50 years			T = 75 years		
0.0^+	8	0.6	0.98	8	0.6	0.97
1.0	10	1.0	0.95	10	1.0	0.93
1.0	10	1.0	0.93	10	1.0	0.79
0.0^+	14	1.2	0.81	14	1.2	0.72
	T = 100 years					
0.0^+	8	0.6	0.96			
1.0	10	1.0	0.90			
1.0	10	1.0	0.72			
0.0^+	14	1.2	0.64			

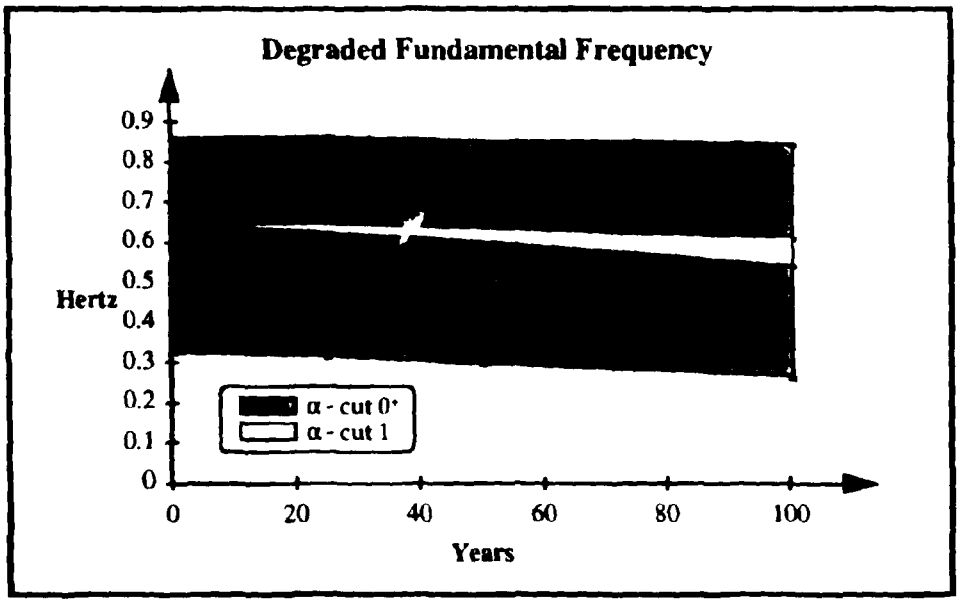

Figure 6.4: Fundamental frequency as a function of time for the axial vibrations of a bar with a linear spring at one support.

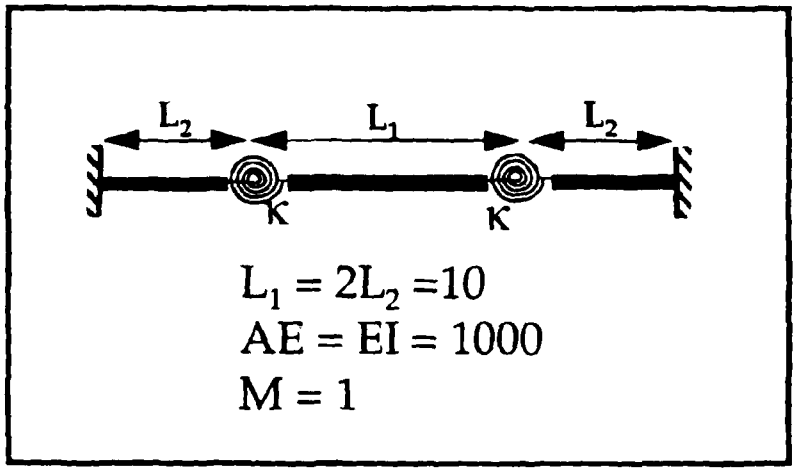

Figure 6.5: Fixed - fixed beam with semi-rigid joints represented as rotational springs.

Table 6.2: Parametric values used in the degradation model.

α-cut	lower bound	upper bound	lower bound	upper bound
	γ, % rigidity		β	
1	5	15	0.0001	0.005
0	2	25	0.0001	0.005

which are used in the analytical model to represent the semi-rigid joints. Here, the stiffness of the springs is expressed as

$$\kappa = \gamma(\text{stiffness of the beam}) \tag{6.4}$$

where,

κ = Stiffness of the rotational spring, moment/radian; and

γ = factor representing % rigidity compared to the beam stiffness.

It is assumed that the springs degrade in stiffness such that

$$\gamma(t) = \gamma_o e^{-\beta t} \tag{6.5}$$

where,

γ_o = represents the initial % rigidity supported by the spring; and

β = parameter representing degradation rate.

Analyses are performed discretely in 10 year intervals. The uncertainty for the initial and degrading stiffness of the springs represented by γ and β, respectively, is given in Table 6.2.

Figures 6.6 and 6.7 show the graphical results for the second natural frequency of the beam and spring system at 100 years. The second lowest mode shape has an inflection point near the center of the beam. Due to this curvature this mode is more sensitive to the spring stiffness than the first mode (which does not have an inflection point). Thus, the frequency for the second mode is presented here. The results are depicted as a three dimensional fuzzy set with uncertainty increasing as a function of

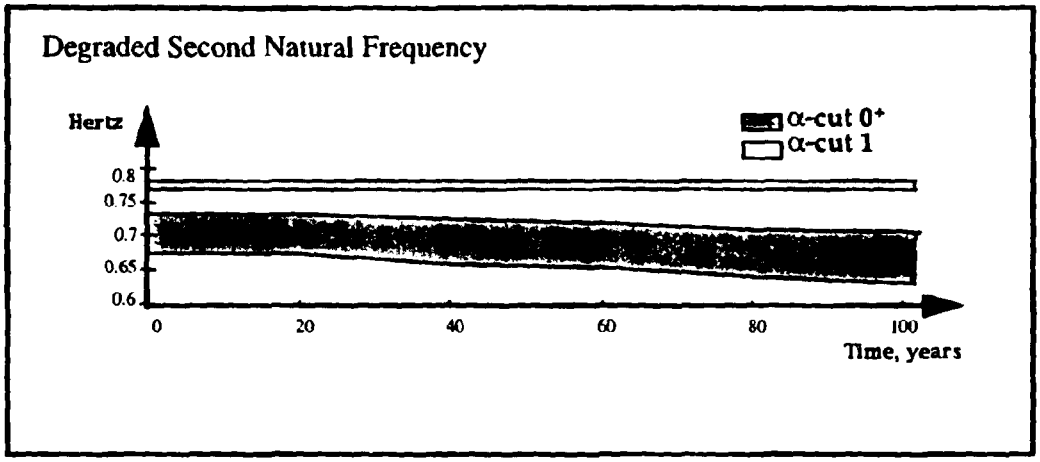

Figure 6.6: Degrading natural frequency for the 2nd mode of vibration as a function of time.

time. In Fig. 6.6 α-cut 0^+ bounds are denoted by the extreme bounds shaded grey and the α-cut 1 bounds denoted by the white region. Note that since this application is confined to the use of convex fuzzy sets, α-cut 1 is a subset of α-cut 0^+. Figure 6.7 shows the additional uncertainty in the frequency due to the consideration of a 100 year lifespan. The calibrated frequency is represented by the white fuzzy set, and the additional uncertainty due to degradation in 100 years is represented by the fuzzy set shaded black. Here, the calibration error and the degradation error are superimposed such that the black region depicts the added uncertainty due to the degradation in 100 years.

6.4 Discussion

The previous examples have demonstrated the use of fuzzy sets in predicting the potential degradation in dynamic properties of structure. In the first example, implementation of the degradation model is demonstrated through the calculation of fuzzy sets at discrete instances in time. Degradation of member stiffness due to corrosion and the stiffness of semi-rigid joints is presented. The degradation relationships are

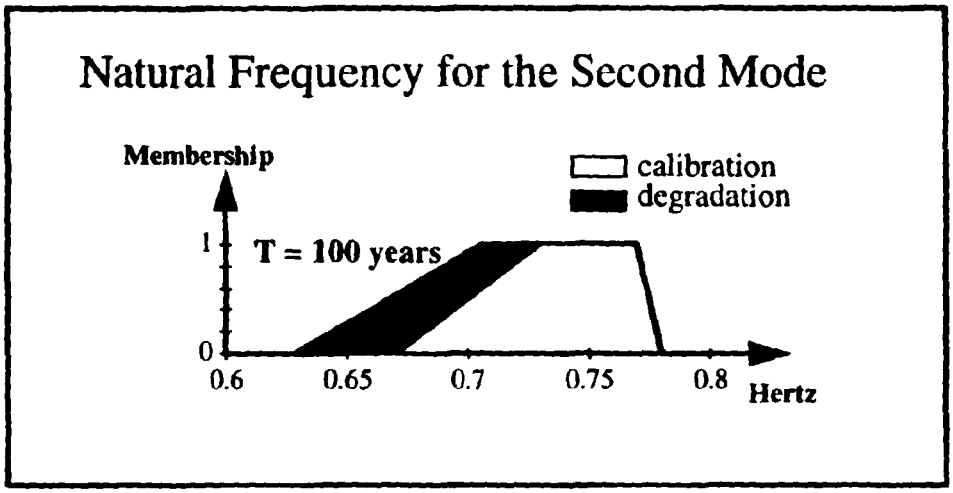

Figure 6.7: Degraded natural frequency versus calibrated natural frequency.

applied to initial representations of uncertainty in the calibration model.

Implementation of the degradation model combines the fuzzy sets representing the initial uncertainty in the fundamental parameter with a fuzzy set for the potential degradation of the parameter in time. By combining extreme bounds from each of these fuzzy sets, the upper bounds of a fundamental parameter's fuzzy set will degrade the least while the lower bounds will degrade the most over time. This statement assumes that the frequency will, in general, deteriorate in time. There may be instances when aging will cause the fundamental parameters to increase in value. The result obtained from the degradation model is a fuzzy set for the fundamental parameter which represents increasing uncertainty in time.

The slope, b, given in Eq. 6.1 is a parameter which can be used to predict the change in frequency as a function of time due to potential degradation. This parameter is not a fundamental quantity and must be determined after implementing the degradation model. Once determined, however, b may be used to interpolate the bounding values for the frequency fuzzy sets as a function of time. The parameter b is useful, permitting an analyst to quickly assess the potential changes in frequency.

For example, an iteration applying the calibration and degradation models may suggest the need for a design change. After the design change and reapplication of the calibration model, the analyst may wish to use the parameter b to assess the structure's degradation potential. Care must be taken that b is not used to extrapolate degradation information for points in time not initially considered in the degradation model. Since b is dependent on the fundamental degradation characteristics, b cannot be used to predict degradation beyond the time period with which the model was applied initially.

Implementation of the degradation model requires communication between all the players active in the design phase. The analyst must fully understand the intended use for the structure during the time period in which the degradation model is being applied. Additionally, the analyst must also consider the type of environment the structure is in. These considerations will help him answer questions such as: *How much exposure to corroding effects will this structure have? Will there be a regular dynamic load felt by the structure? How often will the structure experience minor earthquake loadings?, etc.*

This chapter has presented a framework for the application of the degradation model to structural systems which are analytically modeled with a finite element model. Today, there are efforts to build structures with design lives well over two hundred years. Unfortunately, at this time there is little information available pertaining to the degradation properties of the fundamental parameters which contribute to the dynamic response of a structure. These designs must consider the uncertainty due to the deterioration and degradation of material properties and joint conditions. This degradation model which is based on uncertainties modeled as fuzzy sets using expert opinion provides a method of assessing the dynamic characteristics of a structure over such a lifespan. As more knowledge is obtained about the degradation of material properties expert opinion will improve; thus, improving the quality of the results.

CHAPTER 7

Summary and Conclusions

This dissertation presents a framework for modeling uncertainties in dynamic parameters using fuzzy set mathematics. By modeling uncertainties in the dynamic properties of a structure, an analyst can increase his intuition about the structure's potential behavior. Thus, the designer is provided with uncertainty information needed to improve his design. These uncertainty analyses can also be expanded to provide the analyst with information about structural degradation. Following, in Section 7.1 the research developed in this dissertation is summarized. Recommendations for future research with respect to this work are presented in Section 7.2. Finally, this dissertation concludes with Section 7.3 which contains a few closing remarks.

7.1 Summary of Contributions

After the introduction of Chapter 1, Chapter 2 presents uncertainty analysis methods. Every aspect of an engineering problem contains some element of uncertainty. Ultimately, uncertainty in the response of the structure is due to errors in the analytical model and the prediction of potential loads. Typically, probabilistic methods are applied rigorously to predict parametric uncertainty either by calculus or simulation. These processes are, in general, computationally expensive; consequently, they are used only for the most critical structures. Fuzzy sets give bounds describing the uncertainty in a fuzzy parameter at various levels of confidence. Use of fuzzy mathematics allows the analyst to model fundamental uncertainties which contribute to the behavior of a structural system by establishing fuzzy bounds rather than assigning probability distributions.

The calibration model, the first of the adaptive analysis models, is presented in

Chapter 3. This model is capable of quantifying the ultimate uncertainty in the structural dynamic properties based on fundamental uncertainties. The first part of the chapter is devoted to the formulation of the dynamic equations used in the calibration model. Analysis is performed by solving the undamped free-vibration problem for the modal properties. Structural response is obtained from the response spectrum approach. The calibration model solves these dynamic equations with parameters defined by membership functions. The vertex method is used to facilitate the solution process.

Establishment of the fundamental errors are an important aspect in the development of the higher level uncertainties. Section 3.3 is devoted to the development of various types of contributing errors. In this dissertation, procedures are suggested for the development of fuzzy sets for errors in the modulus of elasticity, static loadings, joint stiffness, and floor rigidity. The calibration model is easily applicable to additional uncertainties provided that the logic used in the fuzzy set development is consistent.

Chapter 4 presents a model which can be used to quantify the uncertainty in the input motion felt by the structure. This model considers uncertainty in the frequency content and amplitude of the earthquake motion felt by the structure through the development of a fuzzy response spectra. In this dissertation, fuzzy velocity response spectra are developed for the Loma Prieta earthquake only. However, the procedure has been established to develop spectra for records from multiple earthquakes. Superposition of the uncertainties for the structure's natural frequencies and the input motion allows the analyst to quantify levels of maximum response as fuzzy sets.

The fuzzy response spectra developed in Chapter 4 demonstrate characteristics typical of sites in the San Francisco Bay area. Rock sites, in general, have a larger frequency content than the alluvium sites. This is due to the wide variation in age for the rock in the bay area; thus, the range in shear wave velocity for the rock sites is broad. Additionally, the spectra demonstrate attenuation in amplitude as the distance from the site to the rupture zone increases. These spectra show the possible and most likely levels of amplitude of the ground motion due to different site conditions and distance from the rupture zone. Since, only records from the Loma

Prieta earthquake were used, the results are valid for a single magnitude and rupture mechanism. This information can be used to assess the potential maximum response for a structure at a particular site.

Through the use of examples, Chapter 5 contains a detailed description of the implementation of the calibration model. The calibration model can produce the maximum response for a degree-of-freedom in the analytical finite element model. This information can be further investigated with respect to inter-story drift which is important in assessing the possibilities of nonstructural damage. The first example in this chapter illustrates the calibration model for a small scale two-dimensional example. Natural frequencies and the roof's maximum response is determined for the structure based on uncertainties in the modulus of elasticity, structural mass, and input motion.

A case study also is presented in Chapter 5 which further illustrates the use of the calibration and ground motion models. In the case study, results from the calibration model are compared to the actual dynamic properties of the Santa Clara County Office Building. By considering uncertainty in both mass and stiffness, the resulting frequency fuzzy sets bound the actual frequencies of the structure. Fundamental uncertainties are considered in the finite element model of the structure by implementing repeated solutions. These uncertain frequencies are superimposed with uncertainty in the input motion to obtain an upper bound for the potential maximum response of the degrees-of-freedom in the structural model. The results from the case study are fuzzy sets for the potential maximum response. These fuzzy sets were successful in bounding the actual response of the structure. The actual response is bounded at levels of confidence less than one. This is due to the modal beating which is impossible to predict analytically using the response spectrum method.

The final example in Chapter 5 gives a comparison between the calibration model proposed here and the more traditionally used probabilistic approach. Monte Carlo simulation is used to simulate experimental sampling of three random variables. The results from the simulation technique and the calibration model are shown as a fuzzy set overlaid on a histogram. Four solutions are performed to obtain fuzzy sets for the

structure's natural frequency, while the histogram is the result of 3,000 computer generated samples. The resulting fuzzy sets give conservative bounds for the most likely occurrences. Consequently, when probabilities are needed at high levels of accuracy, the probabilistic methods are recommended. However, to obtain an understanding of the potential values for a parameter, use of the calibration model provides an efficient and accurate result.

Chapter 6 presents the framework used to quantify the potential change in due to the gradual degradation of a structural system. The degradation model is based on the fuzzy estimates for the degradation characteristics of the fundamental parameters. Examples are presented which demonstrate the degradation of frequency for the structure due to corrosion and the loosening of bolted connections. Fuzzy sets are used to model the degradation potential in the time domain based on initial fuzzy sets which describe the uncertainty in time, $t = 0$.

In this dissertation a framework is developed which can be used by an analyst to better understand the uncertainties in dynamic parameters for an analytical structural model. This model which is a finite element representation of the structural system is solved with methods typically used in dynamic analysis. A basis is established for the development of the fundamental uncertainties which affect the dynamic response. However, due to the generality of the process it is impossible to address every issue which adds uncertainty to the problem. The following section gives recommendations for future research in this field.

7.2 Recommendations for Future Research

This research has provided a foundation for the development of adaptive analysis models which consider the uncertainty in dynamic parameters over a structure's lifespan. The purpose of this section is to provide a discussion suggesting additional research which is needed in this field. The following subsections present possible alternate modeling techniques for use the adaptive uncertainty models.

7.2.1 Nonstructural Components

It has been widely accepted that the nonstructural components contribute not only to the masses but also to the stiffness of the structural system. Often, the mass of the nonstructural components is considered in dynamic analysis as dead loads; however, the contributing stiffness from these components to the structural system are rarely considered. These components, such as partition walls and cladding attached to the exterior of the building, can stiffen the structural system which increases the natural frequencies of the building.

Analytical modeling of the added stiffness due to nonstructural components is extremely difficult. The stiffness contribution from partition walls to the structural system depends on the type of partition wall and the interior and exterior connections to the wall. The quality of the connections affects the ability for the wall to transfer loads (not explicitly considered in the design) to and from the structural system. Construction practice also has an impact on the quality of the connections. Additional research is necessary to assess the stiffness contributions of these components due to a number of uncertain factors. Fuzzy sets can be used to quantify the uncertainty in the stiffness contributions of the nonstructural components by considering issues such as construction practice and joint stiffness which can be difficult to model analytically.

7.2.2 Uncertainty in the Structural Damping

Damping is by far considered to be the most uncertain aspect in the modeling of structural dynamic behavior. There is an extremely large amount of uncertainty related to the amount of damping inherent in the structural and nonstructural systems. This is due to the complexity involved with analytically modeling the damping parameters for the structural elements, in addition to the contribution from nonstructural components. Nonstructural components, such as partition walls and cladding, may increase the damping during the structural response. Damping is typically assumed to be proportional to the mass and stiffness properties of the structural element. An advantage to assuming that the damping is proportional to mass and stiffness is that when the mass and stiffness properties are uncoupled the damping characteristics

also are uncoupled. Thus, it is possible to perform dynamic analyses on each mode separately before superimposing the effects of all modes acting together.

The development of a procedure which quantifies the uncertainty in the proportional damping of a structure, both from the analytically modeled structural system and the nonstructural components (which may not be modeled analytically) is needed. Results from the calibration model will benefit from the consideration of uncertainty in a structure's damping characteristics.

7.2.3 Input Motion Uncertainties

Chapter 4 presented a methodology to define fuzzy sets which consider the uncertainty in the input motion felt by a structure at a site. The fuzzy response spectra quantify the uncertainty in the frequency content and the amplitude of the ground motion. In this chapter, each of the spectra developed for velocity response are confined to a trapezoidal shape with three linear sides (the fourth side is the horizontal axis). This shape gives the best estimates for amplitude for mid-range structural periods. Further refinement of this shape to five linear sides will provide more realistic response estimates at low and high periods.

Consideration of additional earthquakes in the development of fuzzy response spectra will help refine the resulting fuzzy spectra. Soil categories can be refined by grouping data based on shear wave velocities rather than the crude division by soil type. Distance groups also will be refined with the additional data. These refinements will give the analyst spectral values for the ground motion with narrower uncertainty bounds. This is not to say that the uncertainty is reduced; however, the ground motion prediction based on an earthquake magnitude, distance to the rupture zone, and soil type, will be less uncertain with the consideration of additional records.

This dissertation developed fuzzy spectra to illustrate the consideration of input motion uncertainties in the calibration model. The results from the calibration model are validated by comparing the fuzzy sets for maximum response to the actual maximum response of the case study structure during the Loma Prieta earthquake.

7.2.4 Aging Properties of Structural Parameters

The degradation model is dependent on information about the aging characteristics of structural parameters over an extended period of time (i.e. at least 100 years). Unfortunately, at the time of this work there has been very little research performed in determining such information. This work assumes that by understanding the potential degradation properties for fundamental parameters it is then possible to extrapolate the uncertainty in the higher level parameters as a function of time. Specifically, as more knowledge is obtained about the degradation of fundamental parameters, the degradation model presented here can adapt to this updated information.

At this point in time very little is known about a parameter's aging characteristics. Prediction of these future characteristics (which are difficult if not impossible to measure) for these parameters can be facilitated using fuzzy logic. As we obtain more data about material aging, it may be more applicable to predict the uncertainties based on statistical methods rather than using fuzzy sets.

7.2.5 Uncertainty Due to Damage

The adaptive analysis models have been developed to quantify errors at three stages of a structure's life: calibration, degradation, and damage. Both the calibration and degradation models have been described here in this dissertation. Development of the damage model is left to future research. The damage model predicts a drastic change in the dynamic characteristics of a structure due to a design level event, such as a strong earthquake. This drastic shift is illustrated for frequency in Figure 7.1.

The fuzzy set for natural frequency before damage is shaded black in Fig. 7.1 represents uncertainty for this parameter at a particular point in time. The unshaded fuzzy set in the figure depicts the possible uncertainty in frequency due to damage, $\mathcal{E}_{dam}$. This fuzzy set is determined from the calibration and degradation models. Uncertainty in the natural frequency after a damaging event is based on the initial uncertainty for the parameter and the type of event. Furthermore, there is uncertainty associated with the time and location the event occurs. For example, in the San Francisco area three major faults known to actively cause earthquakes are: San

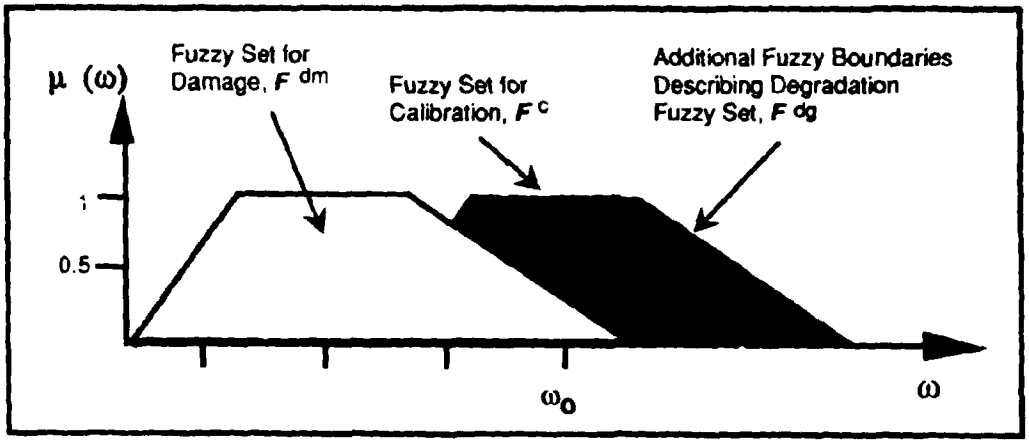

Figure 7.1: Shift in uncertainty for natural frequency due to a damaging event.

Andreas, Hayward, and Calaveras. Additionally, there are numerous smaller faults also capable of initiating earthquakes. Development of the damage model should include the uncertainty involved with which fault ruptures, the location along the fault, and the time of the events in addition to an evaluation of the structure's non-linear response. Not only will the damage fuzzy sets denote a shift in uncertainty due to the occurrence of the event, the fuzzy sets will represent the uncertainty shift in the time domain. Thus, the damage model must include recurrence relationships for earthquakes at various magnitudes occurring at various faults.

7.2.6 Interpretation of Results

Implementation of the adaptive analysis models is performed iteratively, where a structural design is evaluated based on the results of the calibration model. Upon obtaining acceptable results, the design is evaluated based on the degradation model. Finally, as a final check the structural design is evaluated with respect to the damage model. The framework for these adaptive models has been established such that this method can model uncertainties in various types of structural systems, provided the system is modeled using finite elements. Furthermore, the generality of the framework also permits the consideration of additional uncertainties.

Specific guidelines need to be developed to ensure that the user is interpreting the results correctly. These guidelines can steer the analyst through the process of prescribing the fundamental uncertainties as fuzzy sets such that the logic is applied consistently, helping the analyst determine which uncertainties are most important for his purposes. A decision analysis model is needed to help the analyst interpret the results to ensure consistent use in design.

7.3 The Adaptive Analysis Models

This study categorizes structural modeling uncertainties into three main sources of error: calibration, degradation, and damage error, which represent the potential sources of discrepancy between the original structural design model and the constructed system. Previous work focused on quantifying structural modeling error has used system identification techniques or probabilistic techniques to predict the modeling error based on measured response data. However, the need to understand modeling error is greatest prior to construction, during the design of the structure, when response data is not available and the conventional system identification techniques are not applicable.

An adaptive design procedure is presented here which allows the analyst to quantify the uncertainties between the structural finite element model and the as-built structure during the design phase. Fuzzy sets are used to represent the level of confidence associated with various uncertain structural parameters such as natural frequency, frequency ratio, and maximum response. Using the vertex method, the analyses associated with these parametric uncertainties establish the bounds for the fuzzy set and define the membership function for structural response. Membership functions and confidence intervals for the parameters are determined by performing multiple dynamic analyses involving extreme cases of the model assumptions.

The adaptive design methodology is capable of simulating and predicting the various forms of modeling error prior to building construction. This iterative design procedure allows the design engineer to account more effectively for modeling discrepancies and degradation effects. If at any point in the adaptive analysis the potential

exists for unacceptable system response, the designer redesigns the structure and reformulates the associated calibration, degradation, and damage models. When the range in response represented by the fuzzy sets is acceptable for the given design specifications, the iterative procedure converges to an acceptable design.

A possible application for the use of these models based on fuzzy mathematics pertains to the design of a control system. The resulting fuzzy set which represents the uncertainty in the dynamic properties of a structure provides bounds which the analyst can use as a basis to design an active or passive control system. These control systems typically are "tuned" based on the structure's natural frequencies. By quantifying the uncertainty in the potential free-vibration properties and response for the structure it is possible to design a control system which is more robust.

This dissertation has focused on the development of a methodology for the use of fuzzy set mathematics in the quantification of potential errors in structural dynamic properties. Fuzzy set logic is beneficial in this application due to the limited knowledge available about the stiffness and mass contributions from various types of elements which comprise the structural system. Furthermore, the use of fuzzy set mathematics allows the analyst to bound his perceptions of the uncertainties, ultimately bounding the resulting dynamic parameters.

Bibliography

[AB86] James C. Anderson and Vitelmo V. Bertero. Uncertainties in establishing design earthquakes. *Journal of the Structural Division*, 113(8):1709-1724, 1986.

[AB90] Gail M. Atkinson and David M. Boore. Recent trends in ground motion and spectra response relations for North America. *Earthquake Spectra*, 6(1):15-35, 1990.

[AL89] Bilal M. Ayyub and Kwan-Ling Lai. Structural reliability assessment using Latin hypercube sampling. *5th International Conference on Structural Safety and Reliability*, pp. 1177 - 1184, 1989.

[App74] Applied Technology Council. An Evaluation of a Response Spectrum Approach to Seismic Design of Buildings. Technical Report ATC-2, Applied Technology Council, September 1974.

[AT75a] Alfredo H-S. Ang and Wilson H. Tang. *Probability Concepts in Engineering Planning and Design: Volume I - Basic Principles*. John Wiley & Sons, New York, 1975.

[AT75b] Alfredo H-S. Ang and Wilson H. Tang. *Probability Concepts in Engineering Planning and Design: Volume II - Decision, risk, and reliability*. John Wiley & Sons, New York, 1975.

[BCPY85] Colin B. Brown, Jean-Lou Chameau, Richard Palmer, and James T. P. Yao, editors. *Proceedings of NSF Workshop on Civil Engineering Applications of Fuzzy Sets*, West Lafayette, Indiana, October 1985. The National Science Foundation and Purdue University, Purdue University, School of Civil Engineering.

[BG76] Roger D. Borcherdt and James F. Gibbs. Effects of local geological conditions in the San Francisco Bay region on ground motions and the intensities of the 1906 earthquake. *Bulletin of the Seismological Society of America*, 66(2):467–500, 1976.

[BJ82] David M. Boore and William B. Joyner. The empirical prediction of ground motion. *Bulletin of the Seismological Society of America*, 72:S43–S60, 1982.

[BJF93] David M. Boore, William B. Joyner, and T. E. Fumal. *Estimation of Reponse Spectra and Peak Accelerations from Western North American Earthquakes: An interim report.* Open-File Report 93-509, United States Geological Survey, July 1993.

[BK77] S. Baas and H. Kwakernaak. Rating and ranking of multiple-aspect alternatives using fuzzy sets. *Automatica*, 13:47–48, 1977.

[BM58] G. E. P. Box and M. E. Muller. A note on the generation of random normal deviates. *The Annals of Mathematical Statistics*, 29:610–611, 1958.

[BM91] Ruben Boroschek and Steve Mahin. *Response of a Lightly-Damped Torsionally-Coupled Building.* Report UBC/EERC/91/18, University of California, Berkeley and Earthquake Engineering Research Center, Berkeley, California, December 1991.

[Boi85] Auguste C. Boissonnade. *Use of Pattern Recognition and Fuzzy Sets in Seismic Risk Analysis.* PhD thesis, Stanford University, Department of Civil Engineering, January 1985.

[Bor94] Roger D. Borcherdt. New developments in estimating site effects on ground motion: An integrated methodology for estimates of site- dependent response spectra, seismic coefficients for site-dependent building code provisions, and predictive GIS maps of strong ground shaking. *Proceedings of Seminar on New Developments in Earthquake Ground Motion*

Estimation and Implications for Engineering Design Practice, pp. 10:1 - 10:44. Applied Technology Council (ATC 35-1), 1994.

[Cam85] Kenneth W. Campbell. Strong motion attenuation relations: A ten-year perspective. ***Earthquake Spectra***, 1(4):759–804, 1985.

[CDSW88] W. L. Chiang, Weimin Dong, Haresh C. Shah, and Felix S. Wong. Response of structural systems with uncertain parameters: A comparative study of probabilistic and fuzzy sets models. ***Probabilistic Methods in Civil Engineering, 5th ASCE Specialty Conference***, pages 197–200. American Society of Civil Engineers, May 25-27 1988.

[CDW87] W. Chiang, Weimin Dong, and Felix S. Wong. Dynamic response of structures with uncertain parameters: A comparitive study of probabilistic and fuzzy sets models. ***Probabilistic Engineering Mechanics***, 2(2):82–91, 1987.

[Chi88] Wei-Ling Chiang. ***Models for Uncertainty Propagation-Applications to Structural and Earthqauke Engineering.*** PhD thesis, Stanford University, Department of Civil Engineering, March 1988.

[Cif84] Arturo O. Cifuentes. ***System Identification of Hysteretic Structures.*** PhD thesis, California Institute of Technology, Department of Civil Engineering, 1984.

[CSMIP91] ***Processed Strong-Motion Data from the Loma Prieta Earthquake of 17 October 1989 Ground-Response Records.*** Technical Report OSMS 91-06, California Strong Motion Instrumentation Program, 1991.

[CT69] Jon D. Collins and William T. Thomson. The eigenvalue problem for structural system with statistical properties. ***AIAA Journal***, 7(4):642–648, 1969.

[Cza94] R. Martin Czarnecki. Personal Communication, May 1994. Research performed by John A. Blume & Associates.

[DCW87] Weimin Dong, W. L. Chiang, and F. S. Wong. Propogation of uncertainties in deterministic systems. *Computers and Structures*, 26(3):415–423, 1987.

[DK79] A. Der Kiureghian. *A Response Spectrum Method for Random Vibrations*. Technical Report UCB/EERC-79/32, Earthquake Engineering Research Center, University of California, Berkeley, 1979.

[Don86] Weimin Dong. *Applications of Fuzzy Set Theory and Structural and Earthquake Engineering*. PhD thesis, Stanford University, Department of Civil Engineering, August 1986.

[DOU76] Ricardo Dorby, Issa Oweis, and Alfredo Urza. Simplified procedures for estimating the fundamental period of a soil profile. *Bulletin of the Seismological Society of America*, 66(4):1293–1321, 1976.

[DP88] Didier Dubois and Henri Prade. *Possiblity Theory: An Approach to Computerized Processing of Uncertainty*. Plenum Press, New York, 1988.

[DR85] Weimin Dong and Timothy J. Ross. Treatment of uncertainties in structural dynamics models. *Proceedings from Fuzzy Sets in Earthquake Engineering*, Vol. 3, pages 107–119, Beijing, China, 1985.

[DS87] Weimin Dong and Haresh C. Shah. Vertex method for computing functions of fuzzy variables. *Fuzzy Sets and Systems*, 24:65–78, 1987.

[DW86a] Weimin Dong and Felix S. Wong. From uncertainty to approximate reasoning; Part 1: Conceptual models and engineering interpretations. *Civil Engineering Systems*, 3:143–154, 1986.

[DW86b] Weimin Dong and Felix S. Wong. From uncertainty to approximate reasoning; Part 2: Reasoning with algorithmic rules. *Civil Engineering Systems*, 3:192–202, 1986.

[DW86c] Weimin Dong and Felix S. Wong. From uncertainty to approximate reasoning; Part 3: Reasoning with conditional rules. *Civil Engineering Systems*, 4:45–53, 1986.

[DW87] Weimin Dong and Felix S. Wong. Fuzzy weighted averages and implememtation of the extension principle. *Fuzzy Sets and Systems*, 21:183–199, 1987.

[FSFY85] H. Furuta, N. Shiraishi, K. Fu, and J. T. P. Yao. Evaluation of structural serviceability based on fuzzy reasoning. *Proceedings from Fuzzy Sets in Earthquake Engineering*, pp. 218–235, Beijing, China, 1985.

[Fur93] Hitoshi Furuta. Comprehensive analysis for structural damage based upon fuzzy sets theory. *Journal of Intelligent and Fuzzy Systems: Applications in Engineering and Technology*, 1(1):55–61, 1993.

[GR78] V. T. Galambos and M. K. Ravindra. Properties of steel for use in LRFD. *Journal of the Structural Division (ASCE)*, 104:1459–1468, 1978.

[Hay95] Y. Hayashi. *Joint Research Program on Proposal of a Long Life Building and its Design Methods.* Technical report, Ohsaki Research Institute of Shimizu Corporation, Tokyo, Japan, 1995. In Progress.

[HH72] T. K. Hasselman and Gary C. Hart. Modal analysis of random structural systems. *Journal of the Engineering Mechanics Division Proceedings of the American Society of Civil Engineers*, EM3:561–579, 1972.

[Hin85] Andrew J. Hinlke. Linguistic assessment of fatigue damage in butt welds. *Proceedings of NSF Workshop on Civil Engineering Applications of Fuzzy Sets*, pages 219–242, Purdue University, West Lafayette, Indiana, October 1985.

[Hop93] David M. Hopper. Structures and geriatrics from a failure analysis experience viewpoint. *Applied Mechanics Review*, 46(5):213–216, May 1993.

[Hou47] George W. Housner. Characteristics of strong-motion earthquakes. *Bulletin of the Seismological Society of America*, 37:19–27, 1947.

[Hou59] George W. Housner. Behavior of structures during earthquakes. *Journal of Engineering Mechanics Division, ASCE*, 85(EM4), 1959.

[Hou90] George W. Housner. *Selected Earthquake Engineering Papers of George W. Housner*, chapter Engineering Estimates of Ground Shaking and Maximum Earthquake Magnitude; pp. 527 - 539. Civil Engineering Classics. New York, N. Y., 1990.

[HS71] Masaru Hoshiya and Harsh C. Shah. Free vibration of stochastic beam-column. *Journal of the Engineering Mechanics Division Proceedings of the American Society of Civil Engineers*, EM4:1239–1255, 1971.

[Hum90] Jagmohan L. Humar. *Dynamics of Structures*. Prentice Hall, New Jersey, 1990.

[Int86] International Conference of Building Officials. Uniform building code. International Conference of Building Officials, 1986.

[JB81] William B. Joyner and David M. Boore. Peak horizontal acceleration and velocity from strong-motion records including records from the 1979 Imperial Valley, California, earthquake. *Bulletin of the Seismological Society of America*, 71:2011–2038, 1981.

[Joh93] Gayle S. Johnson. Effect of aging on the seismic performance of petrochemical facilities. *Applied Mechanics Review*, 46(5):217–219, May 1993.

[KC86] N. Kishi and W. F. Chen. *Data Base of Steel Beam-to-Column Connections Vols I & II*. Technical report, School of Engineering, Purdue University, 1986.

[KF88] George J. Klir and Tina A. Folger. *Fuzzy Sets, Uncertainty, and Information*. Prentice Hall, Englewood Cliffs, New Jersey, 1988.

[Kno75] Dietbert Knöfel. *Corrosion of Building Materials.* Van Nostrand Reinhold Company, 1975.

[LBM86] Wing Kam Liu, Ted Belytschko, and A. Mani. Probabilistic finite elements for nonlinear structural dynamics. *Computer Methods in Applied Mechanics and Engineering*, 56:61–81, 1986.

[LD86] M. Lamarre and W. Dong. Evaluation of seismic hazard with fuzzy algorithm. *Proceedings of the Third World U. S. National Conference on Earthquake Engineering*, pp. 221–231, Charleston, South Carolina, August 1986.

[MJB83] Martin W. McCann Jr. and David M. Boore. Variablity in ground motions root mean square acceleration and peak acceleration for the 1971 San Fernando, California, earthquake. *Bulletin of the Seismological Society of America*, 73(2):615–632, 1983.

[NH82] Nathen M. Newmark and William J. Hall. *Earthquake Spectra and Design.* Monograph Series: Engineering Monographs on Earthquake Criteria, Structural Design, and Strong Motion Records. Earthquake Engineering Research Institute, 1982.

[NL93] Farzad Naeim and Marshall Lew. *Design Ground Motion Criteria for Seismic-Isolated California Hospitals: Evaluations and Recommendations.* A Report to the County of Los Angeles, October 1993.

[Pai90] Shantaram S. Pai. *Probabilistic Structural Analysis of a Truss Typical for Space Station.* Technical Memorandum 103277, NASA, Lewis Research Center, Cleveland, Ohio, September 1990.

[PC91] Shantaram S. Pai and Christos C. Chamis. *Probabilistic Progressive Buckling of Trusses.* Technical Memorandum 105162, NASA, Lewis Research Center, Cleveland, Ohio, April 1991.

[Sch84] Kurt J. Schmucker. *Fuzzy Sets, Natural Language Computations, and Risk Analysis.* Computer Science Press, 1984.

[Sch88] Philip A. Schweitzer, editor. *Corrosion and Corrosion Protection Handbook.* Marcel Dekker, Inc., second edition, 1988.

[Sch90] G. I. Schueller. *Design for Durability Including Deterioration and Maintenance Procedures.* Working Document - Joint Committee on Structural Safety, November 1990.

[Sei90] Seismology Committee Structural Engineers Association of California. *Recommended Lateral Force Requirements and Commentary.* Structural Engineers Association of California, Sacramento, California, 5th edition, 1990.

[SF85] Naruhito Shiraishi and Hitoshi Furuta. Assessment of structural durability with fuzzy sets. *Proceedings of NSF Workshop on Civil Engineering Applications of Fuzzy Sets*, pages 193–218, Purdue University, West Lafayette, Indiana, October 1985.

[SG86] Costas Souflis and Dimitri A. Grivas. Fuzzy set approach to linguistic seismic load and damage assessment. *Journal of Engineering Mechanics*, 112:650, 1986.

[Shi85] Heki Shibata. Effect on human error for structural design under seismic loading and its evaluation. *Proceedings of NSF Workshop on Civil Engineering Applications of Fuzzy Sets*, pp. 45–63, Purdue University, West Lafayette, IN, October 1985.

[SI69] H. Bolton Seed and Izzat M. Idriss. Influence of soil conditions on ground motions during earthquakes. *Journal of the Soil Mechanics and Foundations Division: Proceedings of the American Society of Civil Engineers*, 95(SM1):99–137, 1969.

[SMLI76] H. Bolton Seed, Ramesh Murarka, John Lysmer, and Izzat M. Idriss. Relationships of maximum acceleration, maximum velocity, distance from

source, and local site conditions for moderately strong earthquakes. *Bulletin of the Seismological Society of America*, 66(4):1323–1342, August 1976.

[SUL76] H. Bolton Seed, Celso Ugas, and John Lysmer. Site-dependent spectra for earthquake-resistant design. *Bulletin of the Seismological Society of America*, 66(1):221–243, February 1976.

[SW92] H. Allison Smith and Sara J. Wadia. Adaptive design models considering lifespan of buildings. *Journal of Intelligent Material Systems and Structures*, 3:585–599, October 1992.

[TA88] Morteza A. M. Torkamani and Ahmad K. Ahmadi. Stiffness identification of a tall building during construction period using ambient tests. *Earthquake Engineering and Structural Dynamics*, 16:1177–1188, 1988.

[Tar88] Bungale S. Taranath. *Structural Analysis and Design of Tall Buildings*. Mc Graw Hill, 1988.

[TAS92] Toshiro Terano, Kiyoji Asai, and Michio Sugeno. *Fuzzy Systems Theory and Its Applications*. Academic Press Inc., 1992.

[Udw86] F. E. Udwadia. *Dynamics of Uncertain Systems*. Report No. FEU-01-86, University of Southern California, Los Angeles, California, 1986.

[Udw87a] F. E. Udwadia. Response of uncertain dynamic systems, I. *Applied Mathematics and Computation*, 22:115–150, 1987.

[Udw87b] F. E. Udwadia. Response of uncertain dynamic systems, II. *Applied Mathematics and Computation*, 22:151–187, 1987.

[Ver93] Lawrence N. Vergin. Dynamic char cteristics of deteriorating engineering structure. *Applied Mechanics Review*, 46(5):220–226, May 1993.

[WDKB81] E. L. Wilson, A. Der Kiureghian, and E. P. Bayo. A replacement for the SRSS method in seismic analysis. *Earthquake Engineering and Structural Dynamics*, 9(2):187–192, 1981.

[Zad65] Lofti A. Zadeh. Fuzzy sets. *Information and Control*, 8:338–353, 1965.

[Zad73] Lofti A. Zadeh. *The Concept of a Linguistic Variable and its Application to Linguistic Reasoning.* Memorandum ERL - M 411, University of California, Berkeley, October 1973.

[Zim91] H.-J. Zimmermann. *Fuzzy Set Theory and its Applications.* Kluwer Academic Publishers, Boston, second edition, 1991.

APPENDIX A

Data Used in Fuzzy Spectra for Loma Prieta

In this appendix the procedure is outlined for the development of the fuzzy velocity response spectrum for alluvium sites less than 30 km from the rupture zone. Data denoting distance to the rupture zone, soil type, and the location of the two corner points A and B, are collected for each site. The steps used in the development of the fuzzy velocity response spectra are itemized below. A few of the figures given in the text of Chapter 4 are duplicated here to clarify the explanations given in this appendix.

- Identification of "Corner Point A" and "Corner Point B" helps to approximate the trapezoidal shape typical of the velocity spectrum (see Fig A.1). Velocity amplification and period are the coordinates used to specify the location of these points.

- Fuzzy sets are defined based on the uncertain location for corner points A and B. This is done by creating plots for amplitude versus distance and the period versus distance for each of the two corner points (four plots in total). Figure A.2 gives a typical plot for period versus distance. This plot is generated by plotting the period values for Corner B for alluvium sites.

  The horizontal lines in the figure at distances of 30 km and 60 km divide the data into the three distance categories. Placement of these divisions have been based on the amount of data available for each group. Effort was made to maximize the amount of data in each distance category, while not creating a category which is unreasonably large.

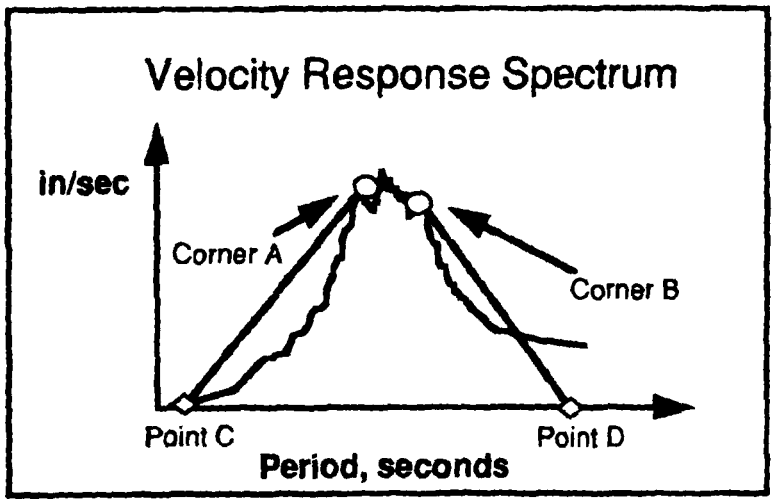

Figure A.1: Corner points A & B for site a dependent spectrum.

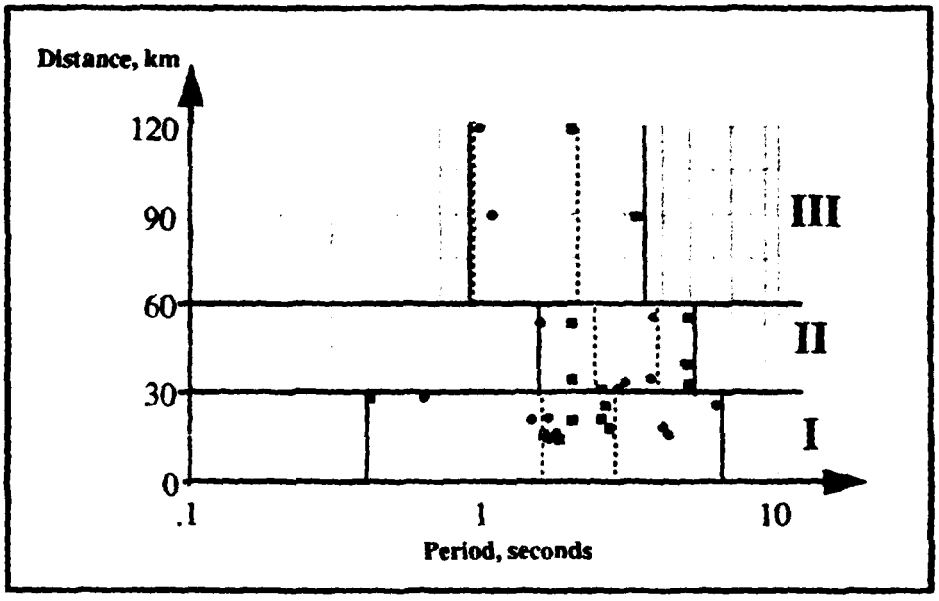

Figure A.2: Period versus distance for alluvium sites (Corner B).

Also, in the figure, there are four vertical lines for each distance category. The solid lines denote the α-cut 0^+ boundaries for period in each distance category. Alpha-cut 1 boundaries are denoted by the dashed lines. This process is repeated to define fuzzy sets for amplitude at each of the three distance categories. Finally, period and amplitude fuzzy sets are generated for Corner A. The result consists of four fuzzy sets which are then used to defined the fuzzy velocity response spectra (shown in Fig. A.3).

- The four fuzzy sets which are used to define the spectrum are two frequency fuzzy sets, one each for Corners A and B, and two velocity amplification fuzzy sets, one each for Corners A and B. These fuzzy sets are shown in Fig. A.3 for alluvium sites less than 30 km from the rupture zone.

  The vertices in Fig. A.3 are mapped to the resulting fuzzy spectrum using fuzzy set theory. Uncertainty in the frequency content for the fuzzy spectrum is obtained by taking the union of the two frequency content fuzzy sets for Corners A and B. The uncertainty in the amplitude of the resulting spectrum at a corner is obtained by taking the intersection of the amplitude fuzzy set for a corner with the frequency fuzzy set for the same corner. The resulting spectrum is a three dimensional fuzzy set as shown in Fig. A.4 (reproduced from Chapter 4). In the figure, the third axis represents membership and is orthogonal to the plane of the page. The two shaded areas are slices taken at membership levels of 0 and 1.

- The final fuzzy set for alluvium sites located less than 30 km from the rupture zone is shown in Fig. A.5. In this figure, two α-cut levels are given.

  The following tables give the distance from the rupture zone and the coordinates for the location of corners A and B for each channel at each site. Rock sites are given in Table A.1, and alluvium sites in Table A.2.

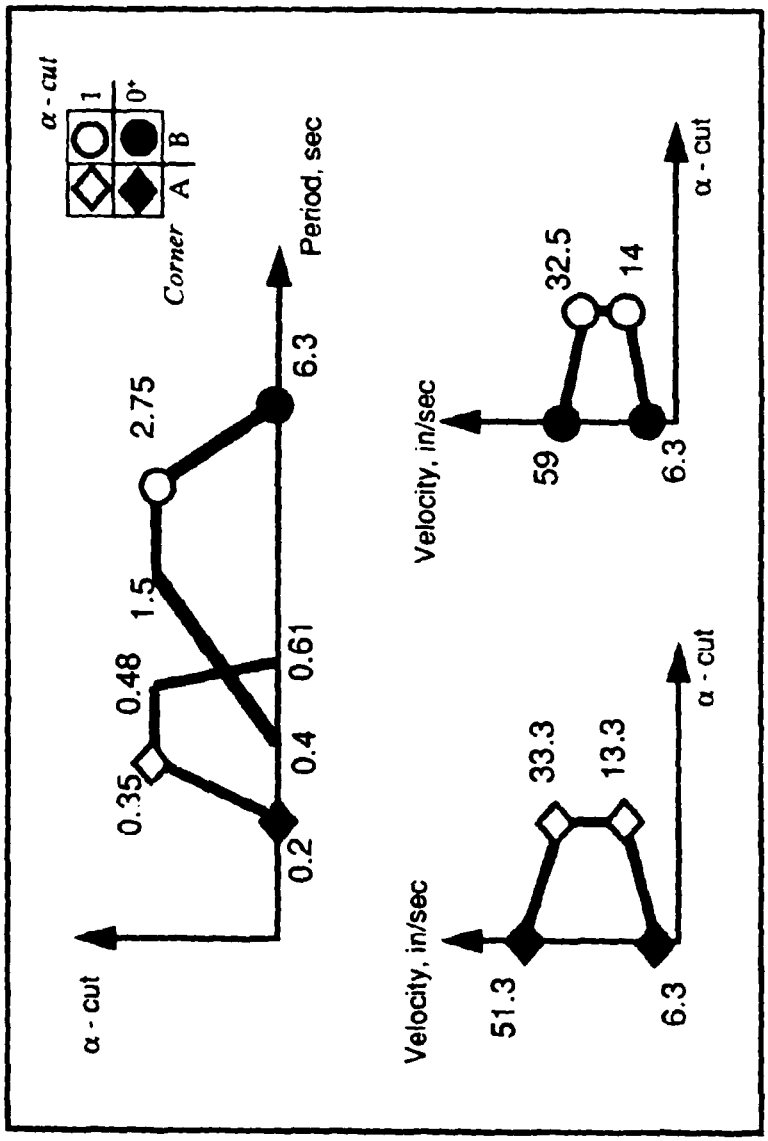

Figure A.3: Fuzzy sets for period and frequency of corners A & B.

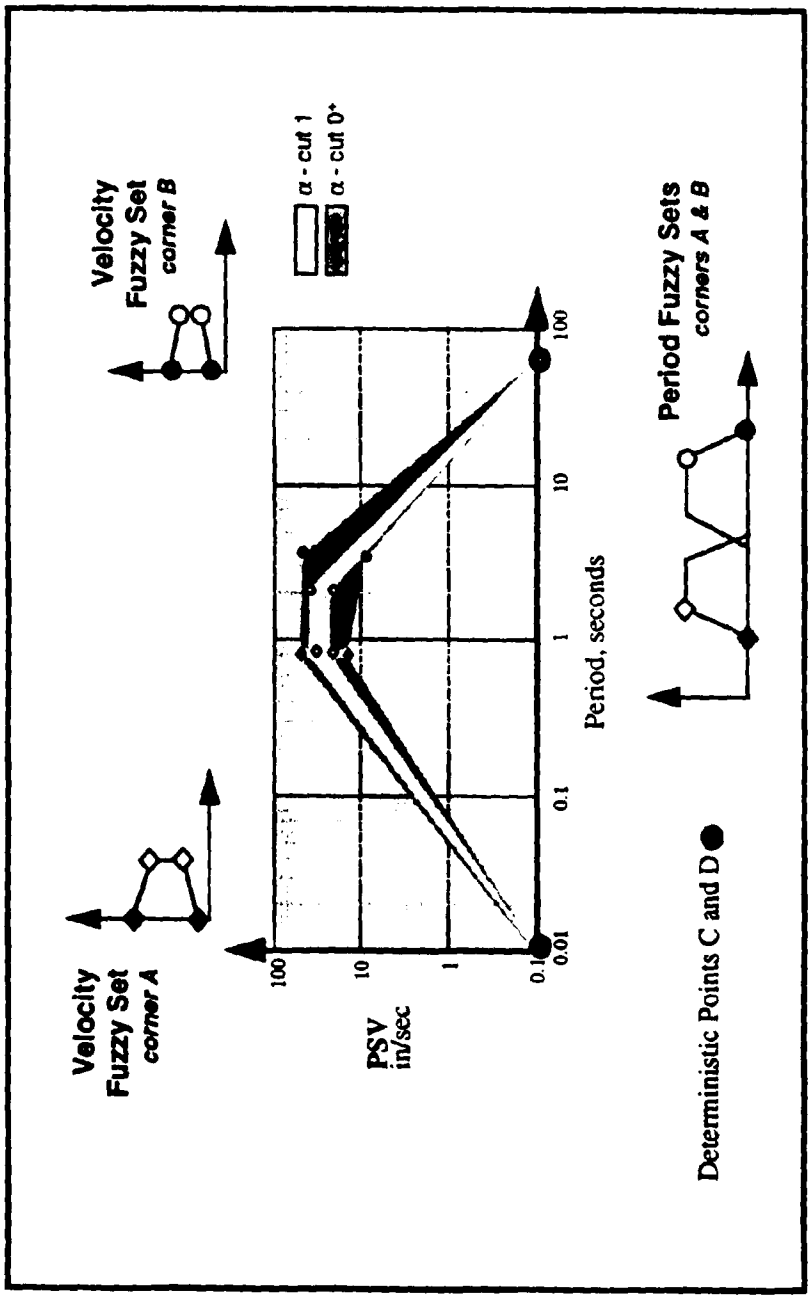

Figure A.4: Establishment of a fuzzy velocity response spectrum.

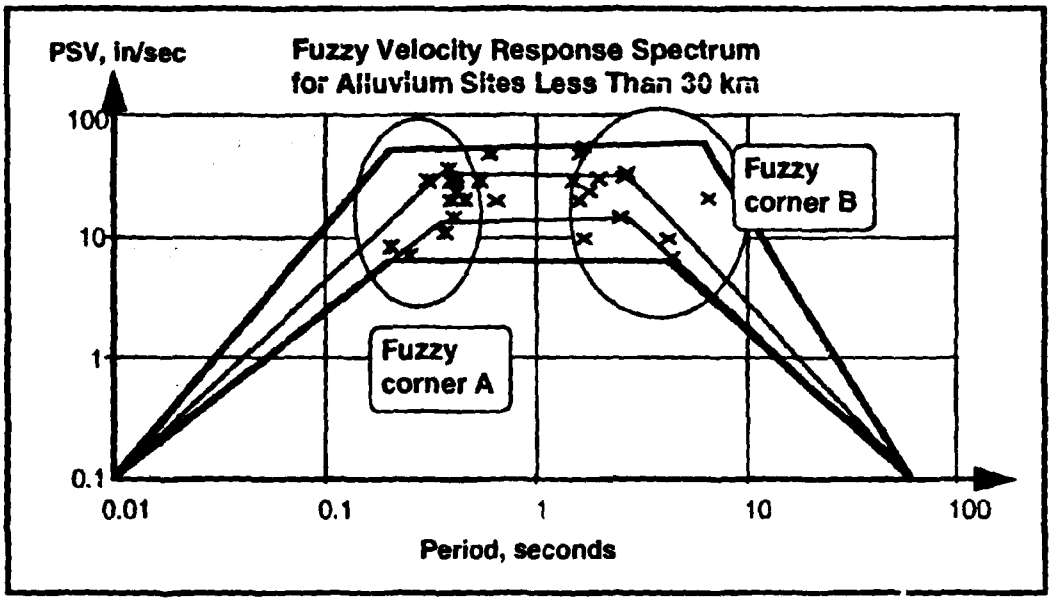

Figure A.5: Fuzzy velocity response spectrum for alluvium sites less than 30 km from the rupture zone at α-cut 0^+.

Table A.1: Rock sites used in fuzzy set development.

Site	Dist. km	Channel I				Channel III			
		Corner A		Corner B		Corner A		Corner B	
		Period sec.	PSV in/s	Period sec	PSV in/s	Period sec	PSV in/s	Period sec	PSV in/s
Corralitos	1	.78	60	3.4	12	0.4	41	2.5	21
Saratoga - Aloha Ave.	9	1.0	20	4.0	30	0.6	25	2.1	39
Gilroy 1	15	0.4	45	1.6	20	0.4	25	3.3	10
Santa Cruz-UCSC	16	0.30	20	4.0	9.5	.4	30	1.1	18
Coyote Lake Dam	21	0.6	42	2.0	20	0.9	20	2.0	11
Gilroy 6 - San Ysidro	24	0.25	13	1.5	15	.4	7	4	7
Woodside Fire Station	36	1	10	3.0	12	1	11	4	16
SAGO South	39	1	14	7	8.5	1	11	5	4
Monterey City Hall	44	0.4	4	1.5	3.5	0.17	3.8	1	4
Skyline Blvd.	44	0.6	10.8	3.0	11	0.55	10	3.5	15
Pulgas Water Temple	44	0.37	7	3.5	12	0.5	12	3.0	13
Hayward - CSUH stadium	53	0.34	5	5	5	0.35	5	6.0	4.8
South S. F. - Sierra Point	65	0.45	6.5	3	4	0.5	4	2.4	4.5
S. F. - Diamond Heights	73	0.45	8	2.7	7	0.7	1.5	2.1	0.5
Piedmont Jr. High School	74	0.5	5.3	6.0	6	0.41	5.2	1.7	6.5
San Francisco - Rincon Hill	76	0.78	7	2.1	9	0.45	3	3.5	4
Yerba Buena Island	77	0.7	8	2.0	7.1	0.88	3.2	4.0	3
S. F. - Telegraph Hill	78	0.2	3.5	1.9	6.7	0.8	4	3.5	3
S. F. - Pacific Heights	78	1.0	9	3.5	6	0.88	10	2.8	9
S. F. - Presidio	79	0.46	16	2.9	11	0.40	7	2.1	8
S. F. - Cliff House	80	1.1	19	2.6	11	0.5	7	4.5	6
Lawrence Berkeley Lab	80	1.4	20	3.9	7	1	10	5.7	4.2
Point Bonita	85	1.2	19	1.9	19	0.88	6.5	2.9	10

Table A.2: Alluvium sites used in fuzzy set development.

Site	Dist. km	Channel I				Channel III			
		Corner A		Corner B		Corner A		Corner B	
		Period sec.	PSV in/s	Period sec	PSV in/s	Period sec	PSV in/s	Period sec	PSV in/s
Capitola	14	0.6	50	1.8	25	0.38	38	1.7	58
Gilroy 2	16	0.46	21	1.6	50	.4	31	1.8	25
Gilroy 3	18	0.30	20	2.7	35	0.42	32	4.2	10
Gilroy 4	20	0.55	30	2.0	31	0.42	30	1.5	30
Agnews State Hospital	25	0.25	7.2	2.6	32	0.36	11	6.4	22
Hollister - South and Pine	33	0.55	20	5.0	31	0.8	60	3.1	35
Salinas John and Work Street	34	0.5	8	2.0	12	.45	5.8	3.8	11
Point Reyes	119	0.8	20	2.0	20	0.75	30	1.0	30
Gilroy - Gavalan College	15	0.42	25	1.6	20	0.39	20	4.4	7
Coyote Lake Dam	21	0.4	15	2.5	15	0.2	8.5	1.7	10
Gilroy 7	28	0.39	30	0.41	30	0.46	20	0.64	20
Halls Valley	31	0.60	15	2.5	10	0.78	21	2.9	6
Mission San Jose	39	0.30	7	5.0	7	0.65	10	5.0	10
John Muir School	53	0.65	12	2.0	16	0.47	10	1.6	20
Hayward BART	55	0.21	8	5	5	1.0	20	3.9	5
Richmond City Hall	89	1.1	15	3.3	6.8	0.9	25	1.1	25

APPENDIX B

Use of the Vertex Method in Modal Analysis

Typically, the response spectrum method is performed deterministically. Values for modal periods for each mode are referenced on the response spectrum to obtain a single value for the maximum response. Then a superposition method, such as SRSS or CQC, is used to obtained an estimate for the potential maximum response for the structural system. The purpose of this appendix is to describe the use of the response spectrum method when uncertain parameters are used rather than deterministic values. Here, the uncertain parameters are represented as fuzzy sets defined by membership functions.

The equations used in this thesis to calculate maximum structural response are given below:

$$\mathcal{L}_n = \phi_n \mathbf{M}\{1\} \tag{B.1}$$

where,

$\mathcal{L}_n$ = the earthquake participation factor for mode n;
ϕ_n = the eigenvector for mode n; and
M = the assembled mass matrix.

$$|\mathbf{V}_{\max}| = \sqrt{\sum_{n=1}^{m} \mathcal{L}_n \phi_n S_v(n)} \tag{B.2}$$

where,

$S_v(n)$ = the maximum velocity obtained from a velocity response spectrum;
m = the number of modes superimposed; and
$\mathbf{V}_{\max}$ = the maximum velocity for the structure.

Calculation of the earthquake participation factor for each mode is performed at the same time as the free-vibration analysis. For each vertex defining the frequency trapezoidal fuzzy set, there is a earthquake participation factor and mode shape. Thus, the extreme conditions used to calculate an extreme bound for frequency are also used to calculate the participation factor and the eigenvector for that vertex.

If a deterministic value is used to reference responses from the fuzzy response spectrum, then the maximum response is a fuzzy set. A period of 2 seconds referenced on the fuzzy velocity response spectrum for rock sites within 30 km of the rupture zone gives the fuzzy set for the maximum velocity shown in Table B.3.

Table B.3: Maximum response fuzzy set at rock sites ($X < 30$ km) for a period of 2 seconds.

α-cut	lower bound in/sec	upper bound in/sec
1.0	11	23
0.0^+	6.1	46

When the period fuzzy set is used to reference responses on the fuzzy spectrum, each vertex of the period fuzzy set refers to a maximum response fuzzy set. Table B.4 gives the response fuzzy sets for a period fuzzy set equal to 'about' 2 seconds. The column of values in the table is the fuzzy set for period. The vertices for the triangular fuzzy set are labeled as A,B, & C as shown in the second column of the table. Fuzzy sets for velocity response for each vertex are given in the last four columns.

Modal superposition using SRSS is performed repetitively using the fuzzy sets for period (with participation factors and eigenvectors) and the fuzzy sets for maximum response. Calculations are performed at each α-cut level as specified by the vertex method. At each α-cut level four solutions are performed to exhaust all possible combinations of vertices. The highest value calculated at each α-cut is selected as the bound for the resulting maximum response fuzzy set.

Equations B.3, B.4, B.5, and B.6 give the parametric combinations for each of the

four solutions at α-cut 0.

$$|\mathbf{V}_{\max}|_1 = \sqrt{\mathcal{L}_1^{L,\alpha=0}\phi_1^{L,\alpha=0}S_v^{L,\alpha=0}(T_1^{L,\alpha=0}) + \mathcal{L}_2^{L,\alpha=0}\phi_2^{L,\alpha=0}S_v^{L,\alpha=0}(T_2^{L,\alpha=0})} \quad \text{(B.3)}$$

$$|\mathbf{V}_{\max}|_2 = \sqrt{\mathcal{L}_1^{L,\alpha=0}\phi_1^{L,\alpha=0}S_v^{U,\alpha=0}(T_1^{L,\alpha=0}) + \mathcal{L}_2^{L,\alpha=0}\phi_2^{L,\alpha=0}S_v^{U,\alpha=0}(T_2^{L,\alpha=0})} \quad \text{(B.4)}$$

$$|\mathbf{V}_{\max}|_3 = \sqrt{\mathcal{L}_1^{U,\alpha=0}\phi_1^{U,\alpha=0}S_v^{L,\alpha=0}(T_1^{U,\alpha=0}) + \mathcal{L}_2^{U,\alpha=0}\phi_2^{U,\alpha=0}S_v^{L,\alpha=0}(T_2^{U,\alpha=0})} \quad \text{(B.5)}$$

$$|\mathbf{V}_{\max}|_4 = \sqrt{\mathcal{L}_1^{U,\alpha=0}\phi_1^{U,\alpha=0}S_v^{U,\alpha=0}(T_1^{U,\alpha=0}) + \mathcal{L}_2^{U,\alpha=0}\phi_2^{U,\alpha=0}S_v^{U,\alpha=0}(T_2^{U,\alpha=0})} \quad \text{(B.6)}$$

where,

U = superscript denoting upper bound for an α-cut; and

T = structural period.

The resulting bound for α-cut 0^+ for the maximum response $|\mathbf{V}_{\max}|_{\alpha=0^+} = \max |\mathbf{V}_{\max}|_n$ for $n = 1,4$. This procedure is repeated at each α-cut level to fully define the upper bound for the maximum response at all levels of confidence.

Table B.4: Maximum response fuzzy set at rock sits ($X < 30$ km) for a period of 2 seconds.

Bounds	Period (sec)	Label	A (in/sec)	B (in/sec)	C (in/sec)	D (in/sec)
α-cut 0^+ (low)	1	A	6.0	6.1	6.1	5.5
α-cut 1	2	B	13	11	11	5.5
α-cut 1	2	C	28	23	23	11
α-cut 0^+ (high)	4.5	D	50	46	46	30